

**Effects of Oxidative Stress on the
Expression and Function of Inducible
Nitric Oxide Synthase (iNOS) in Cultured
Vascular Smooth Muscle Cells**

Praveen Kumar Bingi

**University of Hertfordshire
April 2015**

A thesis submitted to the department of human and environmental sciences of University of Hertfordshire in partial fulfilment of the requirements for the degree of Doctor of Philosophy (PhD)

Summary

Atherosclerosis is widely accepted as an inflammatory disease and most common cause for the cardiovascular diseases. It is a progressive and multi-factorial disease and is presently the foremost cause of morbidity and mortality in the developed world (Wong *et al.*, 2006). There are many risk factors such as hypercholesterolemia, diabetes, smoking, high fat diet, obesity, infections and age that stimulate inflammatory reactions and instigate injury to the endothelium lining the arteries. This causes endothelial dysfunction and allows lipids and toxins to enter the intima through the damaged endothelial layer. This leads to oxidation of lipids and inflammation, which results in plaque deposits, and increased production of reactive oxygen species (ROS) causing oxidative stress (OS). The latter are critical in the pathogenesis of atherosclerosis and produced as a consequence of the disease state (Vogiatzi *et al.*, 2009).

Oxidative stress is defined as an imbalance in the levels of pro-oxidants and anti-oxidants initiating the accumulation of reactive oxygen species (ROS) such as superoxide anion (O_2^-), hydroxyl radical (OH^\cdot) and hydrogen peroxide (H_2O_2). Oxidative stress causes damage to the vascular lining through mitochondrial dysfunction leading to impairment of cellular functions and contributes to the development of diseases including atherosclerosis. In addition, ROS generation may lead to decrease in the bioavailability of nitric oxide (NO), leading to platelet aggregation and vasoconstriction (Ginnan *et al.*, 2008); and may also enhance proliferation and migration of smooth muscle cells while inducing apoptosis of endothelial cells as well as causing oxidation of lipids and alteration of vasomotor

activity (Valko *et al.*, 2005). Mitochondrial damage causes over production of ROS and causes imbalance in the levels of pro-oxidants and anti-oxidants leading to apoptosis and atherogenesis. The excessive ROS generated then react with NO leading to the formation of peroxynitrite (ONOO⁻), which is detrimental to the vascular endothelium lining (Zhang *et al.*, 2012). In contrast to constitutive NO production, excess production of NO by inducible nitric oxide synthase (iNOS) may be pathologically relevant in the pathogenesis of atherosclerosis. However the role of iNOS in atherosclerosis remains elusive. Whilst it is widely believed to contribute to the pathogenesis of the disease, recent studies have shown that iNOS induced nitric oxide (NO) has cardio-protective properties, which could restrict the progression of atherosclerotic lesions (Kanno *et al.*, 2000; Okazaki *et al.*, 2011). Our previous studies have demonstrated that the expression and function of iNOS may be selectively down regulated by pro-oxidants such as antimycin A (AA) and diethyl maleate (DEM) suggesting that part of the detrimental consequences to OS in the disease state may be associated with the obliteration of the iNOS and thus abolition of its cardio-protective properties. Intriguingly hydrogen peroxide (H₂O₂), another common pro-oxidant, did not affect iNOS expression and function, indicating that the observations we made earlier may not simply be due to OS alone. The effects of OS inducers on the expression and function of iNOS could be reversed with atorvastatin. To further explore the underlying mechanisms associated with these effects we have investigated whether AA and/or DEM modulated the activation of key cellular signalling molecules associated with the induction of iNOS, and whether atorvastatin exerted any novel actions through these signalling pathways.

Rat cultured aortic smooth muscle cells (RASMCs) were treated for 24h with antimycin A (25-150 μ M) or DEM (1-10 μ M) or H₂O₂ (25-300 μ M) 30 min prior to stimulation with bacterial lipopolysaccharide (LPS; 100 μ g ml⁻¹) and interferon-gamma (IFN- γ ; 100U ml⁻¹). When used, atorvastatin (1-30 μ M) was added 30 min prior to each of these compounds. In experiments with the determination of ROS, cells were treated with antimycin A (25-150 μ M) or DEM (1-10 μ M) or H₂O₂ (25-300 μ M) for 24h before incubating the cells with a fluoregenic dye. Experiments were also conducted using polyethylene-glycol superoxide dismutase (PEG-SOD) and polyethylene-glycol catalase (PEG-Catalase) in the presence of OS inducers on changes in iNOS expression and/or function and superoxide radical generation. When used, cells were incubated with PEG-SOD 500 U/ml or PEG-Catalase 500 U/ml 30min prior to activation of cells with LPS and IFN- γ . Nitrite production was determined by the Griess assay and total cell protein by the bicinchoninic acid assay. Amount of reactive radical species generated was estimated using confocal laser scanning microscopy and changes in iNOS expression or phosphorylation of mitogen activated protein kinases (MAPK) were determined by western blotting and quantified densitometrically using the image-J software. Statistical analysis was carried out using one-way ANOVA followed by Bonferroni post-hoc test using Graph Pad Prism 5.0.

Antimycin A and DEM resulted in concentration dependent inhibition of NO production and iNOS expression ($p < 0.001$) whereas H₂O₂ was without any effect. Antimycin A, H₂O₂ and DEM induced ROS production in a concentration and time dependent manner ($p < 0.001$) but AA and DEM caused more generation of superoxide radicals ($p < 0.001$) than did H₂O₂ which generated mostly hydroxyl

radicals. Polyethylene-glycol superoxide dismutase but not PEG-Catalase at a concentration of 500 U/ml was able to inhibit the superoxide radical generated by antimycin A and DEM ($p<0.05$). Atorvastatin enhanced nitrite production and iNOS expression ($p<0.01$) in a concentration dependent manner reaching a peak at 10 μ M and considerably declining thereafter. Hence further experiments were continued using atorvastatin 10 μ M. Atorvastatin at 10 μ M significantly ($p<0.001$) and PEG-SOD (500U ml⁻¹) partially reversed the inhibition of NO production and iNOS expression caused by OS inducers. PEG-CAT (500U ml⁻¹) did not affect the inhibitions initiated by OS inducers either on iNOS expression/function and superoxide radical production. These findings suggest that iNOS expression and nitrite production may be down regulated, in part; by pro-oxidants generating superoxide but not hydroxyl radicals and this could explain the differential regulation of these processes by the different OS inducing agents.

Antimycin A and DEM caused concentration dependent inhibition ($p<0.001$) of the phosphorylation of p38 MAPK and Akt. These changes could be prevented when pre-incubated with 10 μ M atorvastatin (DEM: $p<0.01$; antimycin A: $p<0.05$). Thus the presence of OS within the vasculature may suppress the expression of iNOS through the regulation of either p38 MAPK and/or Akt, which may be prevented with atorvastatin. Hence these findings suggest antimycin A and DEM down regulate iNOS expression and NO production through inhibition of phosphorylation of p38 MAPK and Akt. Taken together, the data suggest novel actions for both pro-oxidants and atorvastatin, which may have important implications in coronary artery disease where suppression of iNOS may be deleterious and maintaining its expression may be cardio-protective.

Abstract

The role of inducible nitric oxide synthase (iNOS) and/or nitric oxide (NO) in atherosclerosis remains elusive. Several researchers argued whether iNOS and/or NO are pathogenic or cardio protective. The pathogenesis of atherosclerosis is complex and includes mechanisms associated with inducible nitric oxide synthase (iNOS). We have demonstrated that the expression and function of iNOS may be selectively down regulated by pro-oxidants such as antimycin A and diethyl maleate (DEM). To further explore the underlying mechanisms associated with these effects we have investigated whether antimycin A and/or DEM modulated the activation of key cellular signalling molecules associated with the induction of iNOS. Expression of p38 mitogen activated kinase (MAPK) and Akt were induced by exposure to lipopolysaccharide (LPS) and interferon-gamma (IFN- γ). Oxidative stress (OS) was induced using antimycin A, DEM and hydrogen peroxide (H₂O₂). All three OS inducers caused a significant generation of free radicals whereas only antimycin A and DEM generated superoxide radical (O₂⁻). Also nitrite production and iNOS expression may be down regulated, in part; by pro-oxidants generating O₂⁻ but not hydroxyl radicals (OH⁻). Antimycin A and DEM concentration dependently inhibited the phosphorylation of p38 MAPK and Akt and this was restored when the cells were pre-treated with Atorvastatin whereas H₂O₂ was without any significant effect. Taken together, the data suggest novel actions for both pro-oxidants and atorvastatin which may have important implications in coronary artery disease where suppression of iNOS may be deleterious and maintaining its expression may be cardio-protective.

Declaration

I, Praveen Bingi, hereby declare that this Ph. D. thesis entitled “ Effects of Oxidative Stress on the Expression and Function of Inducible Nitric Oxide Synthesis (iNOS) in Cultured Vascular Smooth Muscle Cells” was carried out by me for the degree of doctor of philosophy and the work presented in it are my own and have been generated by me as the result of my original research.

I declare that all the information provided in this document has been followed in accordance with academic rules and ethical conduct. The contribution of any supervisors and others to the research and to the thesis was consistent with normal supervisory practice.

I certify that this work has not been submitted previously for the award of any other degree, or diploma in my name, in any university or any institution and, to the best of my knowledge and belief, contains no material previously published or written by another person, except where due reference has been made in the text. In addition, I certify that no part of this work will, in the future be used in a submission in my name, for any other degree or diploma in any university or institution without the prior approval of the University of Hertfordshire.

Signature:.....

Date:

Acknowledgement

First and foremost I want to express heartfelt gratitude to my principal supervisor Professor Anwar R Baydoun. It has been an honour to work under his supervision. I appreciate all his contributions in providing his time and ideas to make my Ph. D. experience productive and stimulating. I am heavily inspired for his constant enthusiasm and dedication towards research, which was contagious and motivational enough to overcome tough times in the pursuit of my Ph. D. I hope I could be as lively, enthusiastic and energetic as Prof. Baydoun and able to command an audience as well as he can.

I am also very grateful to my other supervisor, Dr Shori Thakur for her scientific advice and knowledge and many insightful discussions and suggestions. She has always been very supportive and provided me with meaningful advices, which greatly helped me in completing my thesis. I am always thankful for encouraging and giving me constructive feedback during the seminars and meetings.

I extend my special thanks to my past and present colleagues in the laboratory, Ashish Patidar, Anupama Awachat, Hema Pramod, Nasima Chowdary, Pablo Zardoya, Nimer Alsabeelah, Mahdi Alsugoor, Gagan Maan and Adem Nasraddin for making my Ph. D journey very memorable. Their constant encouragement and suggestions made a very pleasant working environment in the lab. The discussions we had and constant exchange of ideas and advices had a great impact in completion of my thesis. I also would like to thank the department technical staff for their support during the demonstrations and handling some of the equipments.

This thesis wouldn't have been possible without the unconditional love and kind support of my parents, Bingi Prakash and Bingi Laxmi. I always cherish the kind of support and confidence you both show on me. You both are my greatest strength and I am blessed to be your son. I would also like to thank my beloved sister for taking care of my parents while I am pursuing my Ph. D. and supporting and understanding me in difficult situations.

I thank you all from the bottom of my heart.

TABLE OF CONTENTS

TABLE OF CONTENTS	X
LIST OF FIGURES.....	XIV
LIST OF TABLES.....	XX
ABBREVIATIONS	XXI
1.0 INTRODUCTION.....	1
1.1 Atherosclerosis	2
1.2 Oxidative Stress.....	5
1.2.1 Reactive radical species	6
1.2.2 Mechanisms for ROS generation in vascular cells	7
1.3 Antioxidants	12
1.3.1 Superoxide Dismutase (SOD).....	13
1.3.2 Catalase.....	14
1.3.3 Heme oxygenase-1 (HO-1).....	15
1.3.4 Nuclear factor erythroid 2-related factor-2 (Nrf-2)	17
1.4 Nitric Oxide	19
1.4.1 Endothelial Nitric Oxide Synthase (eNOS).....	21
1.4.2 Neuronal Nitric Oxide Synthase (nNOS).....	22
1.4.3 Inducible Nitric Oxide Synthase (iNOS)	22
1.4.4 Pathology of the inducible nitric oxide synthase and its implications.....	24
1.5 Statins and their role in atherosclerosis	27
1.6 Aims and Objectives	30
2.0 MATERIALS AND METHODS.....	31
2.1 Cell culture materials and methods.....	32
2.1.1 Preparation of media required for culturing of cells	32
2.1.2 Isolation and culture of rat aortic smooth muscle cells	33
2.1.3 Maintenance of cells in culture	33
2.1.4 Trypsinization of cells.....	34
2.1.5 Cryopreservation of cells.....	34
2.1.6 Cell counting and plating.....	35

2.2 Experimental procedures	36
2.2.1 Treatment of cells with LPS and IFN- γ :	36
2.2.2 Treatment of cells with OS inducers.....	37
2.2.3 Treatment of cells with OS inducers for free radical generation.....	38
2.2.4 Treatment of cells with OS inducers and statins	39
2.2.5 Treatment of cells with OS inducers and polyethylene glycol-superoxide dismutase (PEG-SOD) or polyethylene glycol-catalase (PEG-catalase)	40
2.2.6 Time point analysis of the effects of OS inducers	40
2.3 Griess assay	41
2.4 Cell lysis.....	44
2.5Determination of total cell protein using bicinchoninic acid (BCA):	44
2.6 MTT assay	48
2.7 Western blotting.....	50
2.8Detection of free radical generation by confocal microscopy:	53
2.9 Real-time quantitative reverse transcriptase polymerase chain reaction (qPCR)	57
2.10 Statistical analysis.....	63
3.0 RESULTS.....	64
3.1 Rat aortic smooth muscle cells	65
3.2 Effects of OS inducers on the viability of rat aortic smooth muscle cells.....	66
3.3 Effects of ethanol on nitrite production and iNOS expression in control and activated RASMCs.....	70
3.4 Effect of OS inducers on nitrite production in control and activated RASMCs	73
3.5Effect of OS inducers on the expression of the inducible nitric oxide synthase (iNOS).....	77
3.6 Effect of OS inducers on iNOS mRNA expression in control and activated RASMCs.....	81
3.7Effect of OS inducers on free radical generation.....	85
3.8 Time dependent induction of free radical generation by OS inducers	89
3.9Induction of superoxide radicals by OS inducers	96
3.10EffectofPolyethylene glycol-superoxide dismutase (PEG-SOD)on superoxide radical generation in the presence and absence ofOS inducers.....	99

3.11 Effect of Polyethylene glycol-catalase (PEG-catalase) on superoxide radical generation in the presence and absence of OS inducers	102
3.12 Effect of polyethylene glycol-superoxide dismutase (PEG-SOD) on nitrite production in the presence and absence of OS inducers	105
3.13 Effect of polyethylene glycol-catalase (PEG-catalase) on nitrite production in the presence and absence of OS inducers	107
3.14 Effect of polyethylene glycol-superoxide dismutase (PEG-SOD) on the expression of iNOS in the presence and absence of OS inducers	109
3.15 Effect of polyethylene glycol-catalase (PEG-catalase) on the expression of iNOS in the presence and absence of OS inducers	112
3.16 Effect of atorvastatin on NO production in the presence and absence of OS inducers	115
3.17 Effects of atorvastatin on the expression of iNOS in the presence and absence of OS inducers	122
3.18 Effect of atorvastatin on superoxide radical generation in the presence and absence of OS inducers	130
3.19 Effect of OS inducers on the phosphorylation of p38 MAPK	132
3.20 Effect of OS inducers on the phosphorylation of Akt	134
3.21 Effect of Atorvastatin on the phosphorylation of p38 MAPK in the presence and absence of different concentrations of DEM or antimycin A	136
3.22 Effect of Atorvastatin on the phosphorylation of Akt in the presence and absence of different concentrations of DEM or antimycin A	139
4.0 DISCUSSION	142
4.1 Summary and Conclusions	164
5.0 FUTURE WORK	166
6.0 REFERENCES	168

LIST OF FIGURES

Figure 1.1A diagrammatic representation of stages of atherosclerosis taken from http://www.educatehealth.ca/patient/heart/heart-attack.aspx	4
Figure 1.2 Sources of reactive oxygen species (ROS) and consequences on endothelial function	8
Figure 1.3 Metabolism of Heme and its properties	17
Figure 1.4 Dissociation of Nrf-2 and its function.....	19
Figure 1.5 Synthesis of Nitric Oxide (NO) by the NOS enzyme(Taken from Gorren and Mayer, 1997).....	20
Figure 1.6 Schematic representation of iNOS gene expression and function(Taken from Faraci and Heistad, 1998).....	23
Figure 2.1 Griess reaction for the detection of nitrite.....	41
Figure 2.2A representative Nitrite standard curve	43
Figure 2.3 BCA chelation with a cuprous ion.....	45
Figure 2.4A representative protein standard curve	47
Figure 2.5 Formation of water insoluble Formazan from MTT in the presence of Succinate dehydrogenase.....	49
Figure 2.6 Principal light pathways involved in imaging of the sample in Confocal Microscopy	55
Figure 2.7 DNA polymerase cleaving the green dye from the red.....	58
Figure 3.1 Morphology of RASMCs in culture	65
Figure 3.2 Effect of DEM on viability of RASMCs.....	67
Figure 3.3 Effect of Antimycin A on viability of RASMCs.....	68
Figure 3.4 Effect of H ₂ O ₂ on viability of RASMCs.....	69
Figure 3.5 Effects of ethanol on nitrite production in LPS and IFN- γ activated RASMCs	71

Figure 3.6 Effects of ethanol on iNOS expression in LPS and IFN- γ activated RASMCs	72
Figure 3.7 Effects of DEM on nitrite production in LPS and IFN- γ activated RASMCs	74
Figure 3.8 Effects of antimycin A on nitrite production in LPS and IFN- γ activated RASMCs	75
Figure 3.9 Effects of H ₂ O ₂ on nitrite production in LPS and IFN- γ activated RASMCs	76
Figure 3.10 Effects of DEM on iNOS expression in LPS and IFN- γ activated RASMCs	78
Figure 3.11 Effects of antimycin A on iNOS expression in LPS and IFN- γ activated RASMCs	79
Figure 3.12 Effects of H ₂ O ₂ on iNOS expression in LPS and IFN- γ activated RASMCs	80
Figure 3.13 Effects of DEM on iNOS mRNA in LPS and IFN- γ activated RASMCs .	82
Figure 3.14 Effects of antimycin A on iNOS mRNA in LPS and IFN- γ activated RASMCs	83
Figure 3.15. Effects of H ₂ O ₂ on iNOS mRNA in LPS and IFN- γ activated RASMCs ..	84
Figure 3.16 Effect of DEM on free radical generation in RASMCs	86
Figure 3.17 Effect of antimycin A on free radical generation in RASMCs.....	87
Figure 3.18 Effect of H ₂ O ₂ on free radical generation in RASMCs	88
Figure 3.19 Time dependent induction of free radical generation in RASMCs by antimycin A	90
Figure 3.20 Time dependent induction of free radical generation in RASMCs by DEM	92

Figure 3.21 Time dependent induction of free radical generation in RASMCs by H ₂ O ₂	94
Figure 3.22 Induction of superoxide radicals by OS inducers in cultured RASMCs ...	97
Figure 3.23 Effect of PEG-SOD on superoxide radical generation in the presence of OS inducers in RASMCs.....	100
Figure 3.24 Effect of PEG-catalase on superoxide radical generation in the presence of OS inducers in RASMCs.....	103
Figure 3.25 Effect of PEG-SOD on nitrite production in the presence and absence of OS inducers in LPS and IFN- γ activated RASMCs	106
Figure 3.26 Effect of PEG-Catalase on nitrite production in the presence and absence of DEM and antimycin A in LPS and IFN- γ activated RASMCs	108
Figure 3.27 Effect of PEG-SOD on iNOS expression in the presence and absence of DEM and antimycin A in LPS and IFN- γ activated RASMCs	Error! Bookmark not defined.
Figure 3.28 Effect of PEG-Catalase on iNOS expression in the presence and absence of DEM and antimycin A in LPS and IFN- γ activated RASMCs	Error! Bookmark not defined.
Figure 3.29 Effect of Atorvastatin on viability of RASMCs.....	117
Figure 3.30 Effect of atorvastatin on nitrite production in LPS and IFN- γ activated RASMCs	118
Figure 3.31 Effect of atorvastatin on nitrite production in the presence of DEM in LPS and IFN- γ activated RASMCs.....	119
Figure 3.32 Effect of Atorvastatin on nitrite production in the presence of antimycin A in LPS and IFN- γ activated RASMCs	120

Figure 3.33 Effect of Atorvastatin on nitrite production in the presence of H ₂ O ₂ in LPS and IFN- γ activated RASMCs.....	121
Figure 3.34 Effect of Atorvastatin on iNOS expression in LPS and IFN- γ activated RASMCs	124
Figure 3.35 Effect of Atorvastatin on iNOS expression in the presence and absence of DEM in LPS and IFN- γ activated RASMCs	125
Figure 3.36 Effect of Atorvastatin on iNOS expression in the presence and absence of antimycin A in LPS and IFN- γ activated RASMCs.....	126
Figure 3.37 Effect of Atorvastatin on iNOS expression in the presence and absence of H ₂ O ₂ in LPS and IFN- γ activated RASMCs	128
Figure 3.38 Effect of atorvastatin on superoxide radical generation in the presence and absence of OS inducers in RASMCs	131
Figure 3.39 Effect of OS inducers on the phosphorylation of p38 MAPK in LPS and IFN- γ activated RASMCs.....	133
Figure 3.40 Effect of OS inducers on the phosphorylation of Akt in LPS and IFN- γ activated RASMCs	135
Figure 3.41 Effect of Atorvastatin on the phosphorylation of p38 MAPK in the presence and absence of Antimycin A in LPS and IFN- γ activated RASMCs .	137
Figure 3.42 Effect of Atorvastatin on the phosphorylation of p38 MAPK in the presence and absence of DEM in LPS and IFN- γ activated RASMCs	138
Figure 3.43 Effect of Atorvastatin on the phosphorylation of Akt in the presence and absence of antimycin A in LPS and IFN- γ activated RASMCs	140
Figure 3.44 Effect of Atorvastatin on the phosphorylation of Akt in the presence and absence of DEM in LPS and IFN- γ activated RASMCs.....	141
Figure 4.1 Structural Representation of antimycin A	145

Figure 4.2Structural Representation of diethyl maleate.....	146
Figure 4.3Structural Representation of Hydrogen Peroxide	146
Figure 4.4Structural representation of hydrolysis and oxidation of DCFH.....	151
Figure 4.5 Oxidation of MitoSOX to 2-hydroxy-5-(triphenylphosphonium) hexylethidium by superoxide ($\bullet\text{O}_2^-$).....	153
Figure 4.6Schematic Representation of LPS and IFN- γ Signalling.....	161

LIST OF TABLES

Table 1: Preparation of serial dilutions of NaNO ₂	42
Table 2: Preparation of a protein standard curve	46
Table 3. Preparation of samples for reverse transcription	61

ABBREVIATIONS

AA	Antimycin A
ADP	Adenosine Diphosphate
ANOVA	Analysis of Variance
AP-1	Activating Protein-1
ARE	Antioxidant Response Elements
ATP	Adenosine Triphosphate
ATV	Atorvastatin
BCA	Bicinchoninic Acid
BH ₄	Tetrahydrobiopterin
BSA	Bovine Serum Albumin
cDNA	Complimentary Deoxyribonucleic Acid
CETP	Cholesteryl Ester Transfer Protein
CHD	Coronary Heart Disease
CNS	Central Nervous System
CO	Carbon monoxide
Cu ⁺¹	Cuprous
Cu ⁺²	Copper
DCFH-DA	2, 7-dichlorofluorescein diacetate
DCF	2,7-dichlorofluorescein
DDW	Double Distilled Water
DEM	Diethyl Maleate
DHE	Dihydroethidium
DMEM	Dulbecco's Modified Eagle Medium
DMSO	Dimethyl Sulfoxide

DNA	Deoxyribo Nucleic Acid
EDRF	Endothelium Derived Relaxation Factor
eNOS	Endothelial Nitric Oxide Synthase
ERK	Extracellular Signal-Regulated Kinase
FAD	Flavin Adenine Dinucleotide
FBS	Foetal Bovine Serum
FMN	Flavin mononucleotide
FPP	Farnesylpyrophosphate
GGPP	Geranylgeranylpyrophosphate
GST	Glutathione-S-Transferase
H ₂ O ₂	Hydrogen Peroxide
HBSS	Hank's Balanced Salt Solution
HDL	High-Density Lipoproteins
HIF-1	Hypoxia Inducible Factor-1
HMG CoA	3-hydroxy-3-methyl glutaryl co-enzyme A
HMGI/Y	High Mobility Group Family
HO-1	Heme oxygenase-1
HO-2	Heme oxygenase-2
I/R	Ischemia-Reperfusion
IFN- γ	Interferon-Gamma
IFNR1	Interferon Receptor-1
IFNR2	Interferon Receptor-2
IKK	Inhibitor of kappa B kinase
IL-1	Interleukin-1

iNOS	Inducible Nitric Oxide Synthase
IRAK	Interleukin 1 Receptor Associated Kinase
IRF-1	Interferon Response Factor-1
JAK-2	Janus Kinase-2
JAK-STAT	Janus Kinase-Signal Transducer and Activator of Transcription
JNK	c-jun Terminal Kinase
LBP	LPS Binding Protein
LDL	Low Density Lipoprotein
LFA-1	Lymphocyte Function Associated Antigen-1
LPS	Lipopolysaccharides
MAPK	Mitogen Activated Protein Kinases
MitoSOX	Mitochondrial Superoxide
mM	Milli Molar
MnSOD	Mitochondrial Superoxide Dismutase
mRNA	Messenger Ribonucleic Acid
MS	Multiple Sclerosis
MTT	3-(4, 5-dimethylthiazol-2-yl)-2, 5-diphenyltetrazolium bromide
MyD88	Myeloid Differentiation Primary Response Gene-88
NAD	Nicotinamide-adenine-dinucleotide
NADPH	Nicotinamide-adenine-dinucleotide Phosphate
NaNO ₂	Sodium Nitrite
NF- κ B	Nuclear Factor kappa B
nNOS	Neuronal Nitric Oxide Synthase
NO ₂ ⁻	Nitrite
NO ₃ ⁻	Nitrate
NOS	Nitric Oxide Synthase
NO	Nitric Oxide

Nrf-2	Nuclear factor Erythroid 2-related Factor-2
O ₂	Molecular Oxygen
O ₂ ⁻	Superoxide Anion
OH [•]	Hydroxyl Radical
ONOO ⁻	Peroxynitrite
OS	Oxidative Stress
oxLDL	Oxidized Low Density Lipoproteins
PBS	Phosphate Buffered Saline
PCR	Polymerase Chain Reaction
PEG-Catalase	Polyethylene-glycol Catalase
PEG-SOD	Polyethylene-glycol Superoxide Dismutase
PKC	Protein Kinase C
PVDF	Polyvinylidene Fluoride
RASMCs	Rat Aortic Smooth Muscle Cells
RA	Rheumatoid Arthritis
RC	Respiratory Chain
RNA	Ribonucleic Acid
RNS	Reactive Nitrogen Species
ROS	Reactive Oxygen Species
S.E.M	Standard Error Mean
SAPK	Stress Activated Protein Kinase
SDS-PAGE	Sodium Dodecyl Sulphate Polyacrylamide Gel
SDS	Sodium Dodecyl Sulphate
SOD	Superoxide Dismutase
STAT1	Signal Transducer and Activator of Transcription Alpha
TAB1	TAK1-Binding Protein-1
TLR-4	Toll Like Receptor-4

TNF- α	Tumor Necrosis Factor-alpha
TRAF6	TNF Receptor Associated Factor-6
VCAM-1	Vascular Cell Adhesion Molecule-1
VLDL	Very-Low Density Lipoproteins
WHO	World Health Organization
XDH/XO	Xanthine Dehydrogenase/Xanthine Oxidase
β -actin	Beta Actin
μ M	Micro Molar

1.0 INTRODUCTION

Atherosclerosis is a complex disease with many facets of which the development of oxidative stress (OS) and impaired vascular tone linked to reduced production of nitric oxide (NO) by the endothelial nitric oxide synthase (eNOS) are a common feature. In addition, it has also been widely accepted that overproduction of NO by the inducible nitric oxide synthase (iNOS) under conditions of OS contributes to the pathogenesis of atherosclerosis. This notion, which ascribes a pathological role for iNOS, is however being challenged and iNOS, rather than being pathological, is gaining rapid acceptance as a key cardio protective pathway in atherosclerosis. Moreover, previous research in our group has demonstrated that OS down regulates the expression of the inducible L-arginine-NO pathway which has led to the hypothesis that the deleterious effect of OS may be mediated, in part, through suppression and loss of the protective and beneficial effects of iNOS, thereby contributing to the pathogenesis of atherosclerosis. This has been further addressed in this thesis, which has also been extended to examine whether statins, widely used as lipid-lowering drugs, protected against OS induced regulation of iNOS through novel mechanisms that may be independent of their lipid lowering effects.

1.1 Atherosclerosis

Atherosclerosis is the most common and typical cause of heart attacks, strokes and peripheral vascular disease. It is a progressive and multi-factorial disease and is currently the leading cause of morbidity and mortality in the developed world (Wong *et al.*, 2006). No less than 2.6 million people in the United Kingdom suffer from the disease (<http://www.bhf.org.uk/heart-matters-online/may-june-2013/medical/atherosclerosis.aspx>). The epidemiological studies conducted previously stressed upon the importance of environmental and genetic risk factors in association with

atherosclerosis. However the complexity of the disease aetiology made it difficult to understand the cellular and molecular interactions.

Atherosclerosis was initially considered to be simply a disorder of lipid deposition leading to myocardial infarction, stroke and ischemic gangrene (Hansson *et al.*, 2006). It is, however, now known to be an immune-inflammatory disease where lipids, leukocytes and smooth muscle cells as well as cholesterol-engorged macrophages or foam cells accrue in the intima of the arteries (Zhou & Liao, 2009) leading to the formation of fibro fatty plaques called atheroma. This material gradually encroaches into the lumen of the vessel, eventually leading to blockage of the artery. Plaques may be formed which can weaken the wall of the artery leading to aneurysm and could also cause narrowing of the arteries, thus restricting blood flow (Davis, 2005). This in turn may lead to angina pectoris (chest pain) and subsequently myocardial infarction, heart attack and death.

The difference in dynamics of blood flow allows the lesions to be formed at distinct sites inside the arteries and these tend to be regions of high shear. In the early stage of the disease, lipid laden foam cells form fatty streaks which are not clinically substantial, but the accumulation of smooth muscle cells (SMCs) and lipid rich necrotic debris lead to significant lesions (Coller, 2005). A fibrous cap consisting of monocytes, macrophages and extracellular matrix that enclose a lipid-rich necrotic core characterizes these stringy lesions. These plaques are further hardened and increased by the accumulating through calcification, ulceration and also hemorrhage from small vessels that lead to lesions from media of the blood vessel wall. (Figure 1) (Moore & Tabas, 2011).

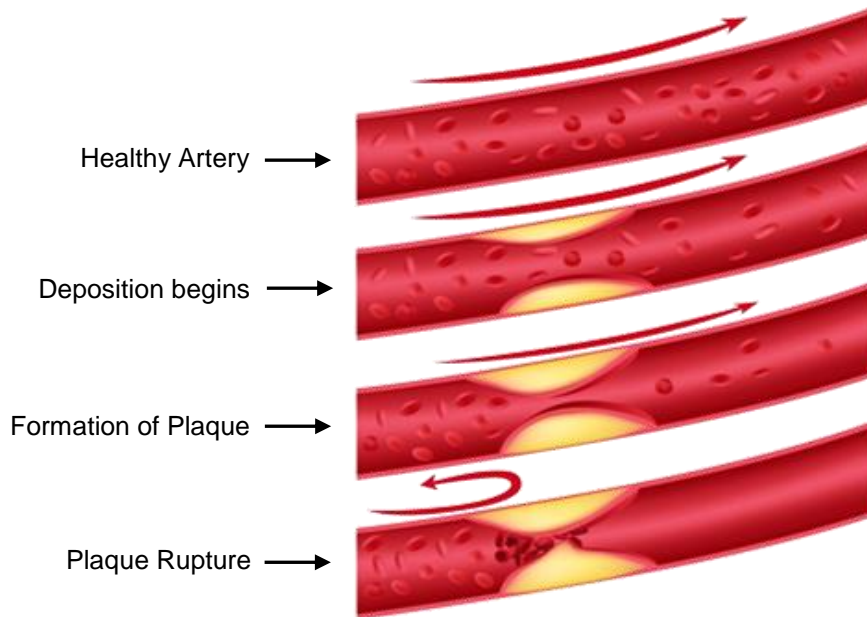


Figure 1.1A diagrammatic representation of stages of atherosclerosis taken from <http://www.educatehealth.ca/patient/heart/heart-attack.aspx>

The trigger for the development of atherosclerosis is now widely accepted to be associated with endothelial dysfunction (Hadi *et al.*, 2005). Indeed many risk factors such as hypercholesterolemia, diabetes, smoking, high fat diet, obesity, infections and age promote inflammatory reactions and OS causing damage to the endothelium lining the arteries (Rasmussen *et al.*, 2005). This causes endothelial dysfunction and allows lipids to enter the intima through the damaged endothelial layer. In parallel, there is also increased recruitment of circulating monocytes, which differentiate into macrophages once in the intima. The macrophages in turn accumulate oxidised low density lipoproteins (Ox-LDL) generated from the oxidation of LDL by reactive oxygen species (ROS). The latter are critical in the pathogenesis of atherosclerosis and are produced as a consequence of the disease state (Vogiatzi *et al.*, 2009).

1.2 Oxidative Stress

Oxidative stress is defined as an imbalance in the levels of pro-oxidants and anti-oxidants in the biological system (Nedeljkovic *et al.*, 2003). It arises when there is an increase in pro-oxidants thereby releasing more amounts of free radicals within the cells (Gobe & Crane, 2010). The biological system loses the capacity to neutralise excess free radicals, which in turn cause complications within the body and facilitates diseases such as atherosclerosis (Vogiatzi *et al.*, 2009).

Oxidative stress causes direct and irreversible oxidative impairment to macromolecules and also alters redox dependent signalling process (Drummond *et al.*, 2011). A wide range of environmental factors such as ultraviolet stress, pathogen invasion, herbicide action and oxygen shortage induce OS. In normal healthy cells, free radicals are produced in an organized manner and acts as important regulators of signalling molecules that are central to cell division, inflammation, immune function, autophagy and stress response. In contrast, uncontrolled production of these reactive oxidants results in OS leading to impairment of cellular functions and, as stated, contributes to the development of diseases including atherosclerosis. This may be mediated through various radical species discussed below.

1.2.1 Reactive radical species

Reactive oxygen and nitrogen species (ROS, RNS) are continuously produced within the body from internal metabolism and external exposure. Oxidative stress causes the formation of ROS and RNS that are oxygen and nitrogen derived small molecules and include radical species such as superoxide anion (O_2^-), hydroxyl radical (OH^\cdot), and peroxynitrite ($ONOO^-$). These free radicals are highly unstable because of their distribution of electrons based on their atomic or molecular structure (Buttery *et al.*, 1996). As a result, they try to become stable by pairing with other molecules and hence are highly reactive. They can also react with other free radicals or take a hydrogen atom from other molecules to achieve a stable state. The levels of these free radicals and the ability of the antioxidant defence system to neutralise these species governs the consequences of OS.

In most of the conditions where ROS is produced, the body's anti-oxidant system is generally able to counteract their effects by inactivating the various ROS produced and in doing so protect against the deleterious effects of these free radicals. However the antioxidant defence is not always sufficient to neutralise ROS and maintain a balance. Thus, excessive ROS generation becomes pathological when their release persists long-term. In atherosclerosis, ROS may contribute to the pathogenesis of the disease through alteration of LDL, reducing the bioavailability of NO and increasing the leukocyte recruitment within the arterial wall.

1.2.2 Mechanisms for ROS generation in vascular cells

Reactive oxygen species are produced from various sources in several compartments within the cell during normal cell regulation or as a consequence when exposed to pathologic or toxic insults. The different compartments within the cell that produce ROS are cell membrane, mitochondria, peroxisomes and endoplasmic reticulum. The normal source of ROS in humans is during oxidative phosphorylation in the mitochondria through the electron transport chain. Reactive oxygen species (ROS) production is nevertheless amplified when electron transport in the respiratory chain (RC) is impaired but the impairment may be buffered to a certain extent without definite ROS formation in mitochondria (Forstermann, 2010). The other sources of ROS formation are mediated by enzymes such as nicotinamide adenine dinucleotide phosphate (NADPH) oxidase, nitric oxide synthase (NOS) and xanthine oxidase as illustrated in Figure 2 (Magenta *et al.*, 2014). The NADPH oxidase is considered as the major source of free radicals and it mainly accelerates the production of O_2^- .

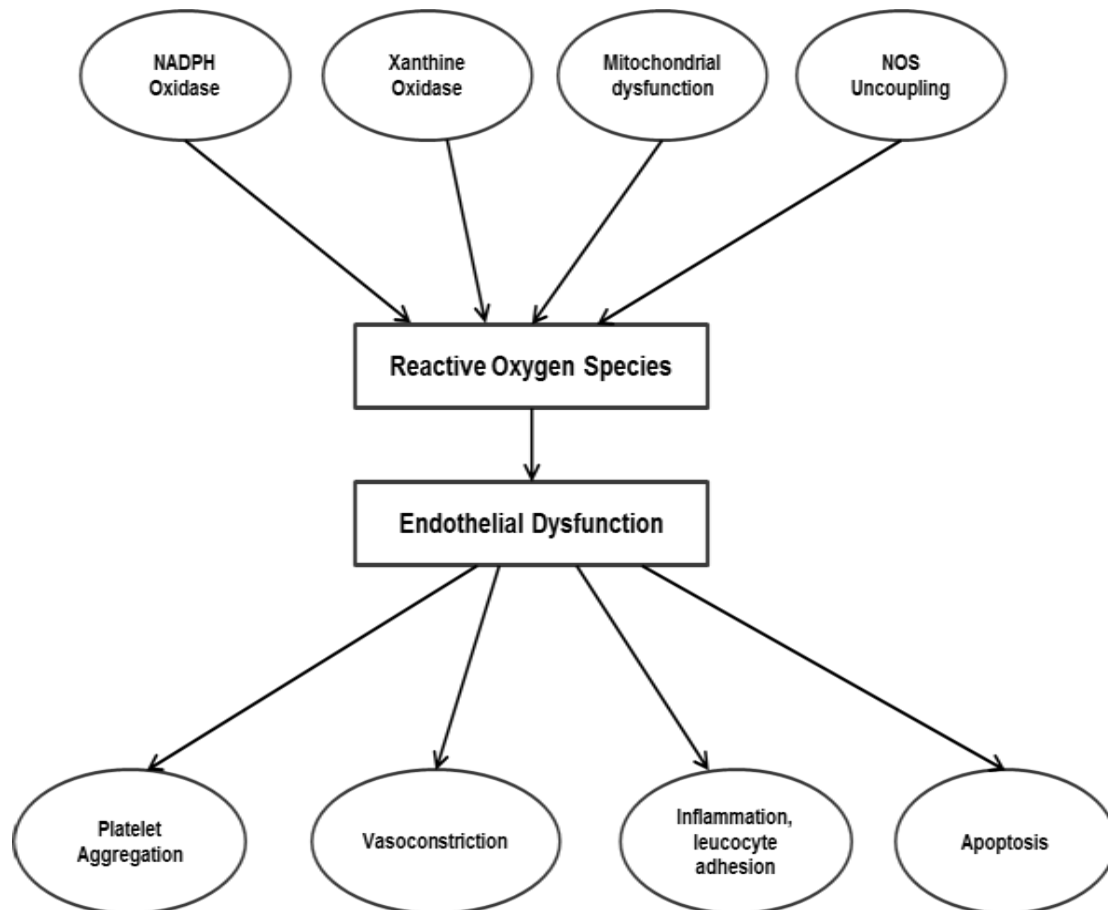


Figure 1.2 Sources of reactive oxygen species (ROS) and consequences on endothelial function

The various enzymatic systems listed above generate ROS from molecular oxygen (O_2). A single electron reduction of O_2 leads to the formation of superoxide (O_2^-) while a two-electron reduction leads to the formation of hydrogen peroxide (H_2O_2). Further, these ROS react with lipids and form active lipid radicals (Kyaw *et al.*, 2004) and may cause endothelial dysfunction. One consequence of this is altered NO bioavailability due to inactivation by superoxide anion (O_2^-) forming peroxynitrite ($ONOO^-$) leading to endothelial dysfunction, vasoconstriction, platelet aggregation, and apoptosis (Cai & Harrison, 2000).

1.2.2.1 Nicotinamide adenine dinucleotide phosphate (NADPH) oxidase family

The NADPH oxidase family consists of different enzymes such as NOX1, NOX2, NOX3, NOX4 and NOX5. These enzymes exhibit differences in their activity and localisation. NOX1 is highly expressed in vascular smooth muscle cells whereas NOX2 is present in neutrophils. NOX3 is highly expressed in vestibular system and produces low levels of superoxide (Bedard and Krause, 2007). NOX4 is generally expressed in all cardiovascular cell types and NOX5 is predominantly found only in humans. All these enzymes play an important role in the pathophysiology of several cardiovascular diseases as they are a major source of ROS and modulate key redox sensitive signalling pathways that regulate growth, proliferation, migration and differentiation. Their expression in macrophages is believed to dictate a critical role in atherogenesis (Guzik *et al.*, 2000) and oxidized LDL itself stimulates NADPH oxidase and facilitates the production of O_2^- , which inactivates NO (Bae *et al.*, 2009). NOX enzymes mediate diverse functions through redox signalling. Vascular NOX generate ROS which is useful in regulating blood pressure and regular cardiovascular health. However the excessive ROS generated will reduce the bio-availability of NO, which then affects the blood pressure as NO regulates the flow of blood (Panday *et al.*, 2015). The p22^{phox}-dependent NOX2 is involved in the activation of nuclear factor kappa B (NF- κ B) and inducible nitric oxide synthase (iNOS) through the proliferation and differentiation of smooth muscle cells (Piao *et al.*, 2005). NOX2 is also known to involve in the angiotensin II signaling and thus play a role in normal functioning of central nervous system. Out of different sources of ROS generation, NOX generated O_2^- has been associated with atherosclerosis. It causes the production of cell adhesion molecules in the vascular endothelium and thus contributes in atherogenesis (Ushio-Fukai *et al.*, 2002).

1.2.2.2 Xanthine Oxidase

During the metabolism of purine, involves the molybdoenzyme, xanthine oxidoreductase that catalyses of oxidation of hypoxanthine and xanthine. Xanthine oxidoreductase is present in two inter-convertible forms, either as xanthine dehydrogenase or xanthine oxidase. Xanthine dehydrogenase involves the reduction of NAD^+ , whereas xanthine oxidase leads to the production of both O_2^- and H_2O_2 in the presence of molecular oxygen (Hajjar & Leopold, 2006). Interestingly, xanthine oxidase appears to be regulated by interferon- γ , which enhances the activity of the enzyme in endothelial cells, strongly implicating a role for inflammation associated with cytokines in atherosclerosis (Dupont *et al.*, 1992). The dysregulation of the enzyme results in impaired vascular function and cardiovascular diseases. Also it inhibits the NO synthase thus reducing the levels of NO. Xanthine oxidase induced oxidative stress in the endothelium triggers the pathogenesis of endothelial dysfunction thus contributing to atherosclerosis. An increase in the xanthine oxidoreductase activity is associated with infarction. Also NADPH and xanthine oxidase are known to be interrelated as one activates the other (Battelli *et al.*, 2014).

1.2.2.3 Mitochondrial generation of reactive oxygen species (ROS)

Mitochondria are the most important source of ROS formation. The damage to the mitochondria in various pathologies is associated with ROS production within the mitochondria (Murphy, 2009). They provide energy to the cell by generating adenosine triphosphate (ATP) through oxidative phosphorylation. This occurs when electrons are transmitted from NADH to molecular oxygen (Murphy, 2009) through a complex of electron transport carriers that include complex I (NADH-ubiquinone oxidoreductase), complex II (succinate-ubiquinone oxidoreductase), complex III

(ubiquinol-cytochrome c reductase), and complex IV (cytochrome c oxidase). More than 98% of electrons are coupled to form ATP whereas the rest leaks out to form O_2^- . However mitochondria contain mitochondrial superoxide dismutase (MnSOD), which neutralises O_2^- . Under pathological conditions the electron transport chain is uncoupled leading to disruption of MnSOD thereby resulting in increased O_2^- production (Sena *et al.*, 2012).

1.2.2.4 Uncoupling of Nitric Oxide Synthases

Nitric oxide synthase derived NO is a potent inhibitor of platelet aggregation and adhesion. It is the most anti-atherogenic defence principle in the vasculature. However NOS can generate O_2^- instead of NO under pathological conditions. The enzymes transfer electrons from the heme group to the substrate L-arginine to form L-citrulline and NO. 5, 6, 7, 8-tetrahydrobiopterin (BH_4) is used as a cofactor in this development. However, decrease in the availability of either BH_4 or L-arginine may uncouple the enzymes resulting in the generation of O_2^- instead of NO (Madamanchi *et al.*, 2005; Roe and Ren, 2012). The O_2^- generated may alter the activity of NOS and react with NO to form $ONOO^-$ which has the ability to oxidize BH_4 to BH_3 resulting in a decrease in BH_4 and hence uncoupling of NOS. Importantly, NOS uncoupling is also common not only in the manifested atherosclerotic state but also in other conditions considered risk factors for atherosclerosis. In this regards, uncoupled eNOS has been seen in patients with endothelial dysfunction that has resulted from conditions such as diabetes mellitus, hypercholesterolemia or essential hypertension (Moens *et al.*, 2008). These consequences reflect the importance of NO under normal physiological conditions, which may be compromised in disease states.

1.3 Antioxidants

Under normal physiological conditions, cells are capable of neutralizing the reactive oxygen species produced with the help of antioxidants. Endogenous cellular antioxidant defences are primarily enzymatic that include superoxide dismutase, catalase and glutathione peroxidase. Superoxide dismutase is present locally in the cytosol and mitochondria and helps in catalysing the reduction of superoxide anion to H_2O_2 and water. Glutathione peroxidases are located in the cytosol and mitochondria and helps in eradicating the majority of H_2O_2 whereas catalase, located in peroxisomes, is responsible for neutralizing high levels of H_2O_2 . Non-enzymatic antioxidants such as vitamin E, vitamin C, β -carotene, coenzyme Q and glutathione act by quenching reactive oxygen species. When the redox balance is altered towards cellular oxidants, oxidative injury to lipids and proteins occur and results in reduced cell viability and modification of cellular function (Lu *et al.*, 2010). The intracellular redox state is assessed by the relative amounts of oxidized and reduced form of each redox pair. Reactive oxygen species therefore are considered as important parameter in evaluating the redox state of the cell and establish a mechanism whereby it modifies the protein conformation and function and regulation of signal transduction.

The redox systems normally found within the cells comprise nicotinamide adenine dinucleotide phosphate, thioredoxin, glutaredoxin, and glutathione. Amongst these, glutathione serves as a principal antioxidant to maintain overall cellular redox balance because the cellular glutathione concentration is 500 to 1000-fold higher than the other redox regulating proteins. Whenever there is a discrepancy in the ratio of

reduced to oxidized glutathione, it directly reflects the imbalance in intracellular redox state (shih *et al.*, 2007). The importance of glutathione is not only based on its abundance but also its ability to counteract H₂O₂, lipid hydroperoxides mainly as a co-factor of enzymes such as glutathione peroxidase or glutathione-S-transferase (GST). Various pathologies have been associated with decreases in the levels of glutathione.

In mammalian cells, glutathione is the most abundant low molecular weight thiol present in both the reduced (GSH) and oxidized (GSSG) forms. The GSH is 10 to 100 fold greater than the GSSG. An upsurge in the levels of intracellular GSSG can be a result of the breakdown of H₂O₂ by glutathione peroxidase. As the concentrations of GSSG in the cell are usually minimal, even minor oxidation of GSH to GSSG can affect substantial elevated levels of intercellular GSSG. The NADPH-dependent glutathione reductase as well as thioredoxin/glutaredoxin system are capable of reducing the oxidized form of glutathione to GSH. Antioxidant enzymes such as GSH peroxidase, using GSH as a cofactor, neutralize peroxides including membrane lipids peroxides formed as a result of oxidative insult. Also GSH peroxidase in the presence of GSH can protect the biological molecules, proteins from free radical burst (Mezzetti *et al.*, 1990).

1.3.1 Superoxide Dismutase (SOD)

Another important antioxidant enzyme is superoxide dismutase (SOD), which is present in all oxygen-metabolizing cells (Gregory *et al.*, 1974) and catalyzes the destruction of oxygen free radical or superoxide anion. This enzyme therefore plays a critical role in reducing OS and its consequences in atherosclerosis and other life-

threatening diseases. The reaction involves the dismutation of superoxide into oxygen and hydrogen peroxide. It acts as the first line of defense and neutralizes the superoxide anions through successive oxidative and reductive cycles of transition metal ions at its active site.



The critical mechanism to prevent the endothelial dysfunction caused by O_2^- is the activity of SOD in the vessel wall. The SOD regulates the bioactivity of NO as O_2^- reacts with NO reducing its bioavailability. Therefore it acts as a balance between the O_2^- and NO and thus maintaining its bioavailability. The important SOD is the extracellular SOD which protects the endothelium derived NO because of its location. Another important SOD is the mitochondrial SOD which neutralizes the generation of O_2^- within the mitochondria during electron transport (Fukai *et al.*, 2002).

1.3.2 Catalase

Catalase is another major antioxidant enzyme and is present in all living organisms. It is encoded by a single gene and is found pre-dominantly in the liver, kidneys and erythrocytes. It is mainly located in the peroxisomes within the cell. It catalyzes the decomposition of H_2O_2 to water and oxygen thus protecting the cell from oxidative damage. The activity of catalase is very high and rapid as it is effective even at low concentrations. In this regard, one molecule of enzyme can convert millions of H_2O_2 molecules to water and oxygen each second and is therefore very effective in converting H_2O_2 to less harmful products, thus preventing deleterious effects to biological systems.



The overexpression of catalase was shown to inhibit ox-LDL in human aortic endothelial cells as H₂O₂ was known to involve in the production of ox-LDL (Yang *et al.*, 2004).

1.3.3 Heme oxygenase-1 (HO-1)

Heme oxygenase-1 (HO-1) is an enzyme produced under stress and involved in catalyzing the degradation of heme to biliverdin, simultaneously releasing iron and carbon monoxide (CO). Heme oxygenase-1 acts as an antioxidant protection system within the cell during oxidative insult through the antioxidant actions of biliverdin and its metabolite, bilirubin, and anti-inflammatory action of CO. It plays a vital role in cellular antioxidant defense and, particularly, in vascular protection (Abraham & Kappas, 2008).

Heme oxygenase was first extracted from rat liver and pig and bovine spleen and was found to have a molecular mass of 32KDa. The two isoenzymes of HO were referred to as HO-1 and the second HO-2. Heme oxygenase-2 having a molecular mass of 34KDa is constitutively expressed whereas HO-1 can be induced using various pharmacological agents and under circumstances such as heat shock and cellular stress (Cruse & Maines, 1988). In whole animal tissues, when treated with its natural substrate heme as well as various metals, xenobiotics, endocrine factors and synthetic metalloporphyrins, the activity of HO-1 is elevated. Hence it might be possible HO-1 induction is the vital process that occurs following

some acute reactions and cellular protection after injury. Heme oxygenase-1 facilitates the elimination of potentially toxic pro-oxidant molecule heme and generates metabolites with antioxidant properties such as CO, bilirubin and biliverdin. Thus, CO and bilirubin are important for the protection caused by HO-1 (da silva *et al.*, 2001).

Figure 3 shows the metabolism of heme to biliverdin and then to bilirubin, which regulates the cellular redox. Bilirubin inhibits NADPH oxidase and Protein-Kinase C (PKC) activity that mediates angiotensin II induced vascular injury. Bilirubin is also linked to OS reduction in experimental model of diabetes by raising the bioavailability of NO essential for endothelial cell integrity.

The possible mechanism by which HO-1 mitigates the diabetes facilitated free radical production and uncoupling of eNOS might be through the inhibition of NADPH and PKC by bilirubin. Glucose increases the levels of O_2^- , which therefore interacts with NO leading to the vascular accumulation of $ONOO^-$. Peroxynitrite further inactivates the NOS cofactor BH_4 to dihydrobiopterin. As a result of this inactivation, NOS enzyme is uncoupled accelerating the production of O_2^- over NO (Milstien & Katusic, 1999).

Also bilirubin through its anti-inflammatory and anti-oxidative properties can increase tolerance to islet allograft (Wang *et al.*, 2007; Lee *et al.*, 2007). These properties, along with its inhibition of proliferation of smooth muscle cells (Ollinger *et al.*, 2005), might constitute the underlying mechanism for its positive effect in the treatment of atherosclerosis. Indeed, atherosclerosis progression was reduced in patients with

high normal levels of bilirubin when compared with that in individuals with low normal levels (Ollinger *et al.*, 2007).

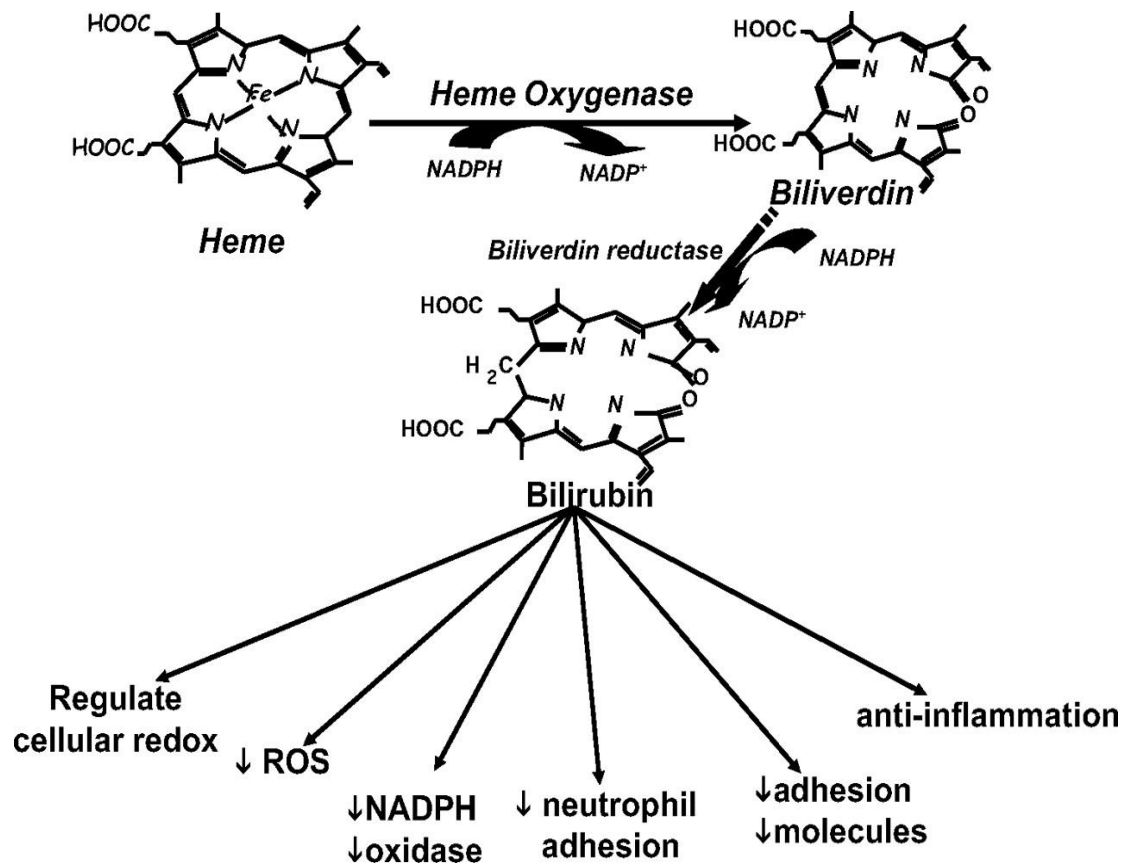


Figure 1.3 Metabolism of Heme and its properties

1.3.4 Nuclear factor erythroid 2-related factor-2 (Nrf-2)

The redox sensitive transcription factor nuclear erythroid 2-related factor 2 (Nrf-2) plays a crucial role in the cellular defense against OS. Nrf-2 is sequestered in the cytosol along with Kelch-like ECH associated protein 1 (Keap 1), a cytoskeletal protein that anchors and represses its transcriptional activity (Alfieri *et al.*, 2011). Keap1 is sensitive to oxidative and electrophilic stress and promotes rapid

degradation of Nrf2. Electrophilic agents or ROS interacts with Nrf2-Keap1 complex and dissociates the complex thus enabling nuclear translocation of Nrf-2. The dissociation of Nrf2-Keap1 complex may be attributed to the alterations in the structure of Keap1 and phosphorylation of serine/threonine residues in Nrf2. The main mechanism for the molecular basis of Nrf2 activation is the oxidation of redox-sensitive cysteines within Keap1 (Tong *et al.*, 2007). The antioxidant effects of Nrf2 through the induction of phase II defense enzymes is regulated by the antioxidant response elements (ARE) in the promoter region of target genes. Nrf2 interacts with ARE and regulates the expression of detoxifying enzymes such as glutathione synthase transferase (GST), HO-1, and NQO1 (Mann *et al.*, 2009). It serves as an important transcription factor in the cytoprotection of tissues against electrophiles and ROS. When the blood flow turns to oscillatory from laminar, shear stress is induced in the vascular wall leading to NO inhibition and superoxide production. This promotes the pathogenesis of atherosclerosis. During this process Nrf2 is suppressed and thereby stimulates proatherogenic environment contrary to its anti-atherogenic effects when the blood flow is laminar (Howden, 2013). Nrf2 is ubiquitously expressed and modulates microglial dynamics in the brain and regulates the expression of inflammatory markers and antioxidant enzymes. It also plays a major role in neurodegenerative disorders such as Parkinson's, Alzheimer's and Huntington's disease (Alfieri *et al.*, 2011).

These antioxidant systems, although effective under normal physiology, are often overwhelmed in chronic disease states including atherosclerosis. Under these conditions, it is likely that other processes other than sequestration of free radicals

may prove beneficial. In this regard, NO is emerging as a cardio protective molecule within the vessel wall.

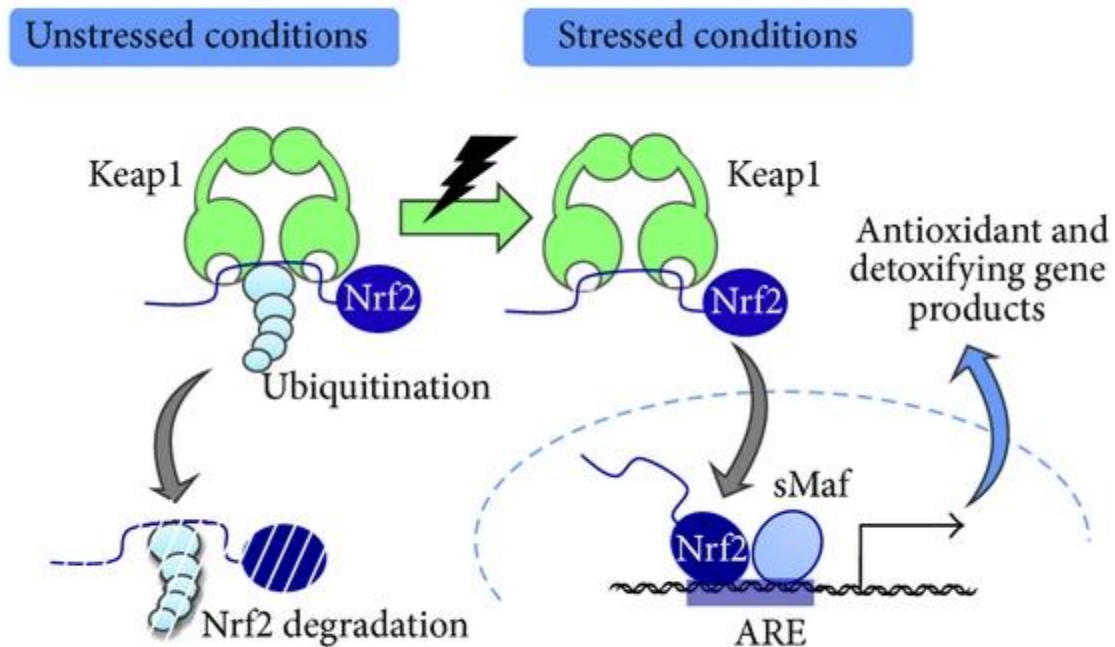


Figure 1.4 Dissociation of Nrf-2 and its function
 (Taken from Kobhayashi *et al.*, 2013)

1.4 Nitric Oxide

Nitric oxide is a ubiquitous molecule naturally found in a range of cell types and organ systems. It is an important signalling molecule, which regulates various physiological and cellular processes in the cells. It was initially termed “Endothelium Derived Relaxation Factor” (EDRF) because of its effect on blood vessel relaxation and vascular tone regulation (Furchgott & Zawadzki, 1980; Chen & Popel, 2009). It has various roles in biological processes including neurotransmission, apoptosis, immune defence and cell motility. Nitric oxide is a key regulator of basal vascular

tone, averts platelet activation as well as cellular proliferation and migration. Nitric oxide also regulates myocardial contractility as well as vascular tone, which have already been mentioned. It is a highly reactive molecule and short lived with a half-life of 3-5 seconds. It is produced by a group of enzymes called NOS of which there are three types: endothelial NOS (eNOS), inducible NOS (iNOS) and neuronal NOS (nNOS) (Vitecek *et al.*, 2012). The NOS enzymes convert arginine to citrulline, producing NO in the process. They utilize reduced nicotinamide-adenine-dinucleotide phosphate (NADPH), flavin adenine dinucleotide (FAD), flavin mononucleotide (FMN), and 5, 6, 7, 8-tetrahydrobiopterin (BH₄) as co-factors (as illustrated in the Figure 4). When there is an increase in intracellular calcium levels, eNOS and nNOS are activated and synthesize NO. The iNOS enzyme is independent of calcium and therefore unaffected by a change in intracellular calcium levels (Ding & Vaziri, 1998).

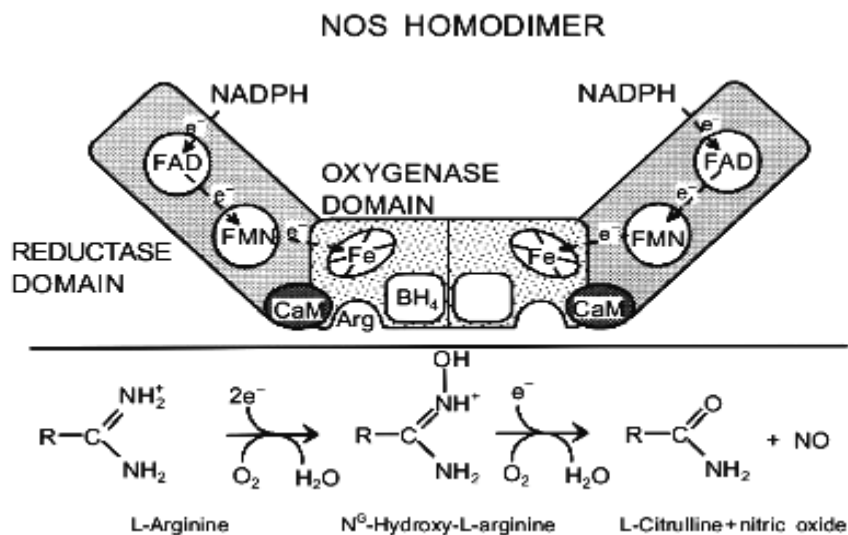


Figure 1.5 Synthesis of Nitric Oxide (NO) by the NOS enzyme (Taken from Gorren and Mayer, 1997).

Nitric oxide released from L-arginine diffuses to smooth muscle cells where they stimulate soluble guanylate cyclase thereby causing enhanced synthesis of cyclic GMP from guanosine triphosphate. The surge in cyclic GMP in smooth muscle cells results in their relaxation (Garcia & Stein, 2006). Nitric oxide also has many beneficial effects, which accounts for various physiological functions. These effects are seen at low physiological concentrations where NO exerts several protective functions in the cardiovascular system, including the regulation of cardiac contractility, inhibition of smooth muscle cell proliferation, inhibition of platelet aggregation, suppression of monocyte adhesion to the endothelium and inhibition of expression of vascular cell adhesion molecule 1 (VCAM-1) and inactivation of nuclear factor kappa B (NF- κ B), which all play a prominent role in atherosclerosis. Thus, reduced bioavailability of NO has therefore been implicated in the pathogenesis of atherosclerosis (Prasad *et al.*, 1999). In contrast, excess amounts of NO may be detrimental and in the presence of O_2 or O_2^- forms $ONOO^-$ which, as already mentioned, is highly reactive and exerts a multitude of deleterious effects including apoptosis and pathogenesis of myocardial infarction, diabetes, chronic inflammatory diseases etc. In this regard, NO derived from iNOS is considered pathological and has until recently been related with the pathogenesis of diseases such as atherosclerosis associated with OS which is discussed further below (See section 1.4.4).

1.4.1 Endothelial Nitric Oxide Synthase (eNOS)

Endothelial nitric oxide synthase or NOS3 is the predominant isoform present in the vasculature. It is mostly expressed in endothelial cells. It is constitutively expressed and activated by G-protein coupled cell surface receptors or by shear stress and

stretch. It requires increases in levels of intracellular calcium that can be induced following receptor activation. This in turn increases the activation of calmodulin and hence its binding to and activation of eNOS. The activity of eNOS could be regulated by a range of co-factors and by its intracellular localization as it facilitates optimal coupling of extracellular stimulation of NO (Frutos *et al.*, 1999). It plays a crucial role in the regulation of vascular tone and preserving vascular integrity. Under physiological conditions eNOS may generate low levels of NO, which may regulate the physiological processes already identified above, and include not only vascular tone but also platelet aggregation and cell migration and proliferation.

1.4.2 Neuronal Nitric Oxide Synthase (nNOS)

Neuronal nitric oxide synthase or NOS1 was one of the first isoforms to be purified and cloned. It is mainly expressed in neuronal tissues. As with eNOS, its activity is regulated by calcium and calmodulin and has been implicated as an important enzyme for synaptic signalling events. The NOS1 enzyme has been implicated in vital physiological functions such as learning and memory (Zhou & Zhu, 2009). Its inhibition in the medulla and hypothalamus can lead to systemic hypertension (Forstermann & Sessa, 2012).

1.4.3 Inducible Nitric Oxide Synthase (iNOS)

Inducible nitric oxide synthase or NOS2 is not normally expressed in cells but can be transcriptionally stimulated by bacterial lipopolysaccharides and cytokines (Figure 5). Typically iNOS is induced in response to cellular stress and produces 100-1000 fold more NO than eNOS and nNOS. Once expressed the enzyme is

constantly active and is not affected by intracellular calcium fluxes. It produces copious amounts of NO for comparatively long periods of time (Leifeld *et al.*, 2002).

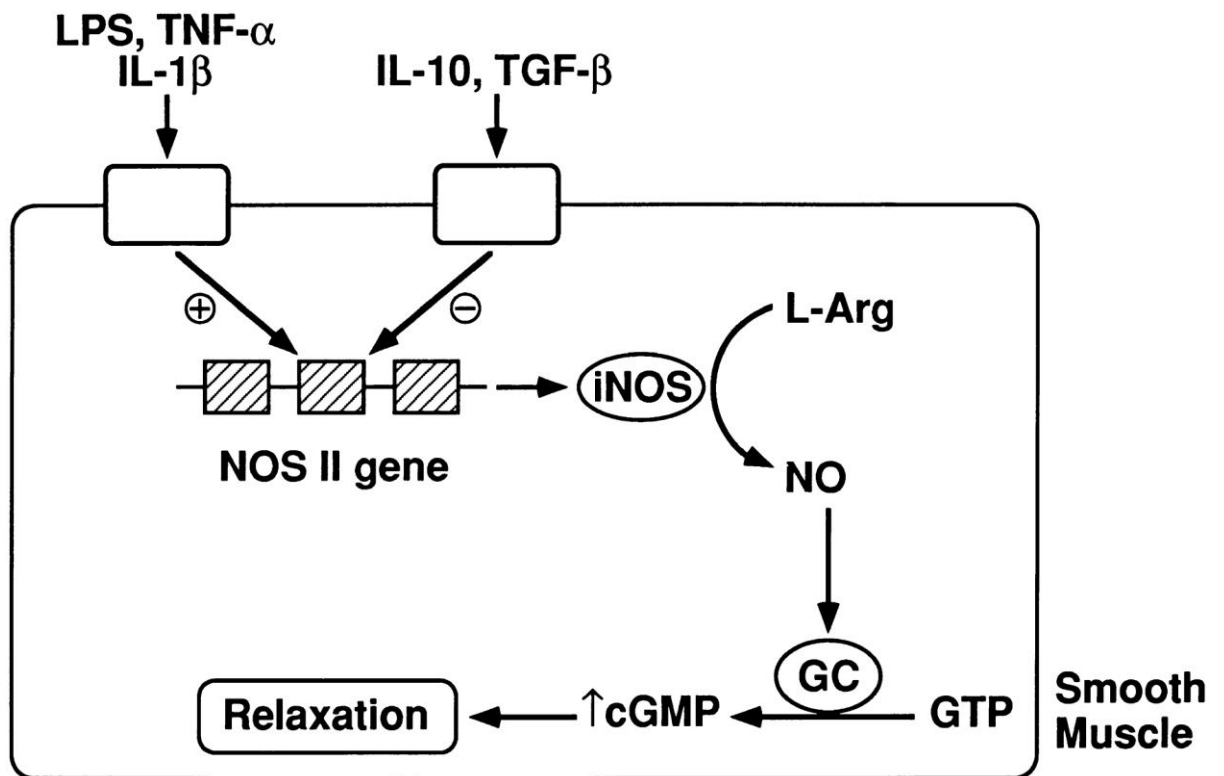


Figure 1.6 Schematic representation of iNOS gene expression and function(Taken from Faraci and Heistad, 1998)

The role of iNOS is complex and controversial and may mediate different aspects of cardiovascular pathologies. The enzyme was initially identified and characterized in macrophages; but it is now expressed in several cell types including endothelial cells, fibroblasts, vascular smooth muscle cells and cardiac myocytes. The iNOS acts as a catalyst and its action is controlled through the availability of calmodulin,

L-arginine and the co-factors, NADPH and tetrahydrobiopterin (as shown in figure 5). Its expression and function has been implicated in a multitude of pathological conditions.

1.4.4 Pathology of the inducible nitric oxide synthase and its implications

In contrast to constitutive NO production, excess production of NO by iNOS may be pathologically relevant in several disease states including the pathogenesis of atherosclerosis. This is supported by the fact that its expression can be induced by inflammatory cytokines associated with the disease state (Channon *et al.*, 2000). The iNOS induced overproduction of NO has also been put forward as a major mechanism by which cytokines exert cardiac contractile dysfunction and initiate cardiovascular disease. In a rabbit infarction model, treatment with specific NOS2 inhibitor greatly improved ventricular function and also improved myocardial blood flow indicating adverse tissue damaging effects of iNOS derived NO production. Furthermore, after cardiac transplantation, iNOS expression correlated with contractile dysfunction in myocytes and vascular smooth muscle cells. Increased production of NO by iNOS may also result in vasodilation during endotoxin and cytokine induced shock (Kiang, 2004); and may similarly contribute to various other diseases such as rheumatoid arthritis (RA; Jarvinen *et al.*, 2003), multiple sclerosis (MS; Hill *et al.*, 2004), Alzheimer's disease (Abd-El-Aleem *et al.*, 2008) and Parkinson's disease (Kavya *et al.*, 2006). In the synovial fluid of RA, NO levels were detected at 6 to 35 fold higher than normal. In the demyelinating lesions of MS, staining of iNOS and nitrotyrosine, a product formed during nitrosative stress, was also detected. When these cells were isolated and cultured *invitro*, a high output of nitric oxide was seen. The expression of iNOS has also been observed in

chronic inflammatory ailments of the airways, the vessels, the bowels, the kidney, the heart and the skin(Kroncke *et al.*, 1998).

During chronic inflammatory conditions, there is increase in the expression of iNOS thus accumulating high levels of NO that can cause DNA damage through its reactive intermediates, which are mutagenic. Recent studies also associate NO as being a key signaling molecule that promotes tumorigenesis, with amplified expression of iNOS involved in tumors of the colon, lung, oropharynx, reproductive organs, breast, and central nervous system (CNS). Moreover, uncontrolled iNOS activation in resident macrophages and smooth muscle cells results in excess production of ONOO⁻, which is pro-atherogenic and pro-thrombogenic and a source of constant nitrosative stress, which is detected abundantly in atherosclerotic lesions in the form of nitrotyrosine. Prolonged stress over a period of time results in atherogenesis especially in those individuals with poor anti-oxidant defence mechanisms. Peroxynitrite could also induce the expression of metalloproteinase in the vascular interstitium that induce atherosclerotic plaque rupture and myocardial infarction (Baker *et al.*, 1999). Moreover, iNOS co-localizes with poly-(ADP-ribose)-polymerase-1 within vascular smooth muscle cells of atherosclerotic human aorta. Poly-(ADP-ribose)-polymerase-1 localizes within the nuclei of smooth muscle cells in the lesions. Hence it causes change in the morphology of mitochondria resulting in considerable damage leading to the deterioration of the condition. This shows the significant role of iNOS and poly-(ADP-ribose)-polymerase-1 in atherosclerotic lesions of humans (Perrotta *et al.*, 2011).

In contrast to the strong argument above for a pro-atherogenic role for iNOS, recent studies have indicated that this isoform may in fact be cardio protective. For instance, it has been reported that iNOS-induced NO has anti-atherogenic effects as it improves endothelial dysfunction, maintains plaque stability and prevents platelet aggregation (Lirk *et al.*, 2002). Additionally, iNOS-induced NO may also prevent cell-mediated oxidative modification of LDL (Buttery *et al.*, 1996) and *in vivo*, attenuate the extent of the atherosclerotic lesion induced by immune injury, as well as protect against OS-induced apoptosis (Rikitake *et al.*, 1998). Moreover, overexpression of this enzyme is reported to reduce infarct size (Arnaud *et al.*, 2001).

Inducible nitric oxide synthase derived NO plays a crucial role as a cardio protective molecule in ischemia/reperfusion injury. Inhibition of iNOS uncoupling, which is instigated by OS, results in reduced infarct size and improved functioning of the left ventricle (Okazaki *et al.*, 2011; Ma *et al.*, 2014). This suggests that contrary to its reported deleterious actions in atherosclerosis, iNOS may in fact protect against the disease development and reduce its subsequent adverse effects. This would however be contradictory to the reported pro-atherogenic effects of iNOS mediated via the formation of ONOO⁻ in the atherosclerotic lesions (Modlinger *et al.*, 2004). As a hypothesis, it is therefore potentially possible that OS may play a major role in shielding the protective functions of iNOS mediated NO release and instigates damaging effects leading to progression of the disease. In this context, iNOS induced NO may alternatively be cardioprotective (Goetzenich *et al.*, 2014) and beneficial rather than deleterious in humans.

1.5 Statins and their role in atherosclerosis

Statins are one of the most extensively prescribed drugs in the United Kingdom and are consumed by almost eight million Britons. They are a class of drugs that are responsible for lowering the levels of cholesterol produced in the liver, exerting this effect by inhibiting the activity of the rate limiting enzyme 3-hydroxy-3-methyl glutaryl co-enzyme A reductase (HMG CoA reductase) and are therefore also referred to as HMG-CoA reductase inhibitors (Wierzbicki *et al.*, 2003). The HMG-CoA reductase catalyzes the reduction of 3-hydroxy-3-methyl glutaryl co-enzyme A (HMG-CoA) to mevalonate, which is the rate-limiting step in hepatic cholesterol biosynthesis thereby inhibiting *de novo* cholesterol synthesis. In addition, they increase the expression of LDL receptors, which are involved in the uptake of LDL. They also cause a reduction in triglyceride levels and a minor increase in high-density lipoproteins (HDL) cholesterol (Nicholls *et al.*, 2014).

In terms of the consequences of their action, statins prevent advancement of atherogenesis by reducing plaque progression. They also act by inhibiting the oxidation of LDL through preservation of the activity of anti-oxidant system and may lower inflammation along the walls of the arteries. Statins also constrain isoprenylation of key proteins involved in oxidant/anti-oxidant-generating pathway thus producing anti-oxidant effects (Shishehbor *et al.*, 2003). In this regard, statin therapy has been shown to suppress O_2^- formation and thus enhanced NO generation through inhibition of isoprenylation of Rac and Rho. Rac is present within the NAD(P)H oxidase complex of both leukocytes and vascular cells. Statins promote the inhibition of Rac isoprenylation, thereby inhibiting its translocation to membranes and hence suppression in O_2^- formation in cultured cells.

Rho is a small GTPase that regulates signaling within the cell. Studies reveal that inhibition of Rho isoprenylation in endothelial cells resulted in greater NO production, presumably due to enhanced stability of eNOS mRNA half-life (Rikitake & Liao, 2005). Furthermore, they weaken the progression of atherosclerosis by retarding the vascular smooth muscle cell proliferation and migration and hence inhibit plaque development and new lesion formation (Stancu & Sima, 2001; Mason, 2003).

The non-lipid effects of statins include increase in NO bioavailability through preventing its oxidative inactivation by O_2^- radicals and by up-regulation, activation and stabilization of eNOS (Kolyada *et al.*, 2001; Ma & Ma, 2014). Statins also exert their non-lipid effects through inhibition of OS, anti-thrombotic actions, regulation of angiogenesis, anti-inflammatory effects, decrease in secretion of metalloproteinase and attenuation of endothelial dysfunction (Lahera *et al.*, 2007; Agouridis *et al.*, 2015). These so called pleiotropic effects are independent of the inhibition of intracellular cholesterol biosynthesis and are secondary to the inhibition of the synthesis of isoprenoid intermediates of mevalonate pathway, such as farnesylpyrophosphate (FPP) and geranylgeranylpyrophosphate (GGPP). These non-lipid actions contribute to the clinical benefits of statins in cardiovascular diseases (Szyguta-Jurkiewicz *et al.*, 2014; Agouridis *et al.*, 2015).

Statins exert its effects through various pathways and one of those appears to be the regulation of the activity of the enzyme cholesteryl ester transfer protein (CETP), which transfers cholesteryl ester to very-low-density lipoprotein (VLDL) and LDL. Most of the studies emphasize that simvastatin and pravastatin inhibit the activity of plasma CETP in normo-lipidemic individuals and also in patients enduring different

kinds of hyperlipoproteinemia. The mechanisms of these effects are unidentified but might facilitate effects outside of lipid metabolism (Kuivenhoven *et al.*, 1998).

Recent studies reveal another novel lipid-independent pleiotropic effect of statins, which is distinct to their inhibitory potential on HMG-CoA reductase. It might exert an anti-inflammatory effect by binding to a specific site of the lymphocyte function associated antigen-1 (LFA-1) on leukocytes. This selective binding prevented any adhesion to LFA-1. These additional properties of statins suggest considerable cardiovascular beneficial properties of these drugs in both normal and hypercholesteromic individuals that go beyond their cholesterol lowering actions. However there is a need for more studies to appreciate the clinical relevance of the non-lipid lowering properties of statins in humans (Weltz-Schmidt *et al.*, 2001).

Oxidised LDL has high affinity and bind to extracellular matrix which promotes inflammation as well as chemo taxis of monocytes. The latter once trapped in the intima form macrophages, which engulf oxLDL to form foam cells that are part of the atherosclerotic lesions, and also activates NF- κ B (Nakata *et al.*, 2007). Statins prevent the oxidation of LDL and in so doing reduce the formation of oxLDL and decrease O_2^- anion production thereby producing beneficial effects in atherosclerosis. Statins also decrease the levels of oxLDL either by decreasing LDL levels or by increasing HDL production. NADPH oxidases are the important source of O_2^- . They inhibit oxLDL-induced NADPH oxidase expression and as a result suppress O_2^- anion production (Wong *et al.*, 2006). In a previous project in our laboratory, statins were found to reverse the suppression of iNOS expression and NO production

caused by pro-oxidants in LPS and IFN- γ activated smooth muscle cells (unpublished observations). Interestingly, this effects which may be beneficial in controlling the development and/or progression of atherosclerosis was selective to certain statins (eg atorvastatin) and not others (eg pravastatin). Thus, although all these effects make statins an important class of drugs for treating coronary artery disease, there is yet a lot more required in order to understand the multitude of effects they exert. In particular it is important to understand how these drugs regulate iNOS expression and what the relevance of this is in OS associated with cardiovascular diseases such as atherosclerosis. This is being addressed in part in this thesis.

1.6 Aims and Objectives

The main aim of this thesis is to extend initial observations showing that iNOS expression and function may be regulated under conditions of OS by exploring the underlying mechanism through which this may be mediated. In particular, the studies aim to establish whether suppression of iNOS expression is dependent on the species of free radical generated and further identify the signalling pathway through which this may occur. Additionally, parallel studies will examine the effects of select statins on OS induced changes in iNOS expression and NO production as well as the mechanisms that may be associated with the actions of the selected statins.

2.0 MATERIALS AND METHODS

2.1 Cell culture materials and methods

2.1.1 Preparation of media required for culturing of cells

2.1.1.1 Cell culture medium: Freshly prepared complete culture medium was used for culturing and sub culturing of cells. Complete culture medium was prepared by supplementing Dulbecco's modified Eagle's medium (DMEM) (Fisher scientific, UK) with 10% Foetal bovine serum (FBS) (Fisher scientific, UK), 100 U/ml penicillin and 100 µg/ml streptomycin (Fisher scientific, UK). DMEM contains essential nutrients and vitamins, FBS provides serum supplement, which promotes the growth and proliferation of cells in culture.

2.1.1.2 Phosphate buffered saline (PBS): Sterile 1x phosphate buffered saline (PBS) was prepared from 10x stock solution (Invitrogen, UK) by 1 in 10 dilutions in autoclaved double distilled water (DDW).

2.1.1.3 Trypsin: Sterile 1x trypsin was prepared from 10x stock solution (Invitrogen, UK) by diluting 1 in 10 in sterile 1x PBS so that the final concentration of the solution contains 0.05% trypsin.

Once prepared, all the above solutions were stored at 4⁰C and used within 3 months from the date of preparation.

2.1.2 Isolation and culture of rat aortic smooth muscle cells

Rat aortic smooth muscle cells (RASMCs) were used for the experiments. Culture conditions for the isolation of these cells from male Sprague-Dawley rat aorta were optimised. The protocol used has been developed from that described previously by Wileman *et al.*, (1995). Aorta was collected in complete culture medium and taken into the tissue culture hood. The aorta was cleaned by washing away blood clots and removing connective tissue attached to the vessel before cutting open to expose the endothelium. A scalpel blade was used to remove the layer of endothelial cells and was separated into 2 pieces. Then the aorta was cut into 2mm sections and 4-5 explants were placed in each T-25 flask endothelium face down. The flasks were then incubated in the upright position for 5 hours in a cell culture incubator gassed with 5% carbon dioxide at 37°C to allow the explants to attach to the surface of the plastic. Each flask was subsequently placed horizontally and a further 5ml of complete culture medium was added to the flask and incubated for 5 days, during which cells migrated from the tissues.

2.1.3 Maintenance of cells in culture

Once isolated, cells were maintained in culture in complete culture medium until confluent. When the cells became confluent, they were trypsinized and transferred into a new flask as explained in section 2.1.4. During the growth period of the cells, the medium in the flask was replenished every two days and the cells were used for experiments from passage 3 to 6.

2.1.4 Trypsinization of cells

Trypsinization of cells was carried out when cells were 80-90% confluent to ensure they were maintained in a healthy viable state. Briefly, the medium was removed from the T-75 flask by aspiration and the monolayer of cells was washed 3 times with 10ml of 1xPBS. 5ml of trypsin was then added to the cells and the flask gently swirled for 5 seconds. Excess trypsin was removed from the flask by aspiration leaving just about 0.5ml. The flask was then tapped gently on the sides until the cells were detached. Complete culture medium was added to the cell suspension to inactivate the trypsin. This process was completed rapidly to ensure that the cells were not exposed to trypsin for too long as this may be toxic and may cause cell death. Finally the cell suspension was diluted for plating as required,

2.1.5 Cryopreservation of cells

Confluent monolayers of cells in T75 flask were washed 3 times with 10ml of 1x PBS and the cells trypsinised as described above. 8ml of complete culture medium was added to the cell suspension and transferred into a centrifuge tube, which was centrifuged at 1100 rpm at 4⁰C for 5 min. The medium was discarded by aspiration without disturbing the pellet which was re-suspended in freezing medium containing 48% DMEM, 40% FBS, 10% dimethyl sulfoxide (DMSO; Sigma-Aldrich, UK) and 2% Penicillin/Streptomycin. The cells in the freezing medium were then transferred into 1ml cryogenic vials and were frozen at -80⁰C for 24 hours using a Mr Frosty before subsequently being transferred into liquid nitrogen for long-term storage.

2.1.6 Cell counting and plating

After centrifugation of cells following trypsinization, the medium was discarded by aspiration and the pellet re-suspended in 5ml of complete culture medium. 20 μ l of cell suspension was added to 20 μ l of 0.4% trypan blue (Fisher scientific, UK) in an eppendorf tube. A 20 μ l aliquot was then loaded into the two sides of a Neuber's chamber and this was placed into the counting port of a Countess™ automated cell counter (Invitrogen, UK). The latter determines total cell count and is also able to distinguish viable and non-viable cells. The amount of live cells available for plating was then determined as shown in the example below:

Chamber A:

Total cells counted = 2.4×10^5 /ml

Live cells = 2.1×10^5 /ml

Viability = 89%

Chamber B:

Total cells = 3.1×10^5 /ml

Live cells = 2.5×10^5 /ml

Viability = 80%

Average of live cells from chambers A and B = 2.3×10^5 /ml

Once counted, the volume of cell suspension required for plating was determined as follows:

Required cells to be plated per well in a 6-well plate = 3.7×10^5 cells

Total cells required per plate: $3.7 \times 10^5 \times 6 = 22.2 \times 10^5$ cells per plate

The amount of average live cells per ml = 2.3×10^5

Therefore to get 22.2×10^5 cells X ml of total cell suspension will be required

Hence $X = 22.2 \times 10^5 / 2.3 \times 10^5 \text{ ml} = \underline{\underline{9.65 \text{ ml}}}$

Thus a volume of 9.65 ml of cell suspension was taken and suspended into a total volume of 18 ml and 3 ml added into each well in a 6-well tissue culture plastic.

2.2 Experimental procedures

2.2.1 Treatment of cells with LPS and IFN- γ :

Once plated, cells were allowed to reach confluency before being activated with bacterial lipopolysaccharide (LPS; 100 $\mu\text{g/ml}$) and interferon-gamma (IFN- γ ; 100 U/ml) and incubated for 24 hours to induce iNOS expression and NO production. After 24hrs incubation, the medium was collected and analysed for NO produced by the Griess assay. The cell monolayer was lysed and used in western blotting for iNOS expression.

LPS (Sigma, UK) was prepared at 10mg/ml and aliquoted in 200 μl amounts, which were stored at -20°C . IFN- γ (Calbiochem, UK) was available at 10,000 U/ml from source and was aliquoted in 50 μl volumes before storing at -80°C .

2.2.2 Treatment of cells with OS inducers

Confluent monolayer of cells in a 24-well tissue culture grade plastic were washed twice with 1x PBS and incubated with diethyl maleate (DEM) (1 μ M, 2.5 μ M, 5 μ M and 10 μ M), hydrogen peroxide (H₂O₂) (50 μ M, 100 μ M, 150 μ M and 300 μ M) or antimycin A (25 μ M, 50 μ M, 100 μ M and 150 μ M) for 30 minutes. The cells were subsequently incubated in complete culture medium alone or medium containing LPS (100 μ g/ml) and IFN- γ (100 U/ml) for a further 24 hours before determining NO produced by the Griess assay. The cell monolayer was then lysed and used for western blotting to determine iNOS expression.

Diethyl maleate (DEM) is a maleate ester produced as a result of formal condensation of both carboxy groups of maleic acid with ethanol. In organic synthesis, it is generally used as a dienophile for diels-alder type cycloaddition reaction. It prevents formation of anti-oxidant glutathione by inhibiting glutathione synthase enzyme (Kaur *et al.*, 2006). As a result there is an increase in the pro-oxidant levels causing deleterious effects. Hydrogen peroxide by comparison is a compound with an oxygen-oxygen single bond and is a colourless liquid having viscosity slightly higher than water. It acts as a major factor in free radical associated aging and has an important role as a signalling molecule in the regulation of numerous biological processes (Romero and Lamas, 2014). Hydrogen peroxide is thermodynamically unstable and readily gets converted to water and oxygen thus leading to the formation of OH⁻ radical. Antimycins represent a group of secondary metabolites resulted from *Streptomyces* bacteria. Antimycin A with an empirical formula C₂₈H₄₀O₉N₂ prevents the oxidation of ubiquinol by binding to the Qi site of cytochrome c reductase during the electron transport chain of oxidative

phosphorylation in the mitochondria. This leads to the disruption of formation of proton gradient through the inner membrane. As a result protons become incapable to stream through the ATP synthase complex resulting in inhibition of ATP synthesis. Instead, a large quantity of toxic free radical superoxide is formed which causes OS. Antimycin A has been extensively used to detect the specific sites of reactive radical species produced in mitochondria isolated from skeletal muscle.

DEM (Sigma-aldrich, UK) was prepared in 50% ethanol at a stock concentration of 50mM and then diluted to give 1 μ M, 2.5 μ M, 5 μ M and 10 μ M in complete culture medium. H₂O₂(Sigma-aldrich, UK) was prepared at 20mM in milli Q water and diluted to 50 μ M, 100 μ M, 150 μ M and 300 μ M in complete culture medium. Antimycin A (Sigma-aldrich, UK) was prepared in 75% ethanol 50mM and diluted to 25 μ M, 50 μ M, 100 μ M and 150 μ M in complete culture medium.

2.2.3 Treatment of cells with OS inducers for free radical generation

50-60% confluent monolayer of cells in a 12-well tissue culture grade plastic were washed twice with 1x PBS and incubated with diethyl maleate (DEM) (1 μ M, 2.5 μ M, 5 μ M and 10 μ M), hydrogen peroxide (H₂O₂) (50 μ M, 100 μ M, 150 μ M and 300 μ M) or antimycin A (25 μ M, 50 μ M, 100 μ M and 150 μ M) for 1min, 5min, 15min, 30min, 1hr, 3hr, 6hr and 24hr. Cells were then washed twice with x1 PBS to remove any traces of medium.

2,7-dichlorofluorescein (Sigma-Aldrich, UK) was dissolved in DMSO at a stock concentration of 10mM and diluted to a working concentration of 20 μ M in x1 PBS. MitoSOX Red (Fisher Scientific, UK) was prepared at a stock concentration of 5mM

in 13µl of DMSO before diluting it to a final concentration of 5µM in Hank's balanced salt solution (HBSS; Fisher Scientific, UK). Cells were incubated with 20µM of 2,7-dichlorofluorescein or 5µM MitoSOX Red for 10 minutes, washed 3 times with x1 PBS with a 5-minute interval between each wash before viewing under the confocal laser scanning microscope.

2.2.4 Treatment of cells with OS inducers and statins

Confluent monolayer of cells in a 24-well tissue culture grade plastic were washed twice with 1x PBS and incubated with atorvastatin (1µM, 3µM, 10µM and 30µM) for 30 minutes before incubating with DEM (1-10µM), antimycin A (25-150µM) or H₂O₂ (50-300µM) for a further 30 minutes. Cells were then incubated in complete culture medium alone or medium containing LPS (100 µg/ml) and IFN-γ (100 U/ml) for a further 24 hours before determining NO produced by the Griess assay. The cell monolayer was then lysed and used for western blotting to determine iNOS expression.

Atorvastatin (Sigma-aldrich, UK) was prepared at the stock concentration of 10mM by dissolving in dimethyl sulfoxide (DMSO; Fisher Scientific, UK) and then diluted to 1µM, 3µM, 10µM and 30µM in complete culture medium.

2.2.5 Treatment of cells with OS inducers and polyethylene glycol-superoxide dismutase (PEG-SOD) or polyethylene glycol-catalase (PEG-catalase)

Polyethylene glycol-superoxide dismutase (Sigma-Aldrich, UK) was prepared at a concentration of 2110 U/ml in de-ionised water and diluted to 500 U/ml in complete culture medium. Polyethylene glycol-catalase (Sigma-Aldrich, UK) was dissolved in de-ionised water at a concentration of 30,000 U/ml and diluted to 500 U/ml in complete culture medium.

Confluent monolayer of cells in a 24-well tissue culture grade plastic were washed twice with 1x PBS and incubated with PEG-SOD (500 U/ml) or PEG-catalase (500 U/ml) for 30 minutes before incubating with DEM (10 μ M), antimycin A (100 μ M) or H₂O₂ (300 μ M) for a further 30 minutes. Cells were then incubated in complete culture medium alone or medium containing LPS (100 μ g/ml) and IFN- γ (100 U/ml) for a further 24 hours before determining NO produced by the Griess assay. The cell monolayer was then lysed and used for western blotting to determine iNOS expression.

2.2.6 Time point analysis of the effects of OS inducers

Confluent monolayer of cells in a 24-well tissue culture grade plastic were washed twice with 1x PBS and activated with LPS (100 μ g/ml) and IFN- γ (100 U/ml) prior to incubation with DEM (10 μ M) or antimycin A (100 μ M) at 5min, 15min, 30min, 1hr, 3hrs, 6hrs, 12hrs, 18hrs and 24hrs post activation with LPS and IFN- γ . NO production was determined by the Griess assay 24hr after incubation with LPS and IFN- γ . The cell monolayer was then lysed and used for western blotting to determine iNOS expression.

2.3 Griess assay

The Griess assay is a spectrophotometric assay which is used to measure nitrite (NO_2^-) levels, one of the two primary stable and non-volatile breakdown products of NO. As NO is unstable it breaks down to NO_2^- and nitrate (NO_3^-). This assay is established on a diazotization reaction initially described by Griess in 1879. It involves a chemical reaction of nitrite with 0.2% N-1-naphthylethylenediamine dihydrochloride (Griess reagent I; Sigma-Aldrich, UK) to form a diazonium salt, which then reacts with 2% sulfanilamide (Griess reagent II; Sigma-Aldrich, UK) in 5% phosphoric acid to form a pink azo dye as shown in figure 6. This assay reveals the levels of nitrite in a diverse range of biological and experimental fluids such as plasma, serum, urine and tissue culture medium.

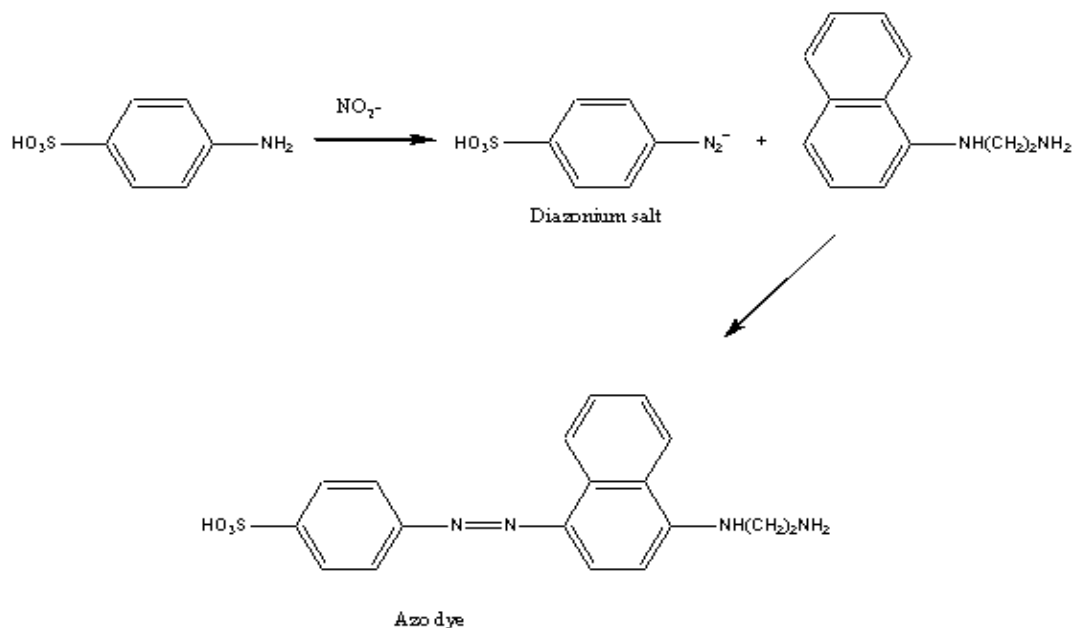


Figure 2.1 Griess reaction for the detection of nitrite

Assay: Briefly, a sodium nitrite standard curve was first constructed by dissolving 0.0345gm of sodium nitrite (Sigma-Aldrich, UK) in 5 ml of complete culture medium to give a 100mM stock solution. A 10 μ l aliquot was taken from the stock and diluted to 1ml with complete culture medium to give a 1mM working solution. Nitrite standards were then prepared as shown in the table below (Table 1). A 100 μ l aliquot of each standard was added in triplicate to separate wells in a 96-well plate. Also, 100 μ l of each sample was added in triplicate to the remaining wells on the plate. The Griess reagent was prepared by mixing solutions I and II in a 1:1 ratio. 100 μ l of the reagent was added to both standard and sample wells and each plate was placed on an orbital shaker for 15 min at room temperature before reading the absorbance values at 540 nm. An example of a standard curve routinely obtained is shown in figure 7.

Table 1: Preparation of serial dilutions of NaNO₂

Concentration of NaNO ₂ (mM)	μ l of 1mM NaNO ₂	μ l of DMEM	Final Concentration of NaNO ₂ (nmoles/100 μ l)
0	0	1000	0
0.01	10	990	1
0,02	20	980	2
0.03	30	970	3
0.04	40	960	4
0.05	50	950	5
0.1	100	900	10

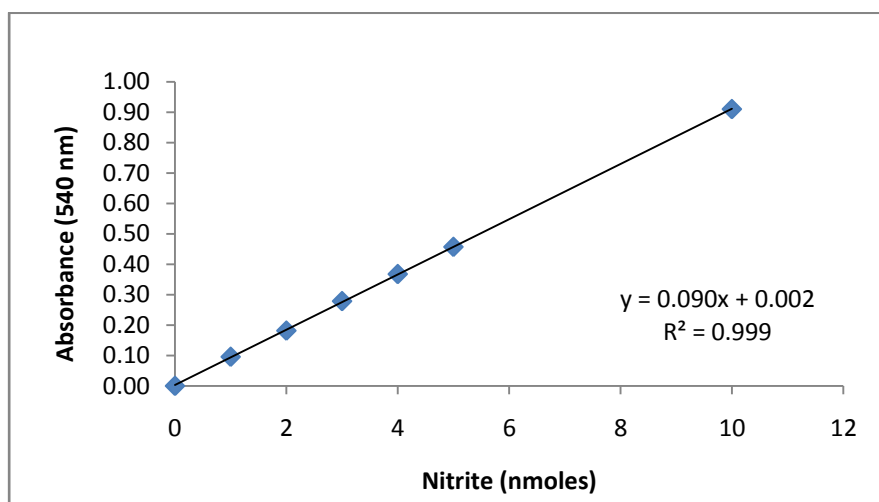


Figure 2.2A representative Nitrite standard curve

Concentrations of NaNO_2 ranging from 0-0.1mM were prepared in complete culture medium. Each concentration was added in triplicates in a 96-well plate and incubated for 15 minutes with 100 μl Griess I and II reagents. Absorbance values were taken at 540 nm on a Labsystems Multiskan Ascent micro plate reader. Data shown are the mean of three replicates for each concentration.

Analysis: The average absorbance of the blank was subtracted from the average absorbance values of the samples. The subtracted value was substituted in the equation shown below obtained from the standard curve to determine the concentration of nitrite (nmoles/100 μl) in the sample.

$$x = (y - 0.090) / 0.002 \text{ where } y = \text{average absorbance-blank value}$$

$$x = \text{concentration of nitrite (nmoles/100}\mu\text{l)}$$

2.4 Cell lysis

Cell lysis was carried out to extract protein from the cells so that they can be analysed by western blotting. Confluent monolayer of cells in 24-well plates were washed three times with 500µl of ice cold 1x PBS to remove traces of serum and culture medium. 100µl of 1x hot lysis buffer consisting of 2 mM Tris (pH 7.4; Fisher scientific, UK) and 1% sodium dodecyl sulphate (SDS; Sigma-Aldrich, UK) was then added to each well. The cells were scraped into the buffer and the lysates were collected into eppendorf tubes which were subsequently sonicated for 30 seconds interval over 90 seconds. The samples were then boiled for 5 minutes at 95°C and centrifuged for 20 minutes at 13,000rpm. The supernatant was transferred into a new eppendorf tubes and stored at -20°C until analysed.

Generation of lysates for the detection of phospho proteins: Confluent monolayers of cells in 24-well plates were washed three times with 500µl of ice cold 1x PBS to remove traces of serum and culture medium. 100µl of 1x lysis buffer consisting of 2 mM Tris (pH 7.4), phosphatase inhibitor cocktail 2 (1:100 dilution; Sigma-Aldrich, UK) and 1% SDS was added to each well. The cells were scraped into the buffer and the lysates were collected into eppendorf tubes which were subsequently sonicated for 30 seconds interval over 90 seconds. The samples were then boiled for 5 minutes at 95°C and centrifuged for 20 minutes at 13,000rpm. The supernatant was transferred into a new eppendorf tubes and stored at -20°C until analysed.

2.5 Determination of total cell protein using bicinchoninic acid (BCA):

This assay is used to determine the amount of protein present in the sample. The first step involves the reduction of copper (Cu^{+2}) to cuprous (Cu^{+1}) by protein in an

Table 2: Preparation of a protein standard curve

Protein per well (µg)	10mg/ml BSA (µl)	DDW (µl)	Final concentration (µg/µl)
0	0	1000	0
1	20	980	0.2
2	40	960	0.4
3	60	940	0.6
5	100	900	1
10	200	800	2
15	300	700	3
20	400	600	4
25	500	500	5

BCA reagent B (Fisher scientific, UK) that contains 4% w/v copper (II) sulphate pentahydrate ($\text{CuSO}_4 \cdot 5\text{H}_2\text{O}$) was mixed with BCA reagent A (Sodium carbonate, Sodium bicarbonate, bicinchoninic acid and Sodium tartrate in 0.1M sodium hydroxide; Fisher scientific, UK) in 1 in 50 dilution. A 96-well plate was set up as follows:

Control wells: 5µl DDW + 5µl lysis buffer (x1) + 100µl BCA solution

Standard wells: 5µl standards + 5µl lysis buffer (x1) + 100µl BCA solution

Sample wells: 5µl DDW + 5µl lysate + 100µl BCA solution

The plate was incubated for 45min at room temperature on an orbital shaker and the absorbance was read at 620nm on a Labsystems Multiskan Ascent plate reader. Each standard or sample was analysed in triplicates. The average absorbance of the blank standard was subtracted from the average absorbance of other standard values. A protein standard curve was plotted using standard protein concentrations ($\mu\text{g}/\mu\text{l}$) on the x-axis and corrected absorbance values of the standards (measured absorbance-blank absorbance (nm)) on the y-axis. An example standard curve routinely obtained is shown in Figure 9.

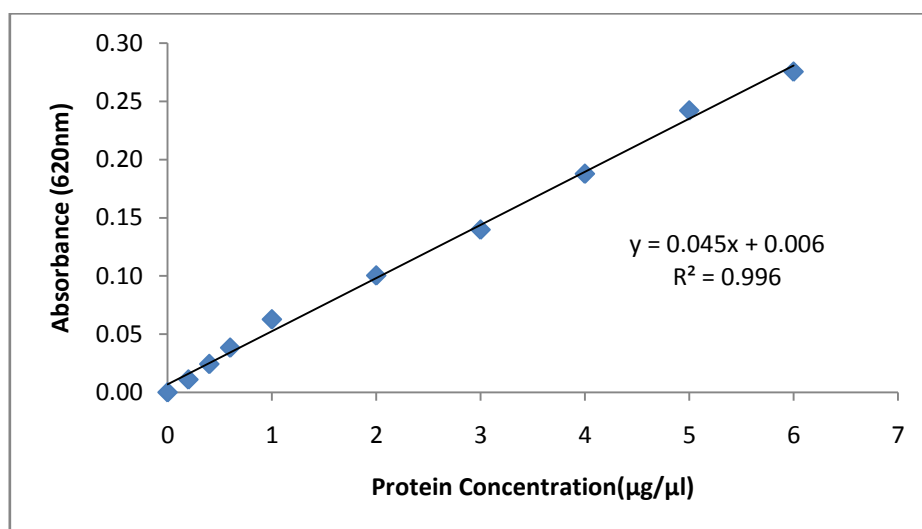


Figure 2.4A representative protein standard curve

Concentrations of BSA ranging from 0-30 μg were prepared in DDW. Each concentration was added in triplicates in a 96-well plate and incubated for 1hr with 100 μl BCA reagent solution. Absorbance values were taken at 620 nm on a Labsystems Multiskan Ascent micro plate reader. Data shown are the mean of three replicates for each concentration.

Analysis:The average absorbance of the blank was subtracted from the average absorbance values of the samples. The subtracted value was substituted in the equation shown below obtained from the standard curve to determine the protein concentration ($\mu\text{g}/\mu\text{l}$). The protein concentration obtained was then used to determine the loading volume for western blot analysis.

$x=(y-0.090)/0.002$ where y = average absorbance-blank value

x = concentration of protein ($\mu\text{g}/\mu\text{l}$).

2.6 MTT assay

The MTT assay is a colorimetric assay involving the breakdown of yellow water-soluble tetrazolium salt 3-(4, 5-dimethylthiazol-2-yl)-2, 5-diphenyltetrazolium bromide (MTT) to dark-blue, water-insoluble formazan crystals (as shown in figure 10). This reaction is catalysed by the mitochondrial enzyme succinate dehydrogenase and it occurs only in living cells. Hence this assay is useful in determining the viability of cells as the higher the absorbance the higher the proportion of live cells (Hughes *et al.*, 2003).

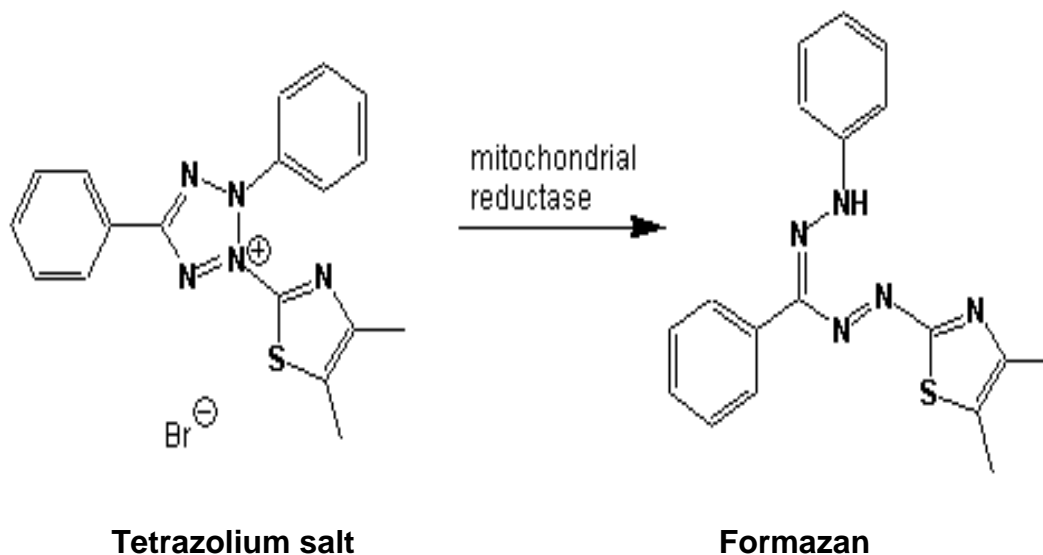


Figure 2.5 Formation of water insoluble Formazan from MTT in the presence of Succinate dehydrogenase

In the assay, confluent monolayers of cells in 96-well plates were treated with complete culture medium alone or with medium containing DEM (1 μ M, 2.5 μ M, 5 μ M, 10 μ M and 25 μ M), H₂O₂ (150 μ M, 300 μ M, 500 μ M, 1000 μ M and 2000 μ M) or antimycin A (10 μ M, 25 μ M, 50 μ M, 100 μ M, 150 μ M) and incubated for 24hrs. The assay was performed 24 hrs later as explained below.

Assay: 5mg/ml MTT solution (Sigma-Aldrich, UK) was prepared by dissolving 0.05g in 10ml PBS. 2ml was taken and diluted to 20ml with complete culture medium to get 0.5mg/ml concentration. The medium in the 96-well plate was aspirated and 200 μ l of 0.5 mg/ml solution was added to each well and the plates were incubated at 37^oC for 4 hours. The medium was then removed and 200 μ l of isopropanol was added before placing the plates on an orbital shaker for 15 min. Absorbance readings were taken at 540nm on Labsystems Multiskan Ascent plate reader.

2.7 Western blotting

This technique is used to identify the protein of interest using a selective antibody against the targeted protein. It involves the separation of proteins on a polyacrylamide gel (SDS-PAGE), which are then transferred from the gel onto a nitrocellulose or polyvinylidene fluoride (PVDF) membrane so that the antigens become accessible to the antibodies. A primary antibody is added then followed by secondary antibody, which detects the protein of interest. The remaining sites on the membrane are blocked using a milk protein to prevent non-specific binding of the antibody to the membrane. Primary antibody detects the specific protein of interest whereas the secondary antibody targets the primary antibody (Blancher & Jones, 2001).

Assay: Glass plates were first set up and checked for any leaking using water which was subsequently poured out and the plates were allowed to dry before pouring the gel solution.

Resolving gel: The solution (4 gels) was prepared with 4.64ml of DDW, 2.66ml of 30% acrylamide : bis-acrylamide (Fisher scientific, UK), 2.5ml of 1.5M Tris-HCl (pH 8.8), 100 μ l of 10% SDS, 100 μ l of 10% ammonium per sulphate (Sigma-Aldrich, UK) and 6 μ l TEMED (Fisher scientific, UK). 3.5 ml solution was poured between the glass plates. A thin layer of water-saturated iso-butanol was added on top of the gel to remove any air bubbles and allowed the gel to set in the absence of oxygen.

Stacking gel: After the resolving gel had polymerised, a stacking gel solution was prepared which consists of 2.44ml of DDW, 0.52ml of 30% acrylamide : bis-

acrylamide, 1ml of 0.5M Tris-HCl (pH 6.8), 40 μ l of 10% SDS, 20 μ l of 10% ammonium per sulphate and 4 μ l TEMED. The water-saturated isobutanol was removed from the top of the resolving gel and the stacking gel solution was poured between the glass plates. A comb was positioned into the latter and left in place for the wells to form.

After the stacking gel had polymerised, the comb was removed and gels were placed onto a cassette and into an electrophoresis tank consisting of 1x tank buffer. A 10x tank buffer was prepared with 0.25M Tris, 1.92M glycine (Fisher scientific, UK) and 1% SDS and diluted to 1x on the day of use.

Sample preparation: Samples for analysis were prepared by adding 2x loading buffer (250 μ M Tris of pH 6.8, 4% SDS, 10% glycerol, 2% β -mercaptaethanol (Sigma-Aldrich, UK), 0.006% Bromophenol blue (Sigma-Aldrich, UK)) to the lysates generated from treated cells. Samples were boiled at 95⁰C for 5 minutes and centrifuged for 20 minutes at 13,000 rpm.

Gel electrophoresis: The samples were loaded into the lanes with molecular weight marker (Cell signalling, UK) in the first lane. The electrophoresis apparatus (Bio-Rad, UK) was connected to a power pack (Bio-Rad, UK) and the gels ran at 220 volts and 20 milli amps (mA) per gel until the samples migrate to the border of the resolving gel. The current was then increased to 25mA per gel until the dye phase reached the bottom of the gel.

A PVDF membrane (Fisher scientific, UK) and filter paper were cut to the same dimensions as the gels. The PVDF membrane was soaked in pure methanol for 15 seconds and then washed in DDW for 2 minutes to reduce the hydrophobicity of the membrane and enhance the adsorption of proteins that were separated by size in the gel. The membrane and gel were set up in a semi-dry transfer cell by placing wet filter paper first and the membrane followed by the gel and then additional soaked filter paper. Transfer buffer was added to the sandwich on the blotter and incubated for 5 minutes. The 1x transfer buffer was prepared from a 10x stock consists of 48mM Tris base (pH 7.5), 39mM Glycine and 0.0375% SDS. On the day a 1x solution was prepared by carrying out a 1:10 dilution and adding 20% methanol (Fisher Scientific, UK). The transfer cell (Thermo Scientific, UK) was connected to a power supply and run at 25 volts for 20 minutes.

Blocking of the membrane: The membrane was subsequently blocked for a minimum of 1 hour using blocking buffer consisting of 100 μ l Tween 20 (Fisher Scientific, UK), 5% non-fat milk (for phospho proteins 3% bovine serum albumin (BSA) was used), 10 ml of 10x washing buffer (10mM Tris-Base (pH 7.5) and 100mM sodium chloride (NaCl; Fisher Scientific, UK)) in a volume of 100 ml. Blocking prevents non-specific binding of antibodies to the membrane.

After blocking, the membrane was placed in a sealed hybridization bag in a solution containing anti-iNOS monoclonal antibody (BD biosciences, UK) in 1:2500 dilution or anti-phospho p38 MAPK (Cell Signalling, UK) in 1:2500 dilution or anti-HO-1 (Abcam, UK) in 1:250 dilution or anti-phospho Akt (Cell Signalling, UK) in 1:1000 dilution and anti- β -actin monoclonal antibody (Sigma-Aldrich, UK) in 1:5000 dilution in

blocking buffer prepared on the day of use. The hybridization bag was placed on a shaker overnight at 4⁰C. The membrane was washed with x1 washing buffer for 30 minutes, changing the buffer every 10 minutes and then incubated with the secondary antibodies on a shaker for a further 1 hour at room temperature. The secondary antibodies were anti-mouse (Cell signalling, UK) in 1:5000 dilutions and anti-biotin (Cell signalling, UK) diluted 1:1000 in x1 blocking buffer. At the end of this incubation, membranes were washed with x1 washing buffer for 1hr, changing the buffer for every 10 minutes.

Enhanced chemiluminescence detection (ECL): To identify the protein bands, equal volume of ECL detection solution A and B were prepared. Solution A contained 100mM Tris pH 8.5, 4.5mM of p-coumaric acid (Sigma-Aldrich, UK) and 25mM of Luminol (Sigma-Aldrich, UK) and solution B had 100mM Tris pH 8.5 and 0.02% H₂O₂. Each membrane was placed on a sheet of cling film in a cassette. The detection solution was then pipetted onto the membrane and incubated for 5 minutes at room temperature. Excess solution was drained off and the membrane was covered with cling film before exposing to an autoradiography film (Fisher Scientific, UK). The film was developed using a developer solution (Sigma-Aldrich, UK) until the bands appear followed by a rinse with water and fixed in a fixer solution (Sigma-Aldrich, UK). Finally the film was washed under running water and allowed to dry.

2.8 Detection of free radical generation by confocal microscopy:

Confocal microscopy technique is used to increase optical resolution by using point illumination and a pinhole having various sizes that helps to remove out-of-focus light in samples. It can be used for three-dimensional reconstructions of images. The

microscope signifies a thin cross-section of the specimen and when compared to a conventional microscope, it offers a better contrast. In biomedical sciences the major application of confocal microscopy involves imaging live or fixed cells and tissues that have been treated with one or more fluorescent probes.

A laser is connected which provides excitation light to get very high intensities. The laser light is reflected off the dichromatic mirror. The laser then passes through the mirrors that are mounted on motors and these mirrors allows scanning the laser throughout the sample. The probe in the sample fluoresces and is focused onto the detector pinhole aperture. Photomultiplier detector measures the emitted light passing through the detector pinhole. The photomultiplier detector is attached to the computer, which shows the image of the sample (Figure 11).

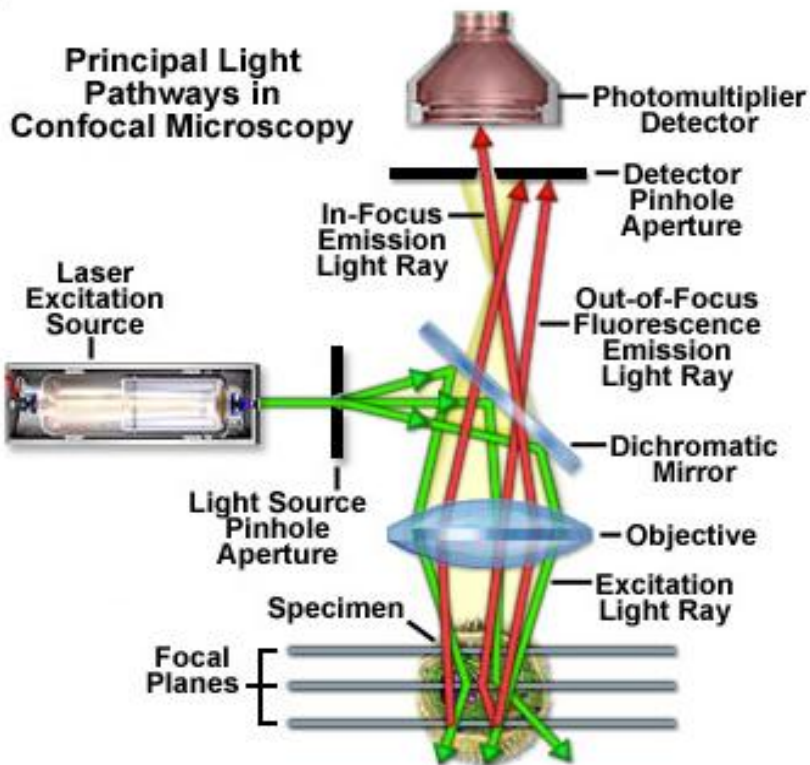


Figure 2.6 Principal light pathways involved in imaging of the sample in Confocal Microscopy

The figure is taken from Microscopy: the source for microscopy education (web link: <http://www.microscopyu.com/articles/confocal/confocalintrobasics.html>)

Detection of reactive oxygen species (ROS) production using dichlorofluorescein (DCF)

The 2', 7' -dichlorofluorescein diacetate is a cell-permeable non-fluorescent probe and is widely used to quantify cellular OS. The non-fluorescent fluorescein derivative, dichlorofluorescein diacetate (DCFH-DA) is converted to DCF after being oxidized by various oxidants and emits fluorescence. The emitted fluorescence is directly proportional to the amount of free radicals. When the adherent cells are treated with the dye, the non-ionic, non-polar DCFH-DA traverses the cell membrane

and intracellular esterases hydrolyze it to nonfluorescent DCFH. In the presence of ROS, DCFH is readily oxidized to highly fluorescent DCF with excitation/emission maxima of 480/530nm.

A 10mg of 2', 7'-dichlorofluorescein diacetate (DCFH-DA) was dissolved in 1ml of methanol to make a 20.5mM stock of DCFH-DA. 20 μ M of working solution was prepared by diluting 20.5mM stock in phosphate buffered saline (PBS) and added to cells, which had been treated under defined conditions. 1ml of 20 μ M working solution was added to the cells grown on Lab-Tek wells and incubated at 37⁰C for 10-15 minutes protected from light. Excess DCFH-DA was aspirated and the cells washed 3 times with 1x PBS with a 5-minute interval between each wash before viewing under an electronic confocal laser-scanning microscope.

Detection of superoxide production using MitoSOXTM Red

MitoSOX Red is a novel fluorogenic dye used for highly selective detection of superoxide, the most predominant free radical produced by the mitochondria. The dye is cell-permeable and targets the mitochondria of the live cells. The O₂⁻ present in the mitochondria oxidizes the MitoSOXTM emitting red fluorescence. MitoSOXTM is readily oxidized by superoxide and not by any other ROS/RNS species and its oxidation can be thwarted using specific O₂⁻ inhibitor, SOD. It has excitation/emission maxima of 510/580nm.

50µg of the MitoSOX™ dye was dissolved in 13µl of DMSO to make a 5mM stock solution which was then diluted further to give a working solution of 5µM in Hank's balanced salt solution (HBSS; Sigma-aldrich, UK). 2ml of the working solution was added to the cells grown on Lab-Tek wells and incubated for 10 minutes at 37°C protected from light. As in the previous experiments, excess dye was aspirated and the cells washed 3 times with 1x PBS with a 5-minute interval between each wash before viewing under an electronic confocal laser-scanning microscope.

2.9 Real-time quantitative reverse transcriptase polymerase chain reaction (qPCR)

Polymerase chain reaction (PCR) has become the keystone of the modern molecular biology the world over. Real-time PCR is an advanced form of the polymerase chain reaction maximizing the benefits of the technique. The real time PCR enables sensitive and reproducible quantification of the amplified complimentary deoxyribonucleic acid (cDNA) as it occurs in real time. Amplification of DNA creates multiple copies of the DNA. There should be enough DNA to be able to be amplified so that we get detectable signal for quantification in order to analyse the sample. It precisely measures the amount of cDNA at each cycle using a fluorescent probe. A thermostable polymerase enzyme is involved in the reaction, which synthesizes a complimentary sequence of bases to any single strand of DNA as shown in Figure 12. The polymerase enzyme amplifies the selected gene in a mixed DNA sample by the addition of small pieces of DNA known as primers complimentary to the gene of interest. These primers enable the DNA sample to bind to the polymerase and begin copying the gene of interest.

During the PCR process, changes in the temperature are permitted to control the action of the polymerase enzyme and efficient binding of primers. The reaction initially started by increasing the temperature to 95°C where the entire double stranded DNA is converted into single strands. The temperature then is reduced to 60°C to enable the primers to bind to its specific gene. Finally the temperature is increased to 72°C for fast and efficient activity of the polymerase enzyme. This temperature change was repeated for 40 cycles. The amount of fluorescence is increased correspondingly with the amplification of each DNA molecule and is measured during each cycle and plotted over time. The amount of PCR product in each cycle is correlated to fluorescence amplification curve, which enables to stipulate the starting quantity of target DNA or RNA. The middle of the curve symbolises the exponential phase where emitted fluorescence exceed background fluorescence. The amount of fluorescence for each sample is represented as cycle threshold (C_t), the point or cycle number at which the fluorescence for that sample exceeds background fluorescence. The higher the C_t value of that sample the lower is the starting quantity of the target DNA as the fluorescence curve exceeds background at a later cycle number. Hence lower C_t values represent higher target DNA or RNA.



Figure 2.7 DNA polymerase cleaving the green dye from the red

Assay

Isolation of ribonucleic acid (RNA): Cells grown in monolayer were lysed directly in the T-25 tissue culture flask using RNA-STAT 60 (1ml per $5-10 \times 10^6$ cells; amsbio, UK). Cells were completely lysed by repetitive pipetting. The homogenate was transferred into eppendorf tubes and allowed to stand for 5 minutes at room temperature for complete dissociation of nucleoprotein complexes. 0.2ml of chloroform per 1ml of RNA-STAT 60 was added to the tubes and was shaken vigorously for few seconds before incubating at room temperature for 2-3 minutes. Homogenates were centrifuged at 12,000g for 15 minutes at 4°C. Subsequently the homogenate was separated into two phases: a lower red phenol chloroform phase and the colorless upper aqueous phase. Ribonucleic acid (RNA) was present solely in the aqueous phase whereas the interphase and lower organic phase contains DNA and proteins. Ideally the volume of aqueous phase should be around 60% of the volume of RNA used for homogenization. Aqueous layer containing RNA was separated using a pipette and transferred into fresh Eppendorf tubes. 0.5ml of isopropanol per 1ml of RNA-STAT 60 was added to the eppendorfs. Samples were stored at room temperature for 10 minutes and then centrifuged at 12,000g for 10 minutes at 4°C. Ribonucleic acid was precipitated in the form of white pellet at the bottom of the tube. The supernatant was removed and the pellet was washed with 75% ethanol by vortexing and subsequent centrifugation at 7500g for 5 minutes at 4°C. 1ml of 75% ethanol per 1ml of RNA-STAT 60 was used. After centrifugation, the supernatant was removed and the RNA pellet was briefly air-dried before dissolving in about 40µl of autoclaved double distilled water.

Removal of contaminating DNA from RNA preparation: TURBO DNase treatment was used to remove the DNA from RNA preparations. 0.1 volume of 10X TURBO DNase buffer was added to the RNA solution. 1µl of TURBO DNase was added to the sample and was mixed properly by repetitive pipetting. Samples were then incubated on a heat plate at 37⁰C for 30 minutes. After incubation 1µl of DNase inactivation reagent was added to the samples and allowed to stand at room temperature for 5 minutes with occasional mixing. Samples were centrifuged at 10,000g for 2 minutes. Colourless supernatants containing RNA were collected into clean eppendorf tubes while pellet at the bottom that had DNase inactivation reagent were discarded.

Quantification of RNA: Ribonucleic acid (RNA) was quantified using the photometric method. 10µl of RNA sample was diluted with 190µl of sterile distilled water. Prior to that, blank readings were taken using 200µl of sterile distilled water. Readings of all the RNA samples were taken using a bio-photometer and measured in µg/mL.

Reverse transcription of RNA to cDNA: The process enables the conversion of RNA to cDNA using a reverse transcriptase enzyme. A high capacity RNA to cDNA kit (Applied Biosystems, UK) was used. 2µg of total RNA was required for the process and the total volume used for the reaction was 20µl. Samples were prepared as follows:

Table 3. Preparation of samples for reverse transcription

Component	+RT	-RT (Control)
2X RT Buffer	10µl	10µl
20X Enzyme mix	1µl	-
RNA Sample	Up to 9µl	Up to 9µl
Nuclease Free Water	Make up to 20µl	Make up to 20µl
Total per reaction	20µl	20µl

Master mix preparation: The master mix was prepared by mixing the fluorescent dye SYBR green (Applied Biosystems, UK) with forward and reverse primer and cDNA of the target gene. Inducible nitric oxide synthase primers used were: 5'-CTGGCTCGCTTTGCCACGGA-3' (forward primer) and 5'-GCTGCGACAGCAGGAAGGCA-3' (reverse primer). A stock of 100µM was prepared by diluting the powdered form in autoclaved double distilled water. A working solution of 10µM was used for the PCR process. The master mix was prepared as follows: 10µl SYBR Green + 1µl of forward primer + 1µl of reverse primer + 2µl of cDNA sample + 6µl of nuclease free water.

Analysis

The average or mean of the replicates of control, target and reference gene samples were calculated.

Mean Control sample C_T Mean reference gene C_T → ▲ C_T normalised

Mean Target sample C_T Mean reference gene C_T → ▲ C_T Target Sample

Final standard deviation = $\sqrt{(\text{S.D of target sample } C_T)^2 + (\text{S.D of reference gene } C_T)^2}$

▲▲ C_T Target Sample = ▲ C_T Target Sample — ▲ C_T normalised

Fold change = $2^{-C_T \text{ Target Sample}}$

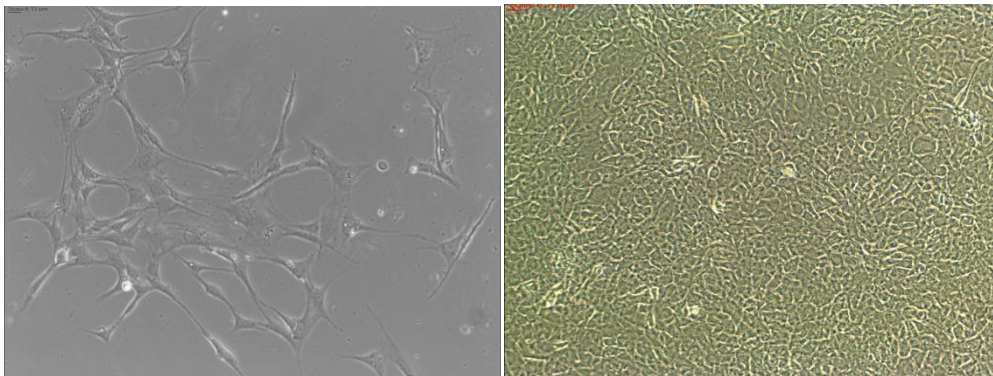
2.10 Statistical analysis

Statistical analysis was carried out using the Graph Pad Prism 5.0. All values are expressed as means \pm S.E.M of measurement of at least 3 individual experiments. Statistics applied was one-way analysis of variance (ANOVA) followed by Bonferroni or Dunnett or Tukey's as a post-hoc test having a significance at $p < 0.001$, $p < 0.01$ and $p < 0.05$.

3.0 RESULTS

3.1 Rat aortic smooth muscle cells

Rat aortic smooth muscle cells (RASMCs) were taken out of liquid nitrogen, transferred into a T-75 flask and grown to confluency using complete growth culture medium. Figure 13 represents smooth muscle cells growing as a monolayer in culture and characterised by a polygonal and epitheloid shape. Figure 3.1(a) shows the cells in the sub-confluent stage of growth 24 hours after transferring into the flask from liquid nitrogen. Figure 3.1(b) shows the cells in a confluent stage, which usually takes 3-4 days, and ready for the next passage or plating into wells for experimentation.



3.1(a)

3.1(b)

Figure 3.1 Morphology of RASMCs in culture

Rat aortic smooth muscle cells were taken out of a cryo vial from liquid nitrogen and cultured using growth culture medium and grown to confluency over 3-4 days in a T-75 flask. The growth medium in the flask was replenished every 2 days. Initial growth and the confluent stages were confirmed by observing the cells in flasks under a OLYMPUS™ electronic microscope at a magnification of 40x and 100x. Figure 3.1(a) was taken after 24hrs of transfer from liquid nitrogen and figure 3.1(b) was taken after 72hrs when cells were confluent.

3.2 Effects of OS inducers on the viability of rat aortic smooth muscle cells

To determine whether OS inducers used in the studies exerted any cytotoxic effects, cells were treated with complete culture medium alone or medium containing various concentrations of DEM, antimycin A and H₂O₂ for 24hrs before performing the MTT assay as described in the methods (section 2.6). Control cells showed no decrease in viability and the metabolism of MTT by these cells was considered as 100% and compared to different concentrations of OS inducers. Diethyl maleate was found to be toxic at 50µM causing a 30-40% decrease in viability of the cells. Lower concentrations did not show any statistically significant change in cell viability when compared to controls (Figure 3.2). Antimycin A showed no significant decrease in the viability of the cells with less than 20% reduction in MTT metabolism observed even at the highest concentration of 150µM used (Figure 3.3). Hydrogen peroxide was also not cytotoxic at lower concentrations (150µM and 300µM) but caused a significant inhibition of MTT metabolism with almost 40-50% decrease in the cell

viability at concentrations of 500 μ M and above (Figure 3.4). There was no change observed in the above data when OS inducers were treated with LPS and IFN- γ .

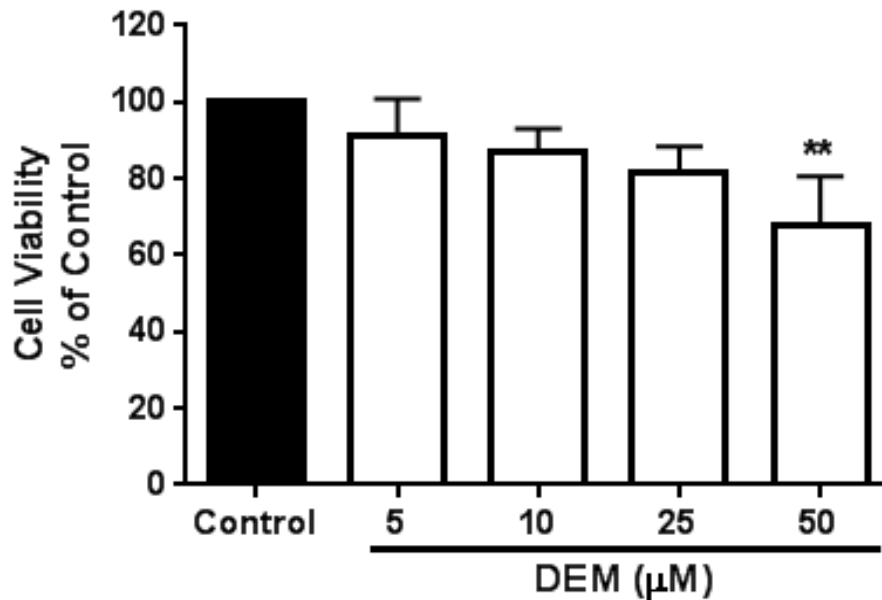


Figure 3.2 Effect of DEM on viability of RASMCs

Confluent monolayers of cells in 96-well plate were treated with different concentrations of DEM for 24hrs as described in section 2.6. Following 24hrs incubation, cell viability was determined by performing the MTT assay as described in the methods. The data is presented as % cell viability with control as a 100%. The data represents the means \pm S.E.M. of at least three individual experiments. ** denote $p < 0.01$ when compared to control.

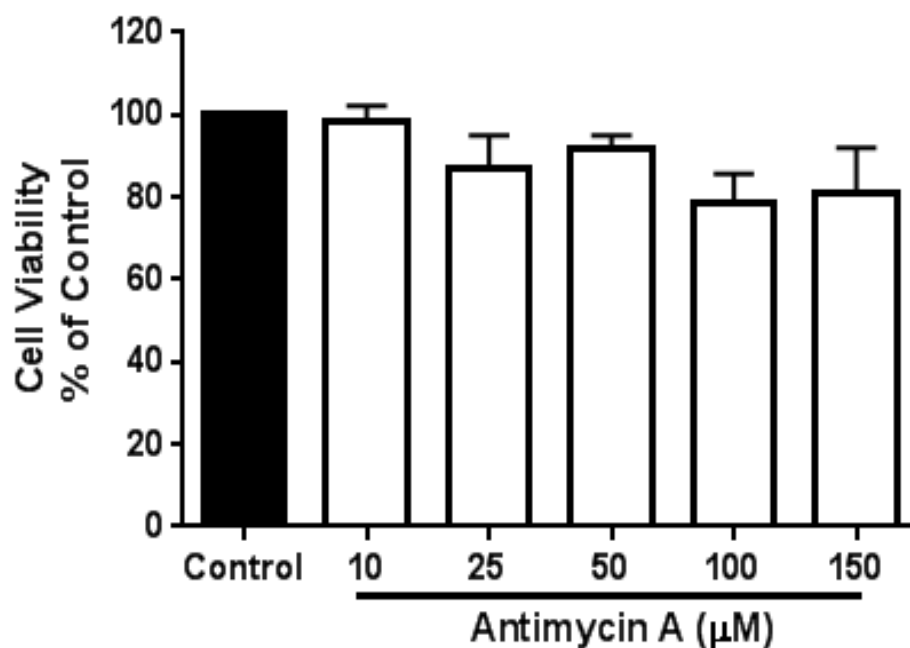


Figure 3.3 Effect of Antimycin A on viability of RASMCs

Confluent monolayers of cells in 96-well plate were treated with different concentrations of antimycin A for 24hrs as described in section 2.6. Following 24hrs incubation, cell viability was determined by performing the MTT assay as described in the methods. The data is presented as % cell viability with control as 100%. The data represents the means \pm S.E.M. of at least three individual experiments.

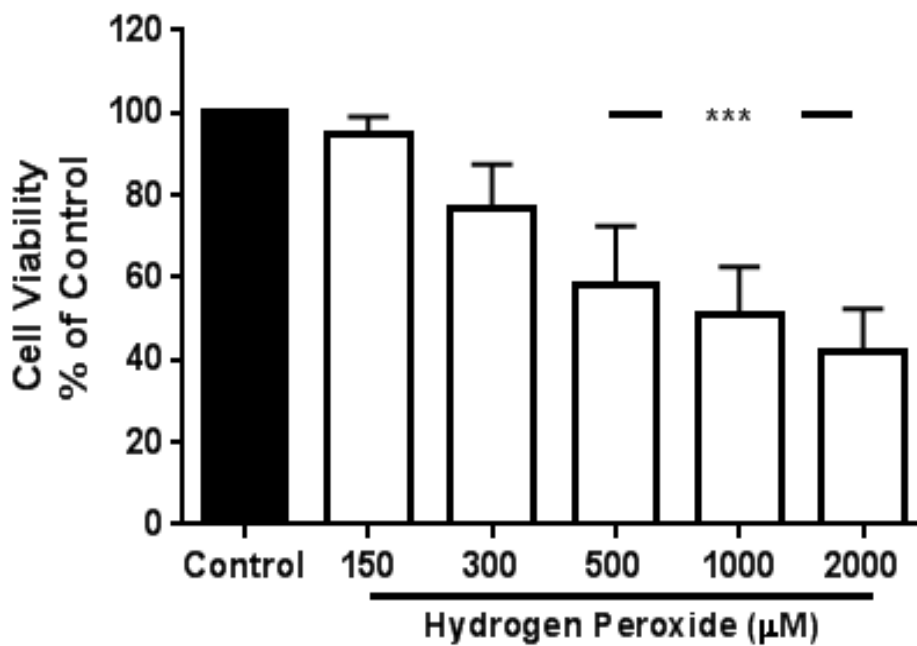


Figure 3.4 Effect of H₂O₂ on viability of RASMCs

Confluent monolayers of cells in 96-well plate were treated with different concentrations of H₂O₂ for 24hrs as described in section 2.6. Following 24hrs incubation, cell viability was determined by performing MTT assay as described in the methods. The data is presented as % cell viability with control as 100%. The data represents the means ± S.E.M. of at least three individual experiments. *** denote p<0.001 when compared to control.

3.3 Effects of ethanol on nitrite production and iNOS expression in control and activated RASMCs

Because ethanol was routinely used as the solvent for dissolving drugs, experiments were carried out to determine whether it had any direct effects on nitrite production and iNOS expression. Cells were therefore pre-treated with different concentrations of ethanol (0.005%-0.1%) for 30 minutes before activating with LPS (100 µg/ml) and IFN- γ (100 U/ml) for 24hrs as described in the methods (section 2.2.1). Nitrite production was estimated using the Griess assay and iNOS expression by western blotting as described in the methods (section 2.3 and section 2.7). Control cells showed no iNOS expression (figure 3.6) or nitrite production (figure 3.5) but cells treated with LPS and IFN- γ showed clear expression of iNOS and significant generation of NO. Treatment with various concentrations of ethanol in the presence of LPS and IFN- γ did not change the expression of iNOS or nitrite production when compared to the levels detected in LPS and IFN- γ -treated cells.

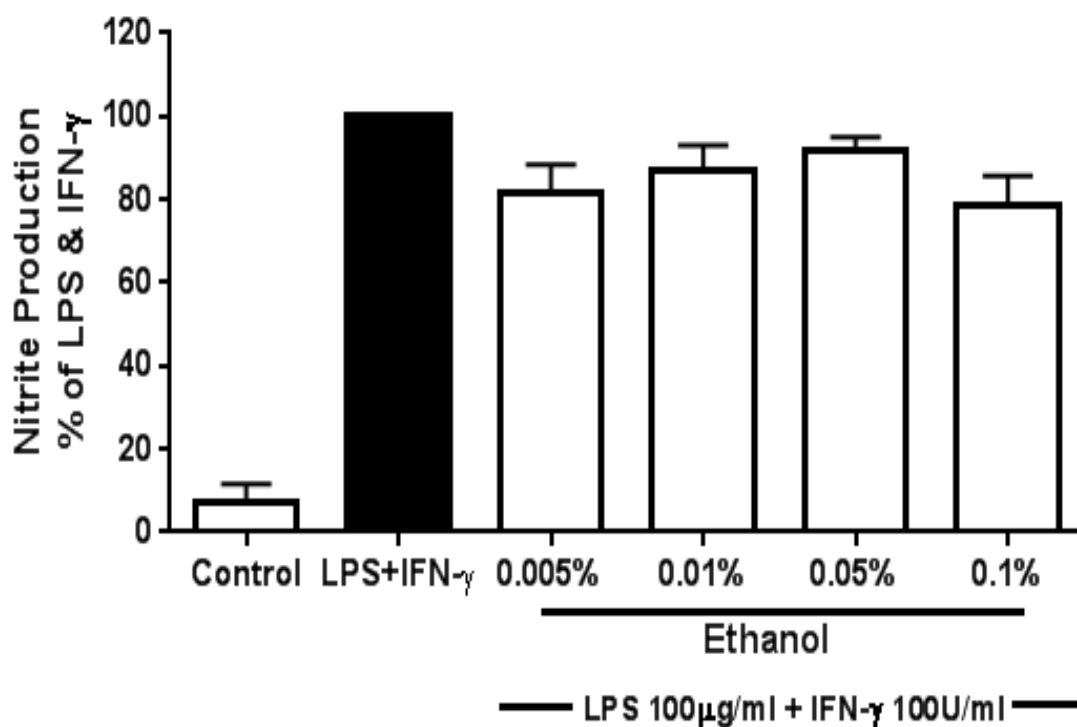


Figure 3.5 Effects of ethanol on nitrite production in LPS and IFN- γ activated RASMCs

Confluent monolayers of RASMCs in 24-well plate were pre-treated with complete culture medium alone or medium containing ethanol (0.005%, 0.01%, 0.05% and 0.1%) for 30minutes prior to incubation with LPS (100 μ g/ml) and IFN- γ (100U/ml) for a further 24hrs. Nitrite production was determined as described in the methods (section 2.3). The data is expressed as % nitrite production with the response to LPS (100 μ g/ml) + IFN- γ (100U/ml) taken as 100%. The data represents the means \pm S.E.M of at least three independent experiments.

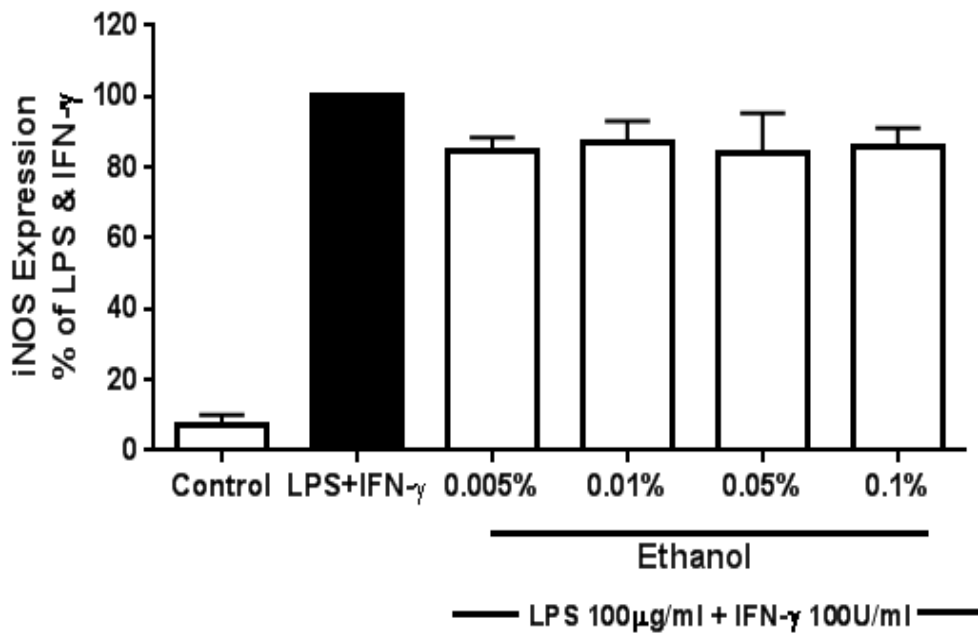
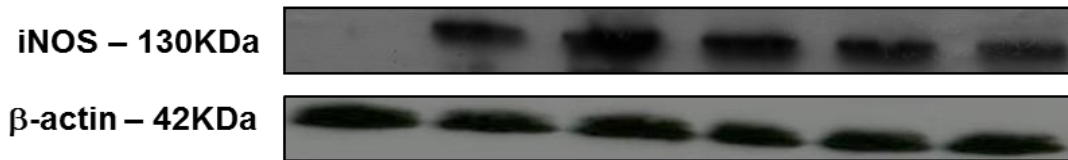


Figure 3.6 Effects of ethanol on iNOS expression in LPS and IFN- γ activated RASMCs

Confluent monolayers of RASMCs in 24-well plates were pre-treated with complete culture medium alone or medium containing ethanol (0.005%, 0.01%, 0.05% and 0.1%) for 30minutes prior to incubation with LPS (100 μ g/ml) and IFN- γ (100U/ml) for a further 24hrs. The expression of iNOS was determined by western blotting as described in the methods (section 2.7). The blot is representative of at least three independent experiments and the bar graph is the densitometric data expressed as % iNOS expression with LPS (100 μ g/ml) + IFN- γ (100U/ml) response taken as 100%. The data represents the means \pm S.E.M of at least three independent experiments.

3.4 Effect of OS inducers on nitrite production in control and activated RASMCs

To determine the effect of OS inducers on nitrite production, cells were pre-treated with different concentrations of DEM, antimycin A and H₂O₂ for 30 minutes before incubating the cells with LPS (100 µg/ml) and IFN-γ (100 U/ml) for 24hrs. Nitrite production was determined using the Griess assay as described in the methods (section 2.3). Control cells showed no nitrite production. LPS and IFN-γ induced significant generation of nitrite and was considered as the maximum response for comparison with OS treated cells. Diethyl maleate caused a concentration dependent decrease in NO production, reducing levels by 20%, 30%, 50% and 70% at 1µM, 2.5µM, 5µM and 10µM respectively (Figure 3.7) whereas antimycin A caused a 40%, 70%, 80% and 90% reduction with 25µM, 50µM, 100µM and 150µM respectively (Figure 3.8). In contrast H₂O₂ (50-300µM) did not cause any inhibition and levels of nitrite were found to be similar to those of LPS and IFN-γ alone as shown in figure 3.9.

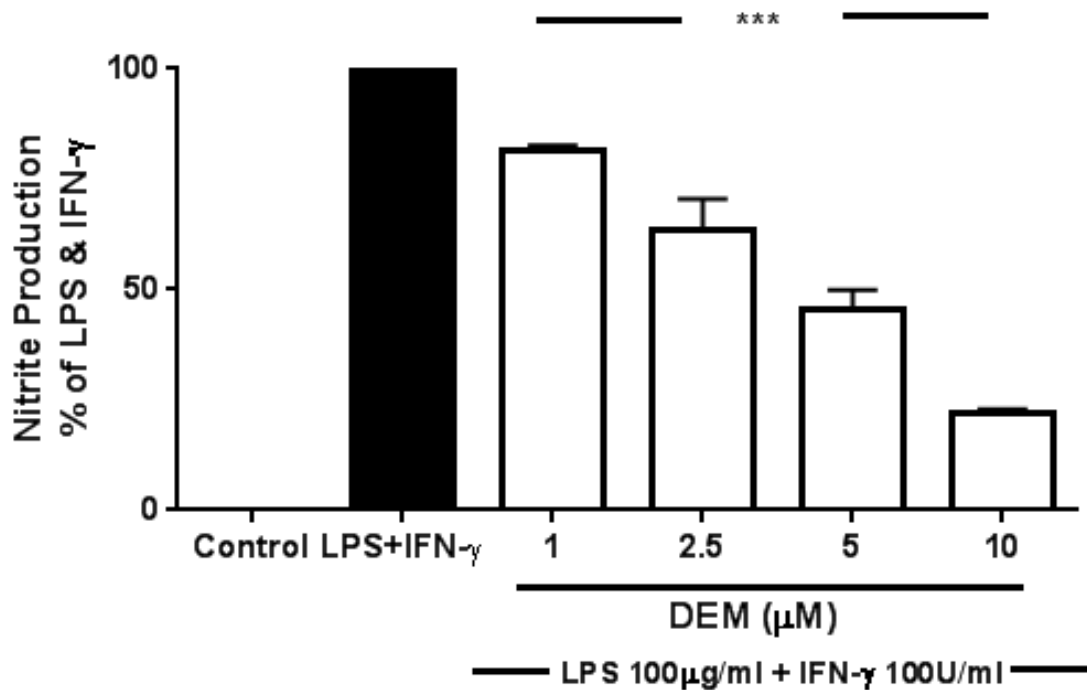


Figure 3.7 Effects of DEM on nitrite production in LPS and IFN- γ activated RASMCs

Confluent monolayers of RASMCs in 24-well plates were pre-treated with complete culture medium alone or medium containing DEM (1 μ M, 2.5 μ M, 5 μ M and 10 μ M) for 30minutes prior to incubation with LPS (100 μ g/ml) and IFN- γ (100U/ml) for a further 24hrs. Nitrite production was determined as described in the methods (section 2.3). The data is expressed as % nitrite production with the response to LPS (100 μ g/ml) + IFN- γ (100U/ml) taken as 100%. The data represents the means \pm S.E.M of at least three independent experiments.*** denote $p < 0.001$ when compared to LPS (100 μ g/ml) + IFN- γ (100U/ml).

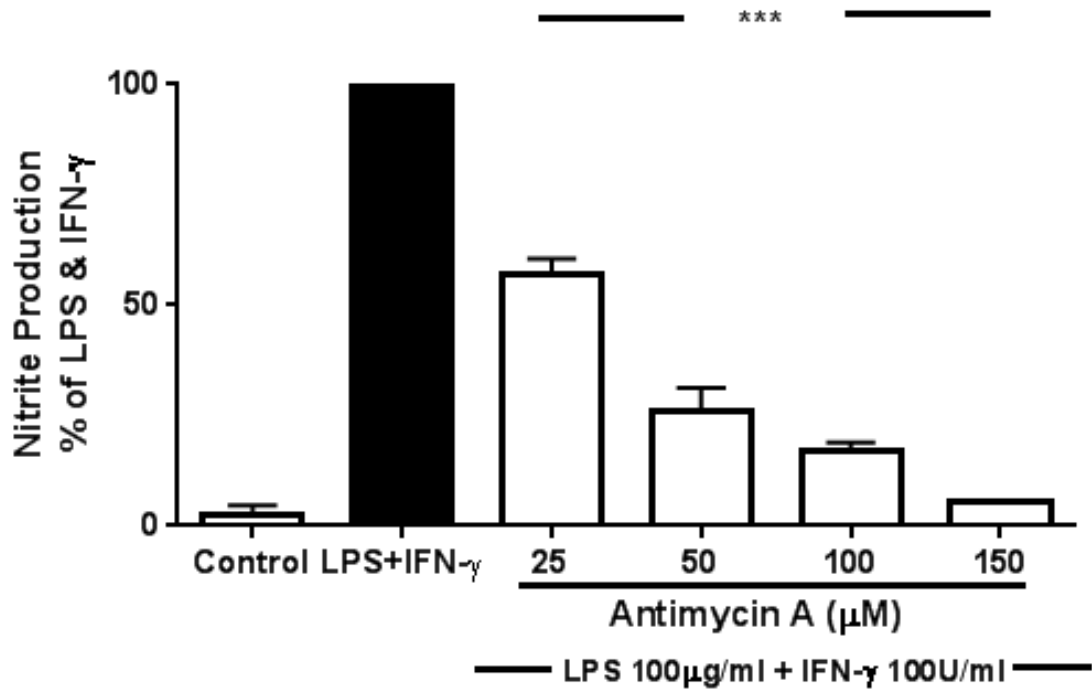


Figure 3.8 Effects of antimycin A on nitrite production in LPS and IFN- γ activated RASMCs

Confluent monolayer of RASMCs in 24-well plate was pre-treated with complete culture medium alone or medium containing antimycin A (25μM, 50μM, 100μM and 150μM) for 30minutes prior to incubation with LPS (100μg/ml) and IFN- γ (100U/ml) for a further 24hrs. Nitrite production was determined as described in the methods (section 2.3). The data is expressed as % nitrite production with the response to LPS (100μg/ml) + IFN- γ (100U/ml) taken as 100%. The data represents the means \pm S.E.M of at least three independent experiments. *** denote $p < 0.001$ when compared to LPS (100μg/ml) + IFN- γ (100U/ml).

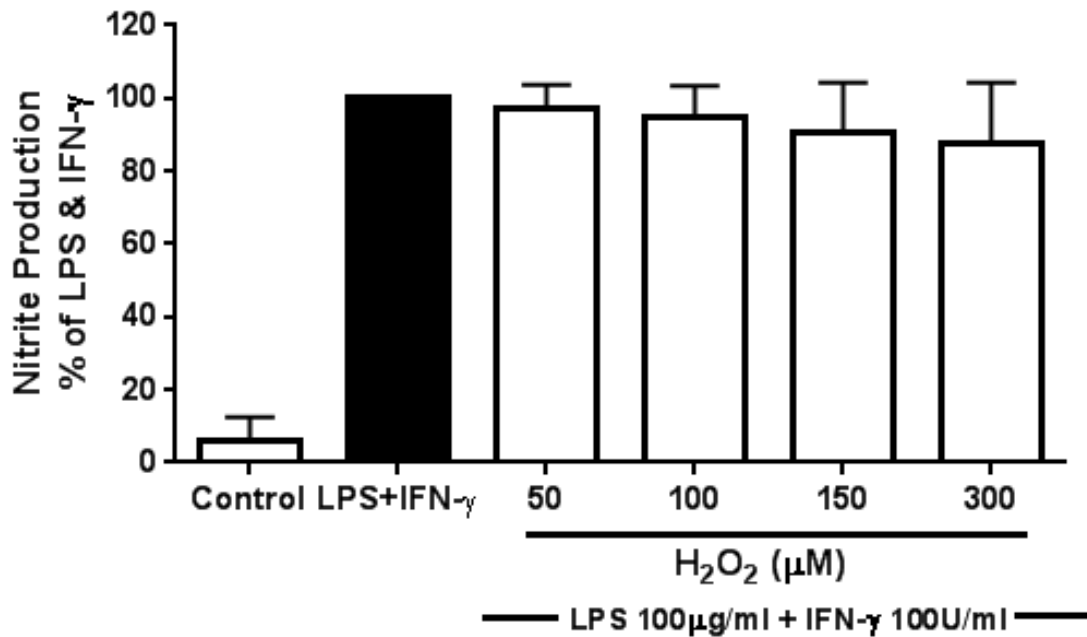


Figure 3.9 Effects of H₂O₂ on nitrite production in LPS and IFN-γ activated RASMCs

Confluent monolayer of RASMCs in 24-well plate was pre-treated with complete culture medium alone or medium containing H₂O₂ (50 μM, 100 μM, 150 μM and 300 μM) for 30 minutes prior to incubation with LPS (100 μg/ml) and IFN-γ (100 U/ml) for a further 24 hrs. Nitrite production was determined as described in the methods (section 2.3). The data is expressed as % nitrite production with the response to LPS (100 μg/ml) + IFN-γ (100 U/ml) taken as 100%. The data represents the means ± S.E.M of at least three independent experiments.

3.5 Effect of OS inducers on the expression of the inducible nitric oxide synthase (iNOS)

To determine the effect of OS inducers on the expression of iNOS, cells were pre-treated with different concentrations of DEM, antimycin A and H₂O₂ for 30 minutes before incubating the cells with LPS (100 µg/ml) and IFN-γ (100 U/ml) for 24 hrs as described in the methods. After 24 hrs, lysates were collected and western blotting was performed to determine the expression of iNOS as described in the methods (section 2.7). In control cells, there was little or no expression of iNOS. Diethyl maleate caused a 15%, 40%, 70% and 90% reduction in the levels of iNOS with 1 µM, 2.5 µM, 5 µM and 10 µM respectively (Figure 3.10) whereas antimycin A caused a 10%, 40%, 70% and 80% reduction with 25 µM, 50 µM, 100 µM and 150 µM respectively (Figure 3.11) when compared to LPS and IFN-γ alone. In contrast to DEM and antimycin A, and consistent with the nitrite data, H₂O₂ (50-300 µM) failed to cause any decrease in the expression of iNOS when compared to LPS and IFN-γ alone as shown in figure 3.12.

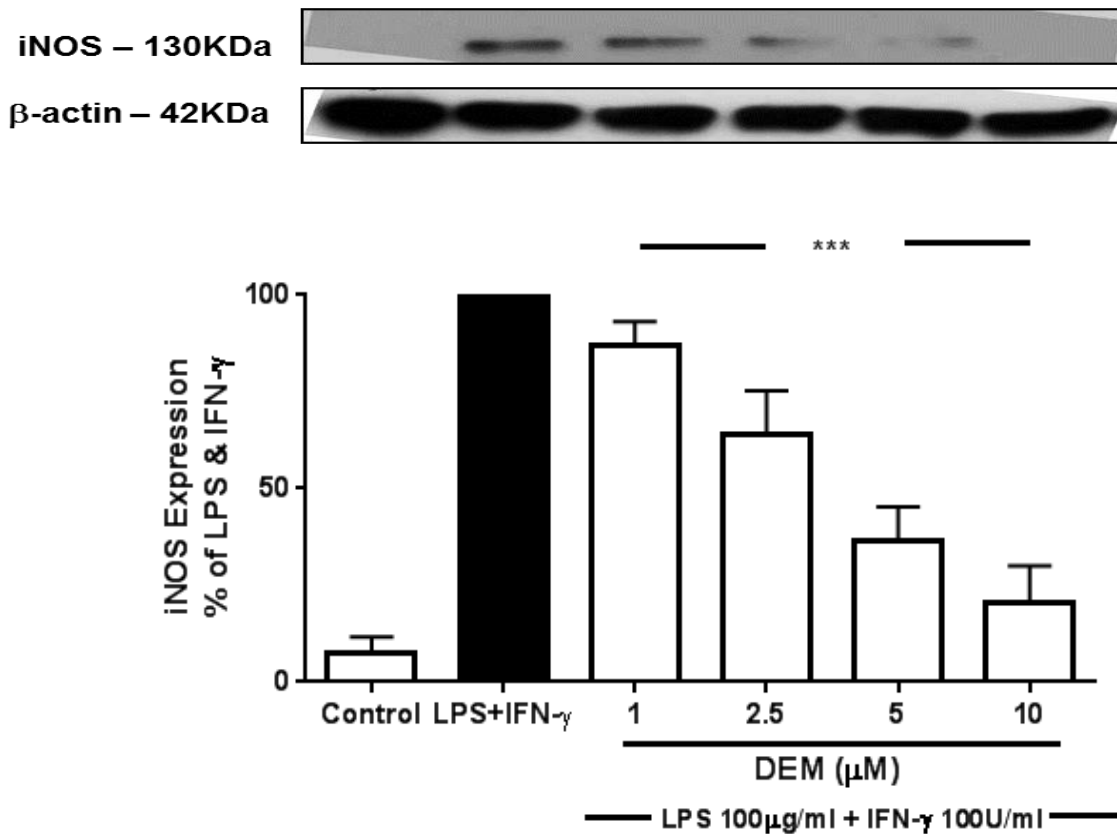


Figure 3.10 Effects of DEM on iNOS expression in LPS and IFN- γ activated RASMCs

Confluent monolayer of RASMCs in 24-well plates were pre-treated with complete culture medium alone or medium containing DEM (1 μ M, 2.5 μ M, 5 μ M and 10 μ M) for 30minutes prior to incubation with LPS (100 μ g/ml) and IFN- γ (100U/ml) for a further 24hrs. The expression of iNOS was determined by western blotting as described in the methods (section 2.7).The blot is representative of at least three independent experiments and the bar graph is the densitometric data expressed as % iNOS expression with LPS (100 μ g/ml) + IFN- γ (100U/ml) response taken as 100%. The data represents the means \pm S.E.M of at least three independent experiments.***denote $p < 0.001$ when compared to LPS (100 μ g/ml) + IFN- γ (100U/ml).

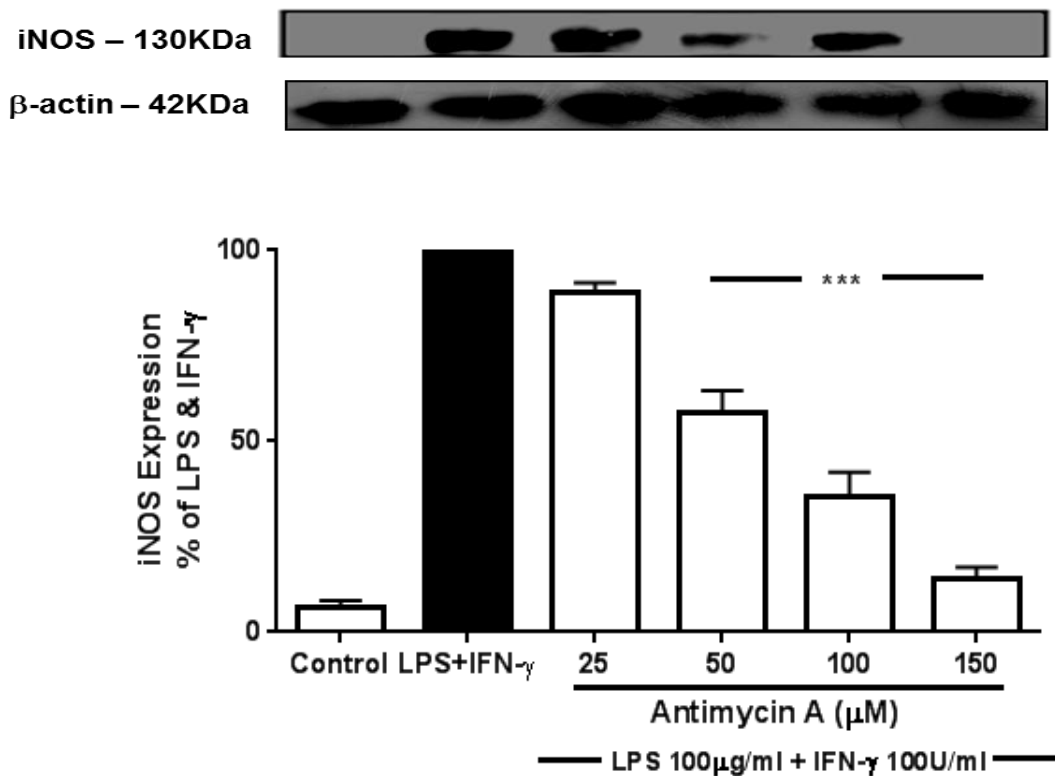


Figure 3.11 Effects of antimycin A on iNOS expression in LPS and IFN- γ activated RASMCs

Confluent monolayers of RASMCs in 24-well plate were pre-treated with complete culture medium alone or medium containing antimycin A (25 μ M, 50 μ M, 100 μ M and 150 μ M) for 30minutes prior to incubation with LPS (100 μ g/ml) and IFN- γ (100U/ml) for a further 24hrs. The expression of iNOS was determined by western blotting as described in the methods (section 2.7). The blot is representative of at least three independent experiments and the bar graph is the densitometric data expressed as % iNOS expression with LPS (100 μ g/ml) + IFN- γ (100U/ml) response taken as 100%. The data represents the means \pm S.E.M of at least three independent experiments. ***denote $p < 0.001$ when compared to LPS (100 μ g/ml) + IFN- γ (100U/ml).

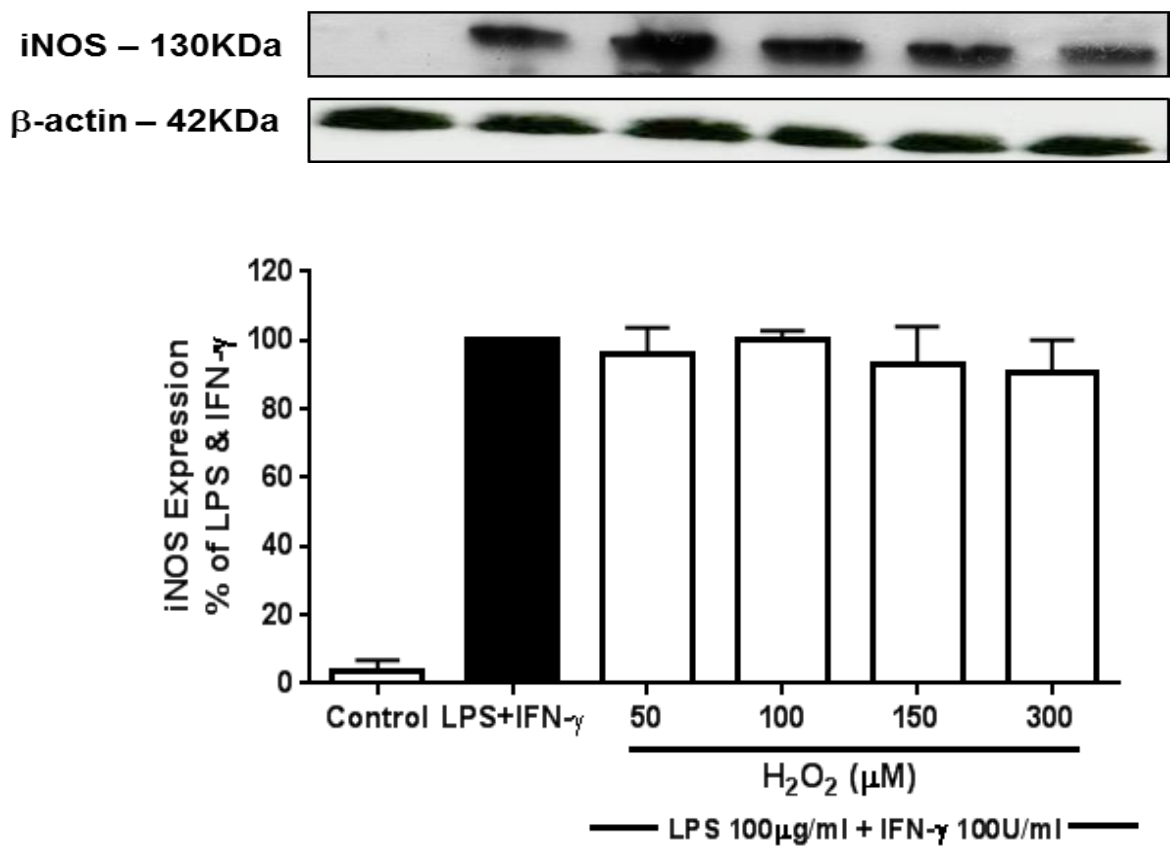


Figure 3.12 Effects of H₂O₂ on iNOS expression in LPS and IFN-γ activated RASMCs

Confluent monolayers of RASMCs in 24-well plate were pre-treated with complete culture medium alone or medium containing H₂O₂ (50μM, 100μM, 150μM and 300μM) for 30 minutes prior to incubation with LPS (100μg/ml) and IFN-γ (100U/ml) for a further 24hrs. The expression of iNOS was determined by western blotting as described in the methods (section 2.7). The blot is representative of at least three independent experiments and the bar graph is the densitometric data expressed as % iNOS expression with LPS (100μg/ml) + IFN-γ (100U/ml) response taken as 100%. The data represents the means ± S.E.M of at least three independent experiments.

3.6 Effect of OS inducers on iNOS mRNA expression in control and activated RASMCs

To determine whether OS inducers regulated iNOS expression at the transcriptional level, analysis of changes in iNOS mRNA was carried out. In these studies, cells were pre-treated with different concentrations of DEM (1-10 μ M), antimycin A (25-150 μ M) or H₂O₂ (50-300 μ M) for 30 minutes before incubating with LPS (100 μ g/ml) and IFN- γ (100 U/ml) for 24hrs. The fold change in iNOS mRNA expression was determined by performing real-time PCR as described in the methods (section 2.9). Control cells showed little or no iNOS mRNA. Cells treated with LPS and IFN- γ alone showed significant expression of iNOS mRNA and this was considered as maximum. Diethyl maleate caused a 20%, 40%, 60% and 70% reductions in LPS and IFN- γ induced iNOS mRNA at concentrations of 1 μ M, 2.5 μ M, 5 μ M and 10 μ M respectively (Figure 3.13). Antimycin A caused a 50%, 60%, 80% and 90% reduction with 25 μ M, 50 μ M, 100 μ M and 150 μ M respectively (Figure 3.14) when compared to LPS and IFN- γ alone. In contrast H₂O₂ (50-300 μ M) did not cause any inhibition and the folds of iNOS mRNA expression were found to be similar to that of LPS and IFN- γ alone (Figure 3.15). These findings are consistent with the trends reported earlier for iNOS expression and NO production.

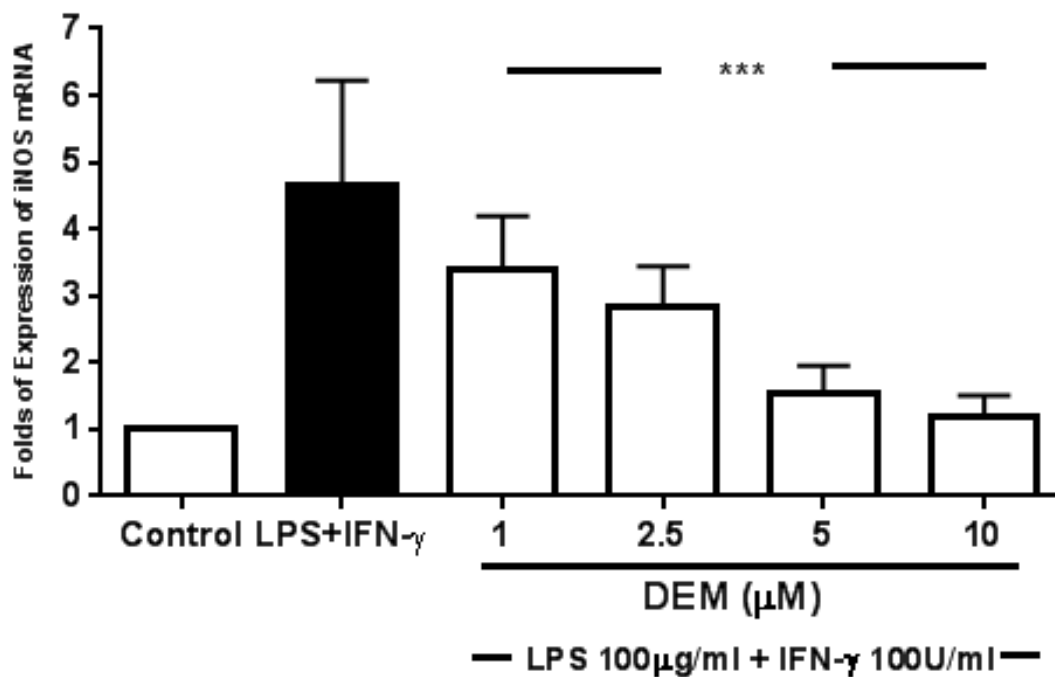


Figure 3.13 Effects of DEM on iNOS mRNA in LPS and IFN- γ activated RASMCs

Confluent monolayers of RASMCs in T-25 flasks were pre-treated with complete culture medium alone or medium containing DEM (1µM, 2.5µM, 5µM and 10µM) for 30minutes prior to incubation with LPS (100µg/ml) and IFN- γ (100U/ml) for a further 24hrs. The levels of iNOS mRNA was determined as described in the methods (section 2.9). The data represents the fold change in expression of iNOS mRNA and is the means \pm S.E.M of at least three independent experiments.*** denote $p < 0.001$ when compared to LPS (100µg/ml) and IFN- γ (100U/ml).

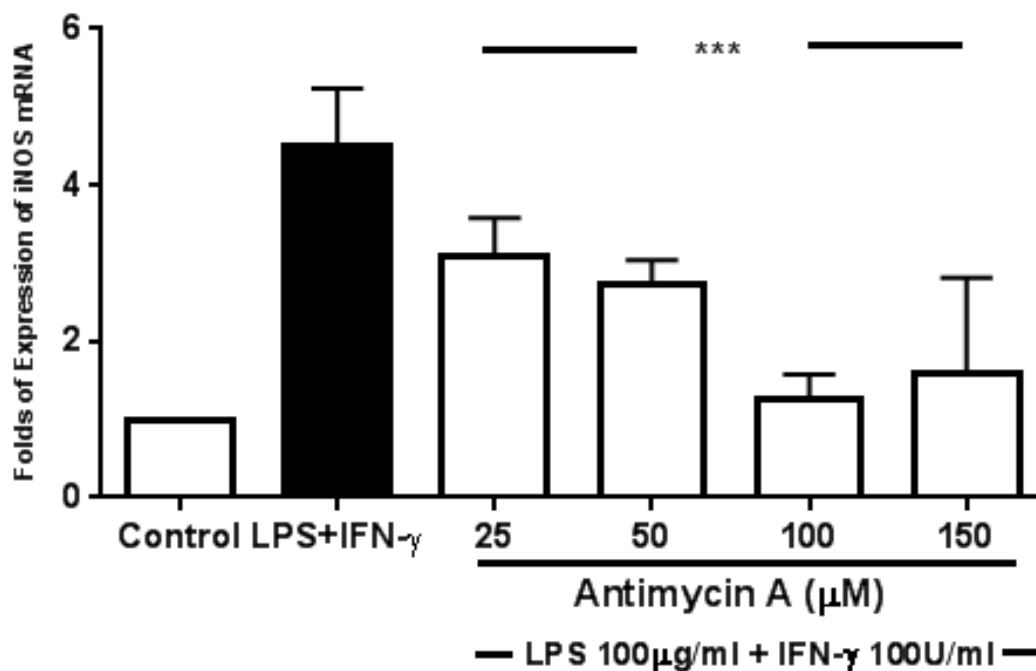


Figure 3.14 Effects of antimycin A on iNOS mRNA in LPS and IFN- γ activated RASMCs

Confluent monolayers of RASMCs in T-25 flasks were pre-treated with complete culture medium alone or medium containing antimycin A (25µM, 50µM, 100µM and 150µM) for 30minutes prior to incubation with LPS (100µg/ml) and IFN- γ (100U/ml) for a further 24hrs. The levels of iNOS mRNA was determined as described in the methods (section 2.9). The data represents the fold change in expression of iNOS mRNA and is the means \pm S.E.M of at least three independent experiments.*** denote $p < 0.001$ when compared to LPS (100µg/ml) and IFN- γ (100U/ml).

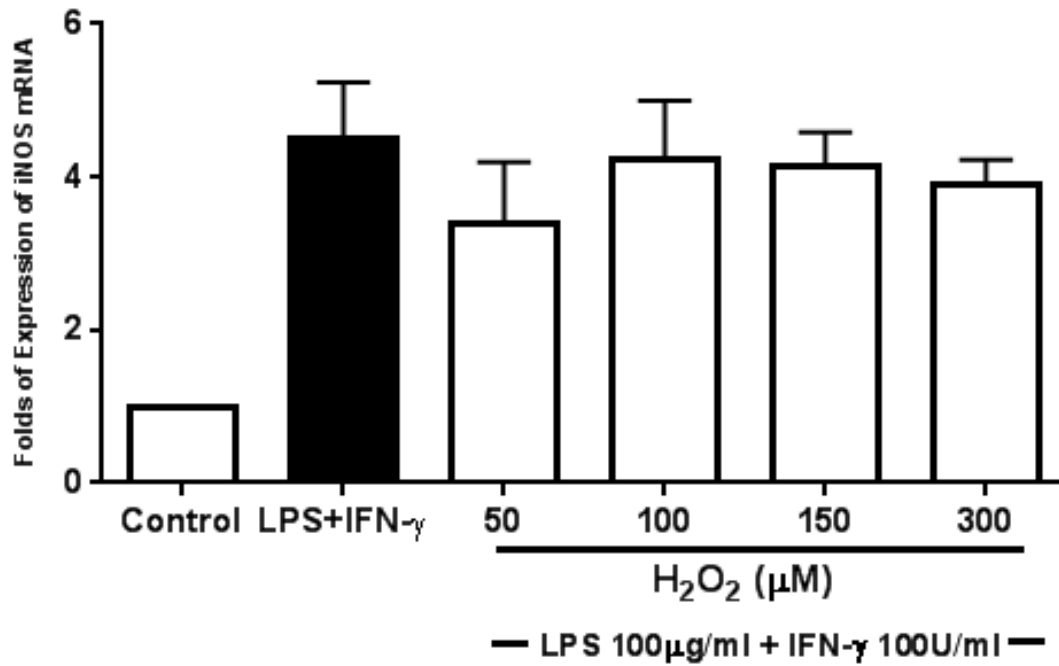


Figure 3.15. Effects of H₂O₂ on iNOS mRNA in LPS and IFN- γ activated RASMCs

Confluent monolayers of RASMCs in T-25 flasks were pre-treated with complete culture medium alone or medium containing H₂O₂ (50 μ M, 100 μ M, 150 μ M and 300 μ M) for 30 minutes prior to incubation with LPS (100 μ g/ml) and IFN- γ (100 U/ml) for a further 24 hrs. The levels of iNOS mRNA was determined as described in the methods (section 2.9). The data represents the fold change in expression of iNOS mRNA and is the means \pm S.E.M of at least three independent experiments.

3.7 Effect of OS inducers on free radical generation

To determine the effect of OS inducers on overall free radical generation, cells were treated with DEM (1-10 μ M), antimycin A (25-150 μ M) or H₂O₂ (50-300 μ M) for 24hrs before incubating with the general ROS detecting dye, 7-dichlorofluorescein (20 μ M) for 10minutes. Cells were then washed with PBS (x1) and viewed under a confocal microscope as described in the methods (section 2.8). Control cells showed little or no detectable levels of free radicals. All three OS inducers on the other hand caused significant generation of free radicals. The highest concentration of each of these OS inducers was taken as 100% and compared to the different concentrations used in the studies respectively. Diethyl maleate at 10 μ M caused the maximum effect whereas 1 μ M increased free radical generation by 50-60% when compared to control (Figure 3.16). With antimycin A, free radical generation was estimated at 30-40% when compared to the maximum levels generated with a concentration of 100 μ M as shown in figure 3.17. Hydrogen peroxide at 50 μ M generated 40-50% and when compared to the maximum 300 μ M (Figure 3.18).

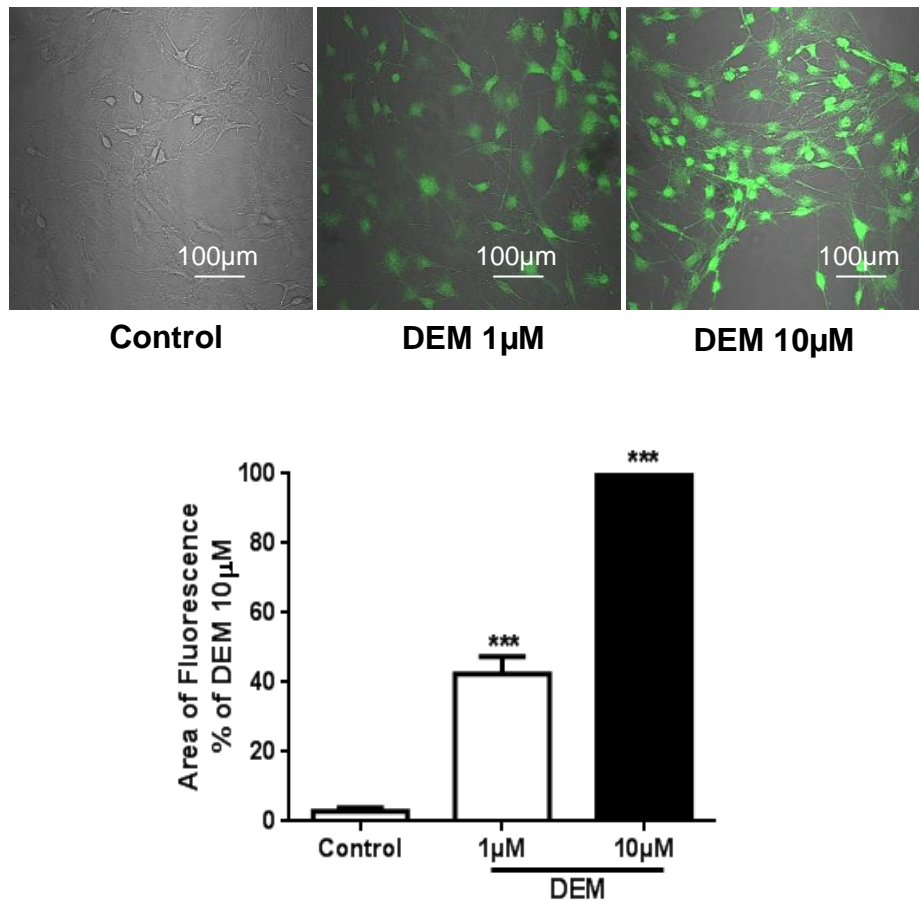


Figure 3.16 Effect of DEM on free radical generation in RASMCs

RASMCs were plated into an 8-well Lab-Tek plate at a seeding density of 30-40% and grown to 60-70% confluency. Cells were then treated with complete culture medium alone or medium containing DEM (1-10 μM) for 24 hrs. Cells were further incubated with 2, 7-dichlorofluorescein (20 μM) for 10 minutes at 37°C, washed with PBS (x1) 3 times with 5 min each wash and then viewed under a Nikon™ TE-2000 confocal laser scanning microscope as described in the methods (section 2.8). The photographs are representative of at least 3 individual experiments. The bar graph is presented as the % area of fluorescence with the response to 10 μM DEM taken as 100%. The data represents the means ± S.E.M of at least three independent experiments. *** denote p < 0.001 when compared to control.

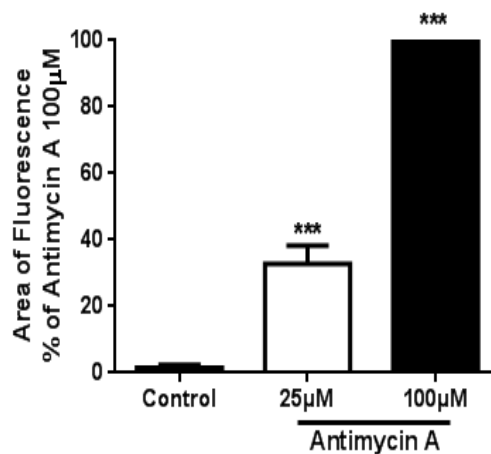
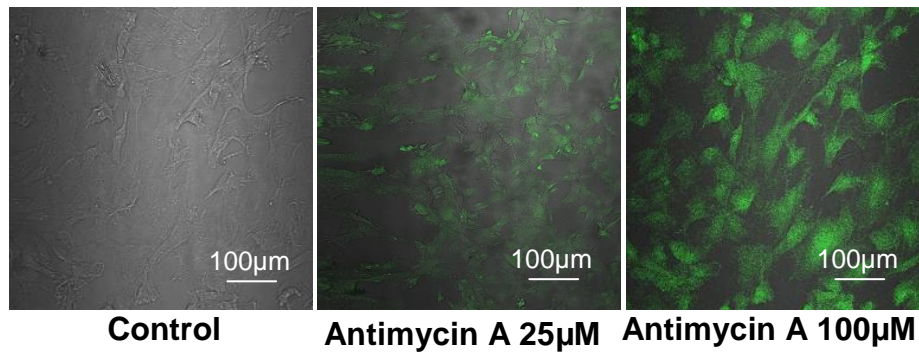


Figure 3.17 Effect of antimycin A on free radical generation in RASMCs

RASMCs were plated into an 8-well Lab-Tek plate at a seeding density of 30-40% and grown to 60-70% confluency. Cells were then treated with complete culture medium alone or medium containing antimycin A (25-150µM) for 24hrs. Cells were further incubated with 2, 7-dichlorofluorescein (20µM) for 10minutes at 37°C, washed with PBS (x1) 3 times with 5min each wash and then viewed under a Nikon™ TE-2000 confocal laser scanning microscope as described in the methods (section 2.8). The photographs are representative of at least 3 individual experiments. The bar graph is presented as the % area of fluorescence with the response to 150µM antimycin A taken as 100%. The data represents the means ± S.E.M of at least three independent experiments. *** denote $p < 0.001$ when compared to control.

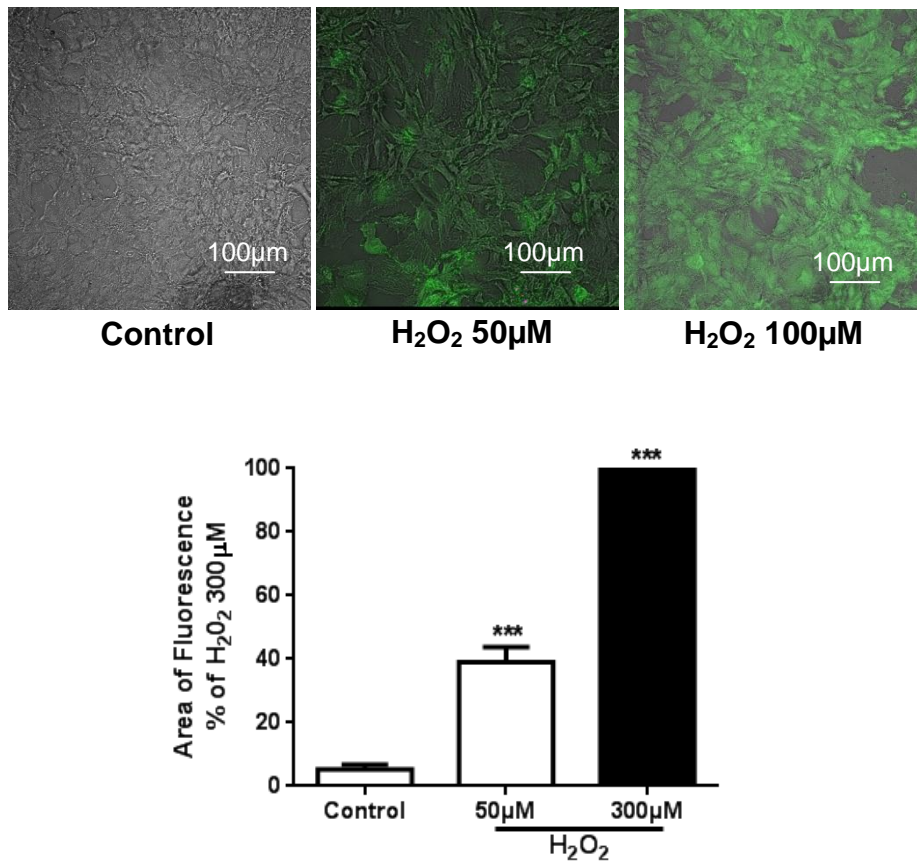
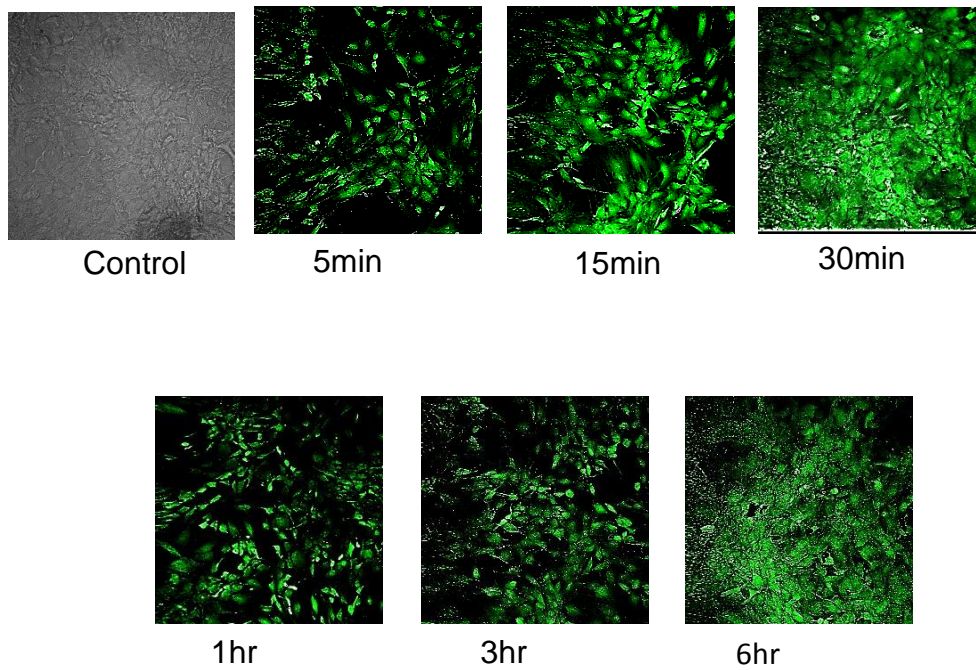


Figure 3.18 Effect of H₂O₂ on free radical generation in RASMCs

RASMCs were plated into an 8-well Lab-Tek plate at a seeding density of 30-40% and grown to 60-70% confluency. Cells were then treated with complete culture medium alone or medium containing H₂O₂ (50-300µM) for 24hrs. Cells were further incubated with 2, 7-dichlorofluorescein (20µM) for 10minutes at 37⁰C, washed with PBS (x1) 3 times with 5min each wash and then viewed under a Nikon™ TE-2000 confocal laser scanning microscope as described in the methods (section 2.8). The photographs are representative of at least 3 individual experiments. The bar graph is presented as the % area of fluorescence with the response to 300µM H₂O₂ taken as 100%. The data represents the means ± S.E.M of at least three independent experiments. *** denote p<0.001 when compared to control.

3.8 Time dependent induction of free radical generation by OS inducers

To determine the time and onset of free radical generation, cells were treated with DEM (10 μ M), antimycin A (100 μ M) or H₂O₂ (300 μ M) for 1min, 5min, 15min, 30min, 1hr, 3hr and 6hr before incubating the cells with 2, 7-dichlorofluorescein (20 μ M) for 10minutes at 37⁰C. Cells were then washed with PBS (x1) and viewed under the confocal microscope as described in the methods (section 2.8). Control cells generated little or no free radicals over the 24hr period. All three OS inducers generated detectable amounts of free radicals at different time points with the maximum amounts detected at 6hr. Hence this was considered as the peak and was taken as 100% when compared to different time points. Antimycin A caused significant (70%) generation of free radicals as early as 5min and reaching a peak at 6hr (Figure 3.19) whereas DEM (Figure 3.20) and H₂O₂ (Figure 3.21) caused 40% and 20% generation of free radicals respectively at 5min but increasing over time to reach a peak at 6hr. Of the three agents, antimycin A generated 30% more free radicals as early as 5min when compared to DEM or H₂O₂ suggesting that it was quick and more effective at inducing free radical production.



Scale bar - 50 μ m

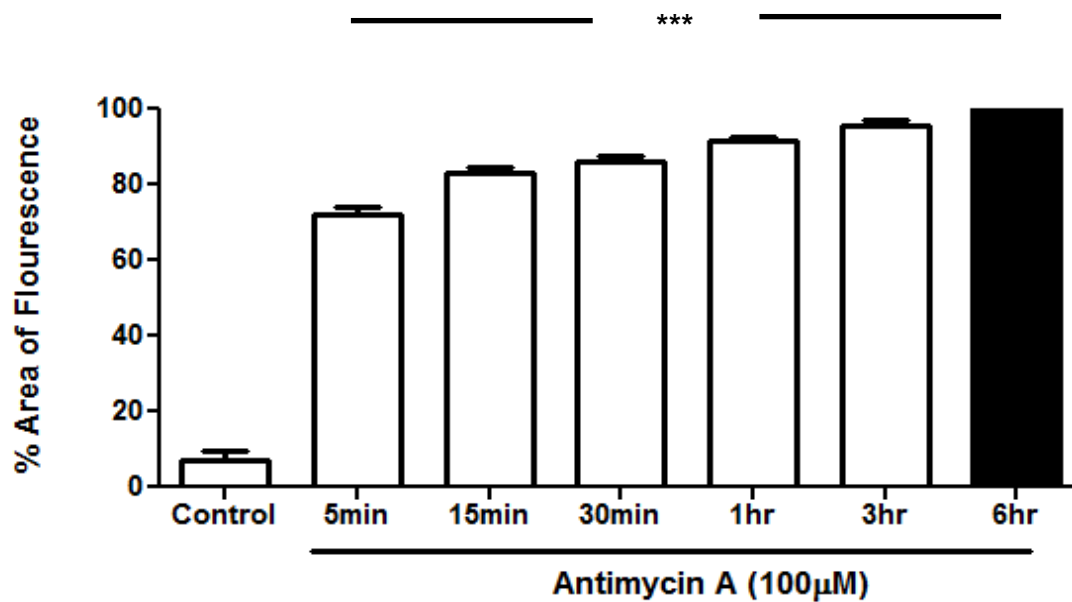
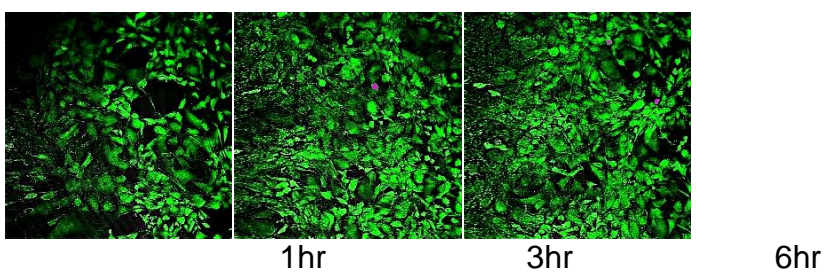
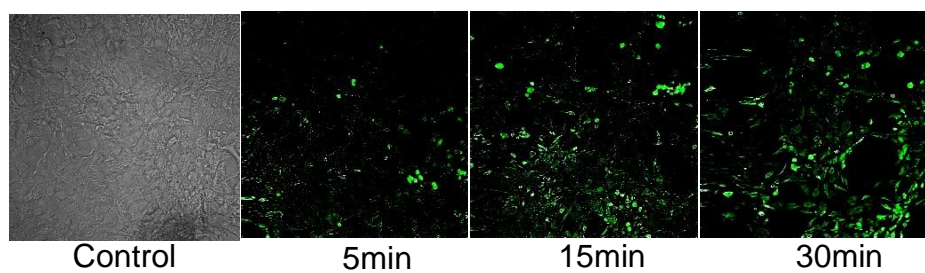


Figure 3.19 Time dependent induction of free radical generation in RASMCs by antimycin A

RASMCs were plated into an 8-well Lab-Tek plate at a seeding density of 30-40% and grown to 60-70% confluency. Cells were then treated with complete culture medium alone or medium containing 100 μ M antimycin A for 5min, 15min, 30min, 1hr, 3hr and 6hr. Cells were further incubated with 2, 7-dichlorofluorescein (20 μ M) for 10 minutes at 37⁰C, washed with PBS (x1) 3 times with 5min each wash and then viewed under a NikonTM TE-2000 confocal laser scanning microscope as described in the methods (section 2.8). The photographs are representative of at least 3 individual experiments. The bar graph is presented as % area of fluorescence with the response to 6hr time point taken as 100%. The data represents the means \pm S.E.M of at least three independent experiments. *** denote $p < 0.001$ when compared to control.



Scale bar - 50 μ m

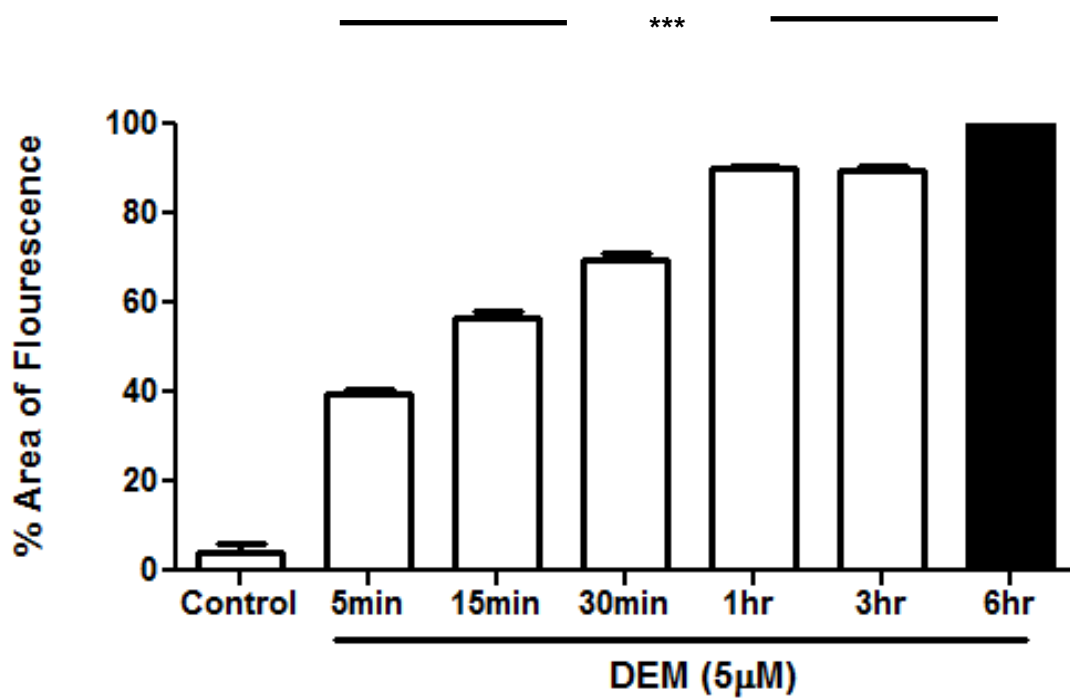


Figure 3.20 Time dependent induction of free radical generation in RASMCs by DEM

RASMCs were plated into an 8-well Lab-Tek plate at a seeding density of 30-40% and grown to 60-70% confluency. Cells were then treated with complete culture medium alone or medium containing 5 μ M DEM for 5min, 15min, 30min, 1hr, 3hr and 6hr. Cells were further incubated with 2, 7-dichlorofluorescein (20 μ M) for 10 minutes at 37⁰C, washed with PBS (x1) 3 times with 5min each wash and then viewed under a NikonTM TE-2000 confocal laser scanning microscope as described in the methods (section 2.8). The photographs are representative of at least 3 individual experiments. The bar graph is presented as % area of fluorescence with the response to 6hr time point taken as 100%. The data represents the means \pm S.E.M of at least three independent experiments. *** denote $p < 0.001$ when compared to control.

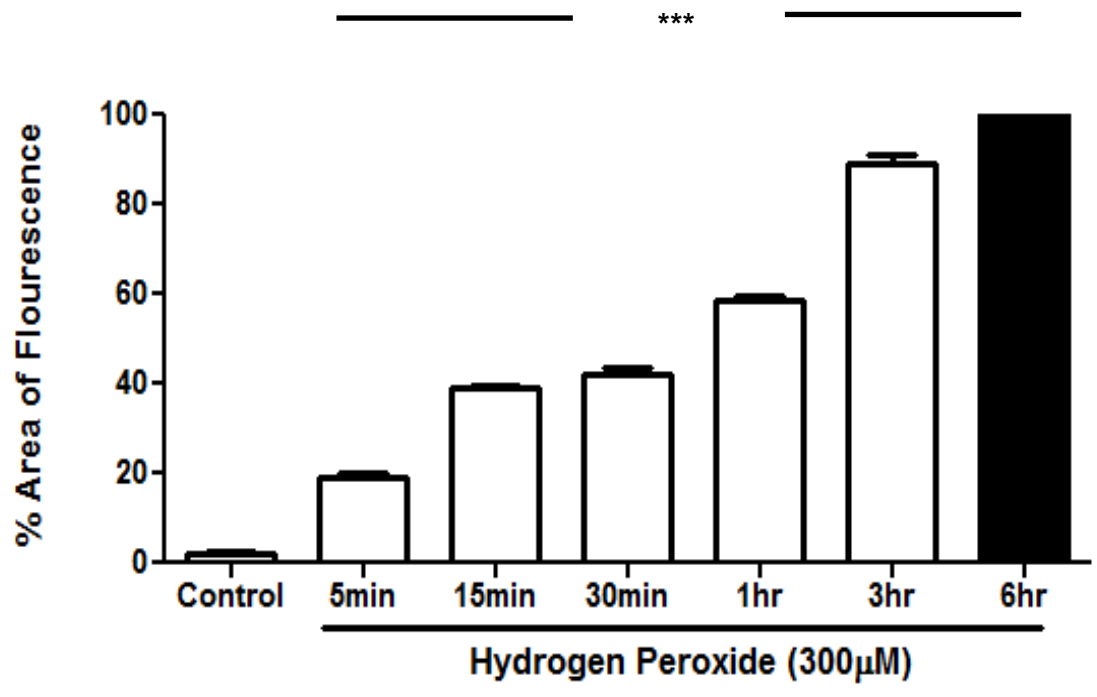
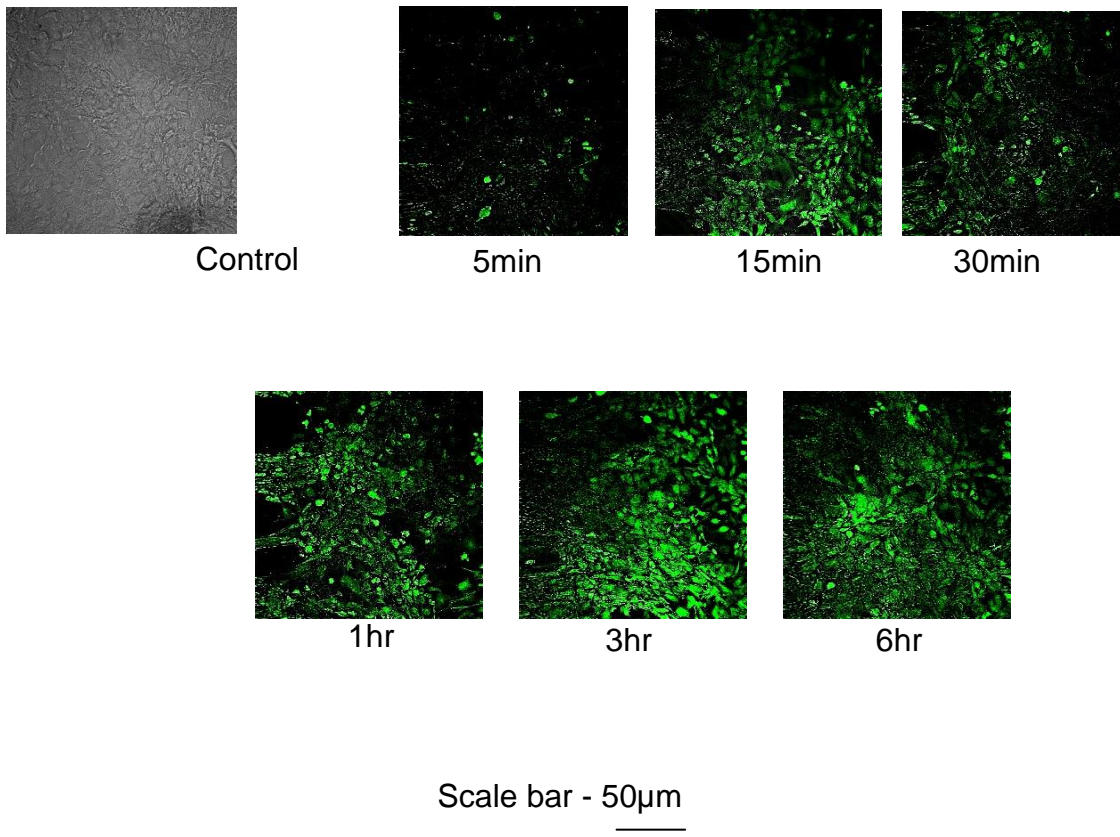


Figure 3.21 Time dependent induction of free radical generation in RASMCs by H_2O_2

RASMCs were plated into an 8-well Lab-Tek plate at a seeding density of 30-40% and grown to 60-70% confluency. Cells were then treated with complete culture medium alone or medium containing 300 μ M H₂O₂ for 5min, 15min, 30min, 1hr, 3hr and 6hr. Cells were further incubated with 2, 7-dichlorofluorescein (20 μ M) for 10minutes at 37⁰C, washed with PBS (x1) 3 times with 5min each wash and then viewed under a NikonTM TE-2000 confocal laser scanning microscope as described in the methods (section 2.8). The photographs are representative of at least 3 individual experiments. The bar graph is presented as % area of fluorescence with the response to 6hr time point taken as 100%. The data represents the means \pm S.E.M of at least three independent experiments. *** denote p<0.001 when compared to control.

3.9 Induction of superoxide radicals by OS inducers

The data presented above show that all three OS inducers generated significant amount of free radicals but as 2, 7-dichlorofluorescein does not distinguish between ROS species, further experiments were carried out using the novel fluorogenic dye MitoSOX red, which is oxidised specifically by superoxide radicals. Cells were treated with DEM (10 μ M), antimycin A (100 μ M) or H₂O₂ (300 μ M) for 24hrs before incubating with MitoSOX red (5 μ M) for 10minutes. Cells were then washed with Hank's balanced salt solution (HBSS) 3 times before viewing under the confocal microscope as described in the methods (section 2.8). Superoxide radical production was at low basal levels in control cells but significantly induced by both antimycin A (100 μ M) and by DEM (10 μ M), the latter inducing ~70% of the levels detected with antimycin A as shown in figure 34. Interestingly, H₂O₂ (300 μ M) initiated relatively little (15%) superoxide radical when compared to antimycin A (Figure 3.22).

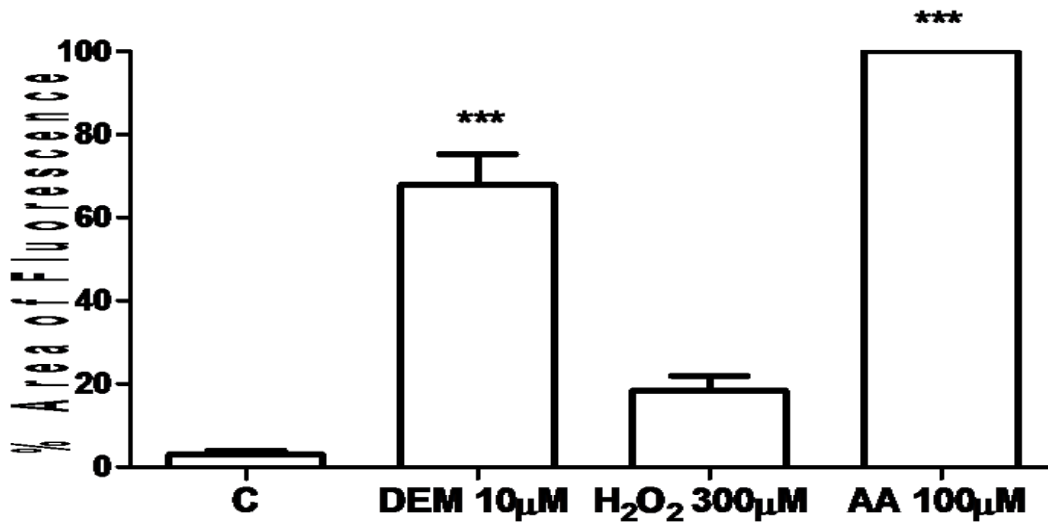
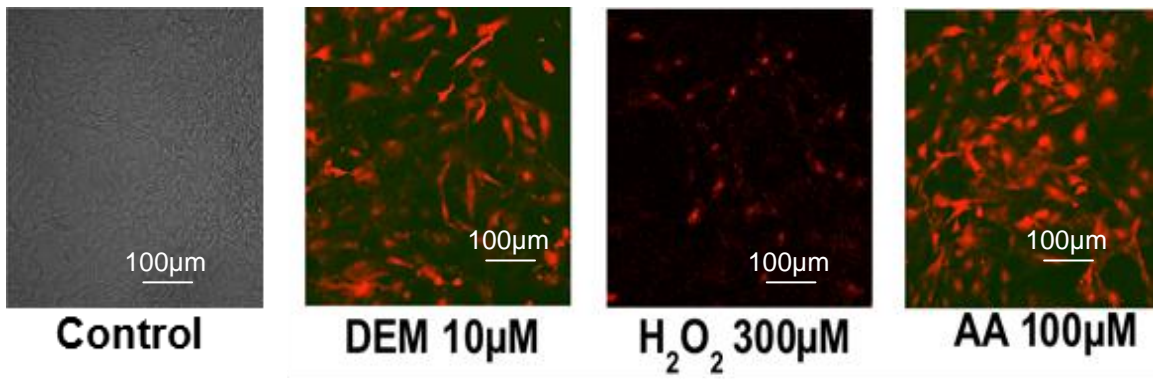


Figure 3.22 Induction of superoxide radicals by OS inducers in cultured RASMCs

RASMCs were seeded into a 12-well plate at 30-40% confluency and grown to 50-60% confluency. Cells were then treated with complete culture medium alone or medium containing DEM (10 μ M), H₂O₂ (300 μ M) or antimycin A (100 μ M) for 24hrs. Cells were further incubated with MitoSOX for 10minutes and washed with HBSS 3 times with 5minutes interval between washes before viewing under the a NikonTM TE-2000 confocal laser scanning microscope as described in the methods (section 2.8). The photographs are representative of at least 3 individual experiments. The bar graph is presented as % area of fluorescence with the response to antimycin A (100 μ M) taken as 100%. The data represents the means \pm S.E.M of at least three independent experiments. *** denote p<0.001 when compared to control.

3.10 Effect of Polyethylene glycol-superoxide dismutase (PEG-SOD) on superoxide radical generation in the presence and absence of OS inducers

To establish that OS inducers did indeed induce O_2^- production, further experiments were carried out using the cell permeable O_2^- scavenger, PEG-SOD. Cells were pre-treated with PEG-SOD (500 U/ml) for 30 minutes before incubating with DEM (10 μ M), antimycin A (100 μ M) or H_2O_2 (300 μ M) for another 30 minutes. Cells were then further treated with MitoSOX red (5 μ M) for 10 minutes at 37⁰C, washed with HBSS 3 times with 5 minutes each wash before viewing under the confocal microscope as described in the methods (section 2.8). Control cells and cells treated with de-ionised water or PEG-SOD (500 U/ml) did not generate any superoxide radical whereas DEM (10 μ M) and antimycin A (100 μ M) but not H_2O_2 (300 μ M) induced significant amount of superoxide radical. Pre-treatment with PEG-SOD (500 U/ml) significantly inhibited superoxide radical generation induced by either antimycin A or DEM reducing the latter by 30-40% and that by antimycin A by 40% (Figure 3.23).

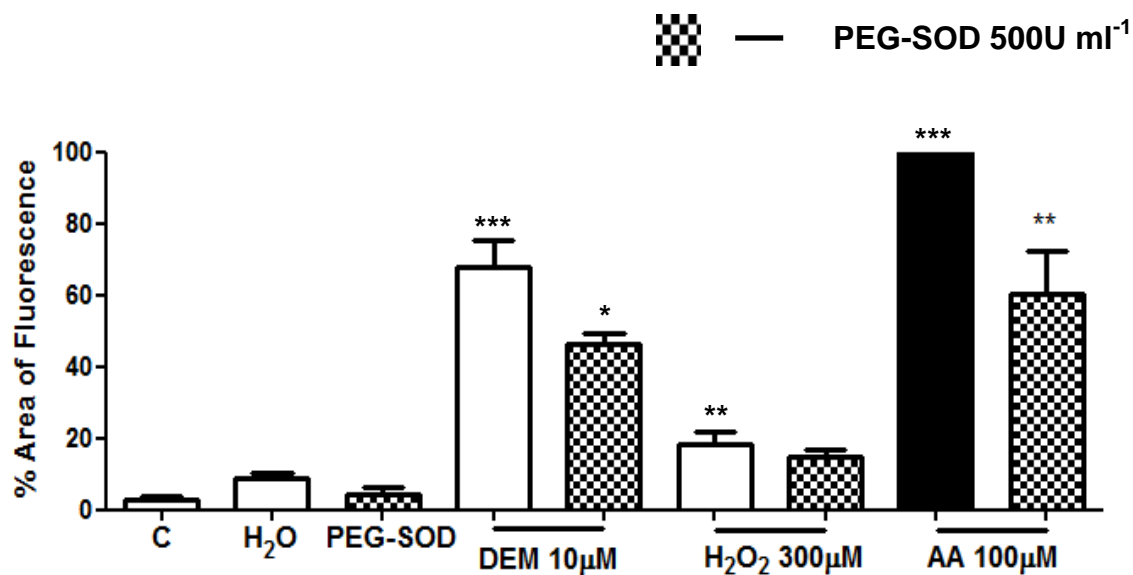
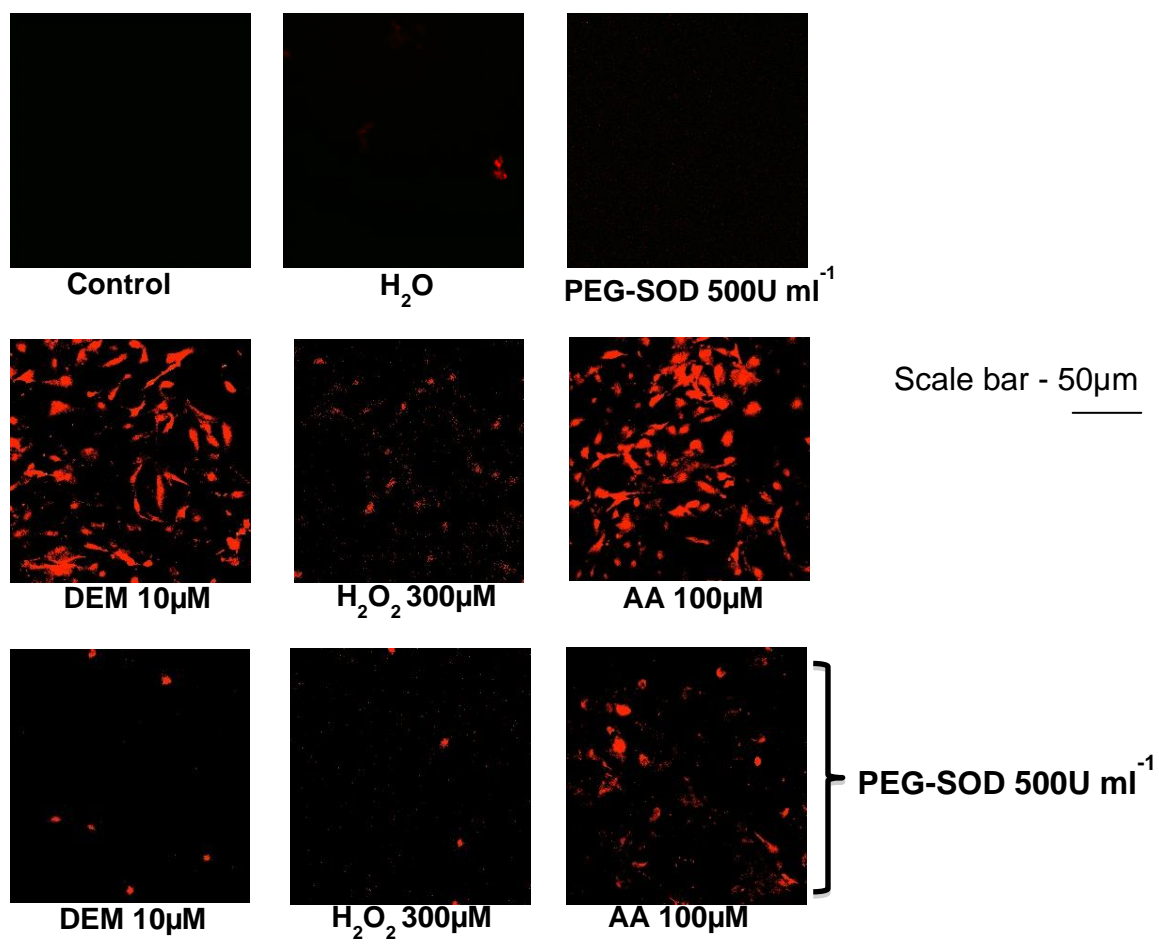


Figure 3.23 Effect of PEG-SOD on superoxide radical generation in the presence of OS inducers in RASMCs

RASMCs were seeded into a 12-well plate at 30-40% confluency and grown to 50-60% confluency. Cells were then treated with complete culture medium alone or medium containing PEG-SOD (500U ml^{-1}) for 30 minutes prior to incubation with DEM ($10\mu\text{M}$), H_2O_2 ($300\mu\text{M}$) and antimycin A ($100\mu\text{M}$) for 24hrs. Cells were further incubated with MitoSOX for 10 minutes and washed with HBSS 3 times with 5 minutes interval between washes before viewing under a NikonTM TE-2000 confocal laser scanning microscope as described in the methods (section 2.8). The photographs are representative of at least 3 individual experiments. The bar graph is presented as % area of fluorescence with the response to antimycin A ($100\mu\text{M}$) taken as 100%. The data represents the means \pm S.E.M of at least three independent experiments. * denote $p < 0.05$ and ** denote $p < 0.01$ when compared to DEM and antimycin A with or without PEG-SOD.

3.11 Effect of Polyethylene glycol-catalase (PEG-catalase) on superoxide radical generation in the presence and absence of OS inducers

In addition to PEG-SOD, experiments were carried out using the cell permeable OH⁻ scavenger, PEG-catalase to determine whether part of the signal detected could be mediated by OH⁻. Cells were pre-treated with PEG-catalase (500 U/ml) for 30 minutes before incubating the cells with DEM (10 μM), antimycin A (100 μM) or H₂O₂ (300 μM) for a further 30 minutes. Cells were then further treated with MitoSOX red (5 μM) for 10 minutes at 37⁰C, washed with HBSS 3 times before viewing under the confocal microscope as described in the methods (section 2.8). As already reported for PEG-SOD, control cells and cells treated with de-ionised water or PEG-catalase (500 U/ml) did not generate any superoxide radical whereas DEM (10 μM) and antimycin A (100 μM) but not H₂O₂ (300 μM) induced significant amount of superoxide radical. Antimycin A alone was taken as 100% as it caused maximum generation of superoxide radical. Interestingly, pre-treatment with PEG-catalase (500 U/ml) altered ROS production by all three OS inducers but this effect was less significant for DEM when compared to antimycin A or H₂O₂ (Figure 3.24).

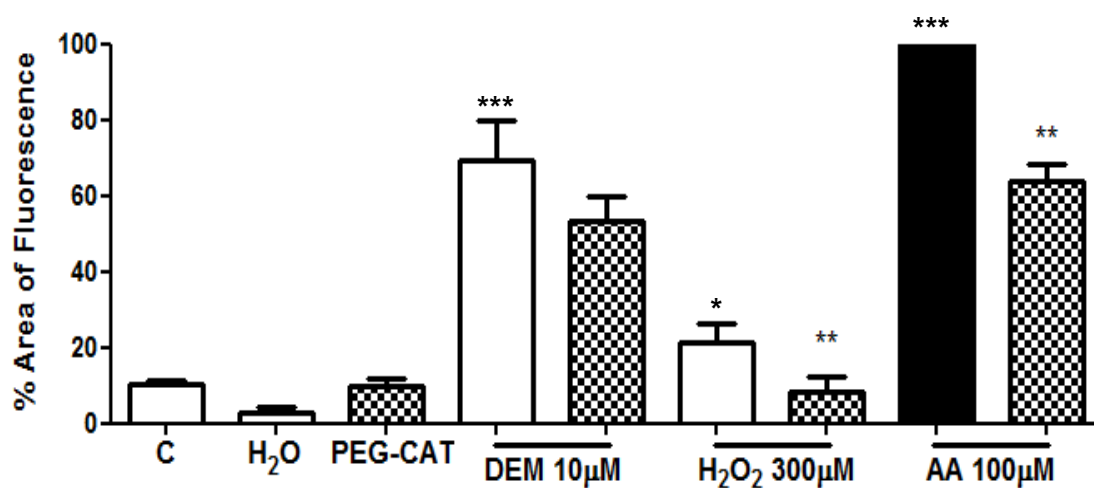
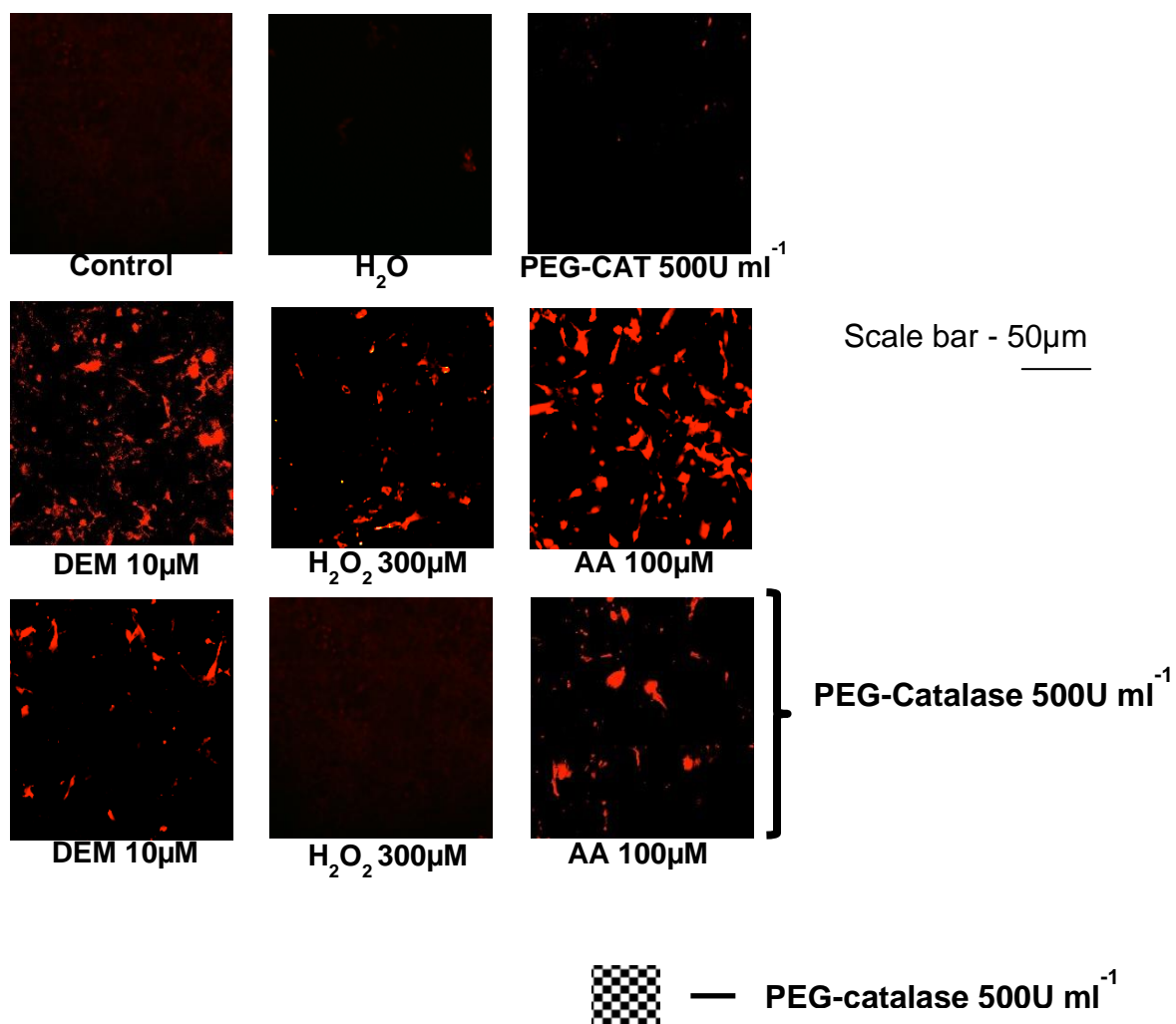


Figure 3.24 Effect of PEG-catalase on superoxide radical generation in the presence of OS inducers in RASMCs

RASMCs were seeded into a 12-well plate at 30-40% confluency and grown to 50-60% confluency. Cells were then treated with complete culture medium alone or medium containing PEG-CAT (500U ml^{-1}) for 30 minutes prior to incubation with DEM ($10\mu\text{M}$), H_2O_2 ($300\mu\text{M}$) and antimycin A ($100\mu\text{M}$) for 24hrs. Cells were further incubated with MitoSOX for 10minutes and washed with HBSS 3 times with 5minutes interval between washes before viewing under a NikonTM TE-2000 confocal laser scanning microscope as described in the methods (section 2.8). The photographs are representative of at least 3 individual experiments. The bar graph is presented as area of fluorescence with the response to antimycin A ($100\mu\text{M}$) taken as 100%. The data represents the means \pm S.E.M of at least three independent experiments. ** denote $p < 0.01$ when compared to H_2O_2 and antimycin A with or without PEG-catalase.

3.12 Effect of polyethylene glycol-superoxide dismutase (PEG-SOD) on nitrite production in the presence and absence of OS inducers

Since O_2^- appear to be a major ROS generated by DEM and antimycin A, studies were carried out to determine the effect of PEG-SOD on the ability of the OS inducers to regulate nitrite production. Cells were pre-treated with PEG-SOD (500 U/ml) for 30 minutes before incubating with DEM (10 μ M), antimycin A (100 μ M) or H_2O_2 (300 μ M) for a further 30 minutes. Cells were then activated with LPS (100 μ g/ml) and IFN- γ (100 U/ml) for 24 hrs as described in the methods (section 2.2.3). Nitrite production was estimated using Griess assay. Control cells and cells treated with PEG-SOD alone did not produce any detectable levels of nitrite. Cells treated with LPS and IFN- γ induced significant amounts of nitrite and the responses were taken as 100%. In the presence of LPS and IFN- γ , PEG-SOD caused a small but significant increase in nitrite production and de-ionised water used, as the vehicle did not alter the LPS and IFN- γ responses. Antimycin A (100 μ M) and DEM (10 μ M) but not H_2O_2 (300 μ M) caused significant reductions in the levels of LPS and IFN- γ induced nitrite production as already reported earlier. These reductions were partially reversed by PEG-SOD at 500 U/ml (Figure 3.25). Cells treated with H_2O_2 (300 μ M) in the presence or absence of PEG-SOD 500 U/ml did not affect nitrite production when compared to LPS and IFN- γ alone (Figure 3.25).

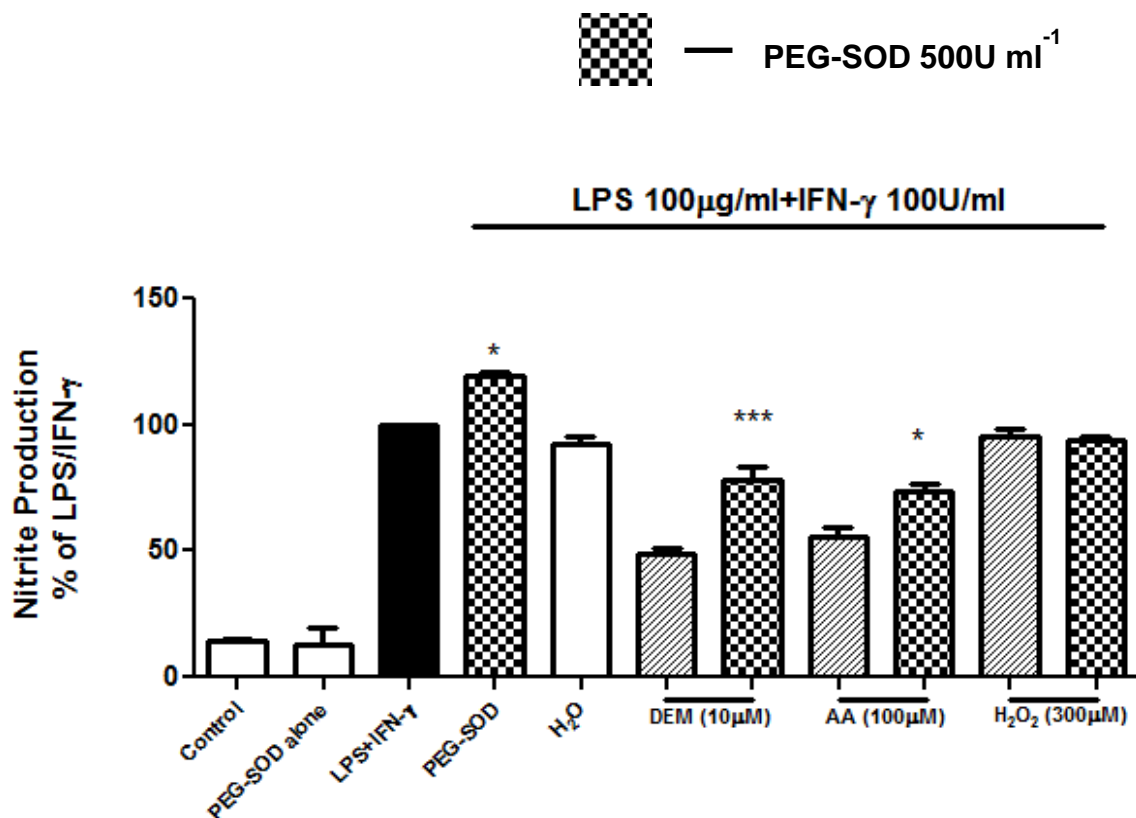


Figure 3.25 Effect of PEG-SOD on nitrite production in the presence and absence of OS inducers in LPS and IFN- γ activated RASMCs

Confluent monolayers of RASMCs in 24-well plate were pre-treated with complete culture medium alone or medium containing PEG-SOD (500U/ml) for 30minutes prior to incubation with DEM (10 μ M), antimycin A (100 μ M) and H₂O₂(300 μ M) for a further 30minutes. Cells were then activated with LPS (100 μ g/ml) and IFN- γ (100U/ml) for 24hrs. Nitrite production was determined as described in the methods (section 2.3). The data is expressed as % nitrite production with the response to LPS (100 μ g/ml) + IFN- γ (100U/ml) taken as 100%. The data represents the means \pm S.E.M of at least three independent experiments. * denote $p < 0.05$ and *** denote $p < 0.001$ when compared to LPS (100 μ g/ml) + IFN- γ (100U/ml).

3.13 Effect of polyethylene glycol-catalase (PEG-catalase) on nitrite production in the presence and absence of OS inducers

To determine the effect of PEG-catalase in the presence and absence of OS inducers on nitrite production, cells were pre-treated with PEG-catalase (500 U/ml) for 30 minutes before incubating with DEM (10 μ M), antimycin A (100 μ M) or H₂O₂ (300 μ M) for a further 30 minutes. Cells were then activated with LPS (100 μ g/ml) and IFN- γ (100 U/ml) for 24 hrs and nitrite production determined using the Griess assay as described in the methods (section 2.3). Control cells and cells treated with PEG-catalase alone did not produce any detectable levels of nitrite. Cells treated with LPS and IFN- γ alone induced significant amount of nitrite and the responses were taken as 100%. In the presence of LPS and IFN- γ , PEG-catalase and de-ionised water, used as the vehicle, did not alter the LPS and IFN- γ responses. Antimycin A (100 μ M) and DEM (10 μ M) but not H₂O₂ (300 μ M) caused a significant reduction in the levels of LPS and IFN- γ induced nitrite production as already reported earlier. PEG-catalase at 500 U/ml did not cause any change in the inhibition of nitrite production caused by DEM (10 μ M) or antimycin A (100 μ M) (Figure 3.26). Cells treated with H₂O₂ (300 μ M) in the presence or absence of PEG-SOD 500 U/ml did not affect nitrite production when compared to LPS and IFN- γ alone (Figure 3.26).

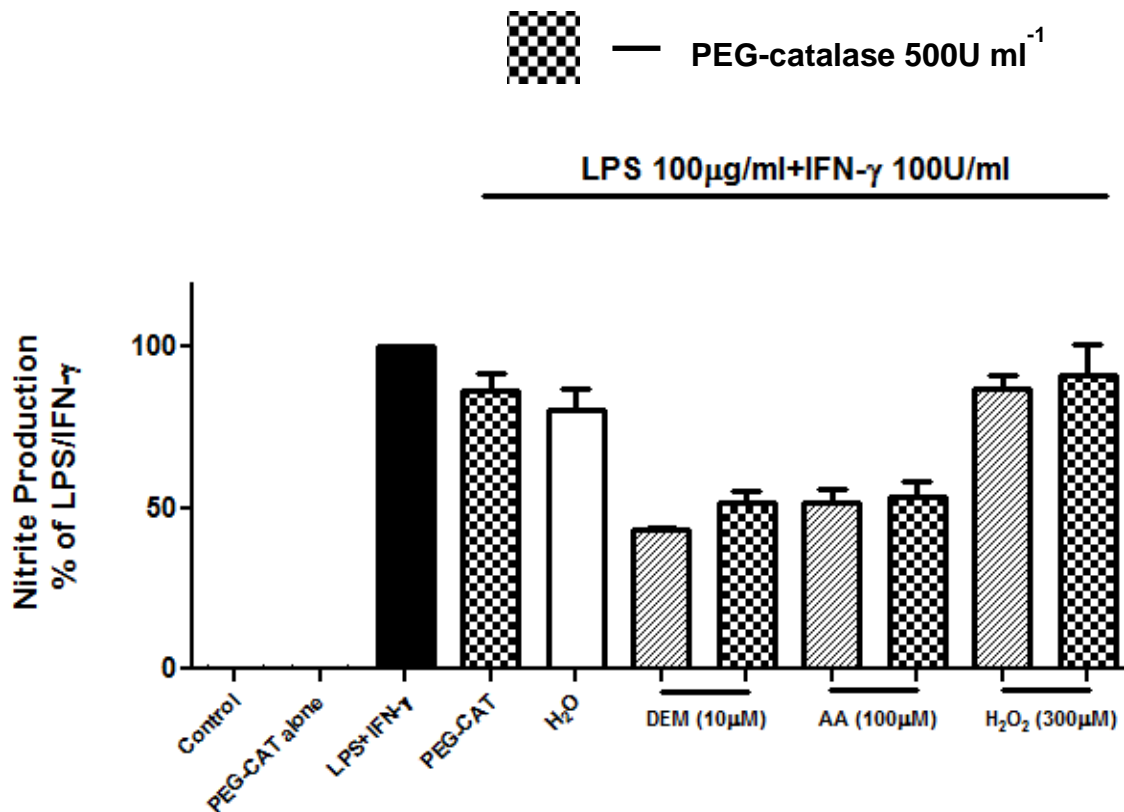


Figure 3.26 Effect of PEG-Catalase on nitrite production in the presence and absence of DEM and antimycin A in LPS and IFN- γ activated RASMCs

Confluent monolayers of RASMCs in 24-well plate were pre-treated with complete culture medium alone or medium containing PEG-catalase (500U/ml) for 30minutes prior to incubation with DEM (10 μ M), antimycin A (100 μ M) or H₂O₂(300 μ M) for a further 30minutes. Cells were then activated with LPS (100 μ g/ml) and IFN- γ (100U/ml) for 24hrs. Nitrite production was determined as described in the methods (section 2.3). The data is expressed as % nitrite production with the response to LPS (100 μ g/ml) + IFN- γ (100U/ml) taken as 100%. The data represents the means \pm S.E.M of at least three independent experiments.

3.14 Effect of polyethylene glycol-superoxide dismutase (PEG-SOD) on the expression of iNOS in the presence and absence of OS inducers

To establish whether the effect of PEG-SOD reported above involved regulating iNOS expression, additional studies were conducted pre-treating cells with PEG-SOD (500 U/ml) for 30 minutes before incubating with DEM (10 μ M), antimycin A (100 μ M) or H₂O₂ (300 μ M) for a further 30 minutes. Cells were then activated with LPS (100 μ g/ml) and IFN- γ (100 U/ml) for 24 hrs as described in the methods. Lysates were collected and subjected to western blotting for iNOS expression. Control cells and cells treated with PEG-SOD alone did not induce any detectable iNOS expression which was seen in cells treated with LPS and IFN- γ . PEG-SOD and de-ionised water in the presence of LPS and IFN- γ did not change the expression of iNOS when compared to LPS and IFN- γ alone. Antimycin A (100 μ M) and DEM (10 μ M) but not H₂O₂ (300 μ M) caused a significant reduction in LPS and IFN- γ induced iNOS expression as reported earlier. PEG-SOD at 500 U/ml was able to partially reverse the inhibition of iNOS expression caused by DEM (10 μ M) and antimycin A (100 μ M) but this effect was more pronounced with DEM than with antimycin A (Figure 3.27). Cells treated with H₂O₂ (300 μ M) in the presence or absence of PEG-SOD 500 U/ml did not affect iNOS expression when compared to LPS and IFN- γ alone (Figure 3.27).

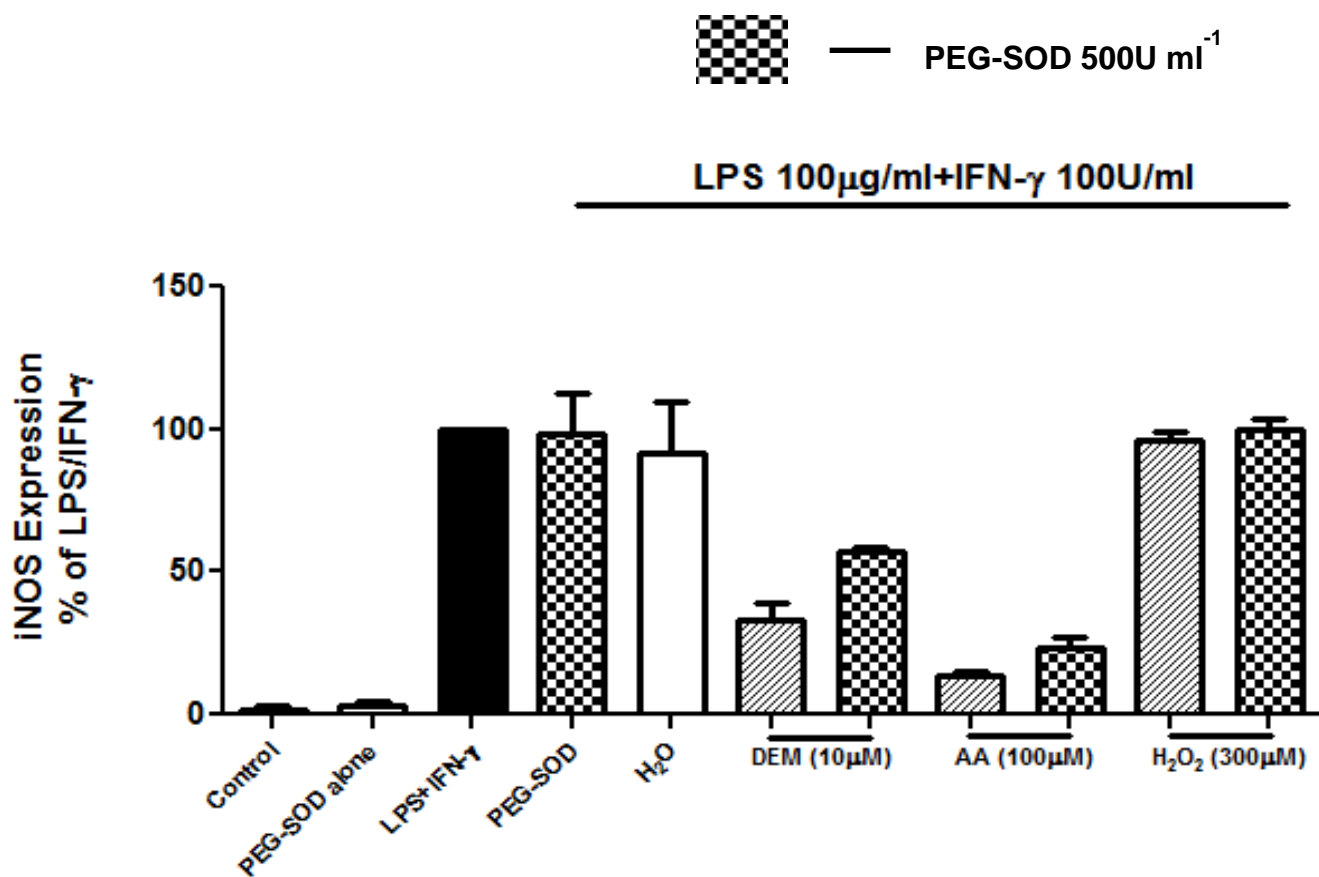


Figure 3.27 Effect of PEG-SOD on iNOS expression in the presence and absence of DEM and antimycin A in LPS and IFN- γ activated RASMCs

Confluent monolayers of RASMCs in 24-well plate were pre-treated with complete culture medium alone or medium containing PEG-SOD (500U/ml) for 30minutes prior to incubation with DEM (10 μ M), antimycin A (100 μ M) or H₂O₂(300 μ M) for a further 30minutes. Cells were then activated with LPS (100 μ g/ml) and IFN- γ (100U/ml) for 24hrs. The expression of iNOS was determined by western blotting as described in the methods (section 2.7). The blot is representative of at least three independent experiments and the bar graph is the densitometric data expressed as % iNOS expression with LPS (100 μ g/ml) + IFN- γ (100U/ml) response taken as 100%. The data represents the means \pm S.E.M of at least three independent experiments.

3.15 Effect of polyethylene glycol-catalase (PEG-catalase) on the expression of iNOS in the presence and absence of OS inducers

In parallel studies to the above, cells were pre-treated with PEG-catalase (500 U/ml) for 30 minutes before incubating with DEM (10 μ M), antimycin A (100 μ M) or H₂O₂ (300 μ M) for a further 30 minutes. Cells were then activated with LPS (100 μ g/ml) and IFN- γ (100 U/ml) for 24 hours. Lysates were collected and subjected to western blotting to determine the expression of iNOS as described in the methods. Control cells and cells treated with PEG-catalase alone did not produce any detectable levels of iNOS expression. Cells treated with LPS and IFN- γ alone induced the expression of iNOS and was taken as 100%. PEG-catalase and de-ionised water in the presence of LPS and IFN- γ did not change the expression of iNOS when compared to LPS and IFN- γ alone. Antimycin A (100 μ M) and DEM (10 μ M) but not H₂O₂ (300 μ M) in the presence of LPS and IFN- γ caused a significant reduction in the expression of iNOS when compared to LPS and IFN- γ alone. PEG-catalase at 500 U/ml had no effect on the inhibition of iNOS expression caused by DEM (10 μ M) or antimycin A (100 μ M). Hydrogen peroxide at 300 μ M in the presence or absence of PEG-catalase (500 U/ml) did not cause any change in the expression of iNOS when compared to LPS and IFN- γ alone as shown in figure 3.28.

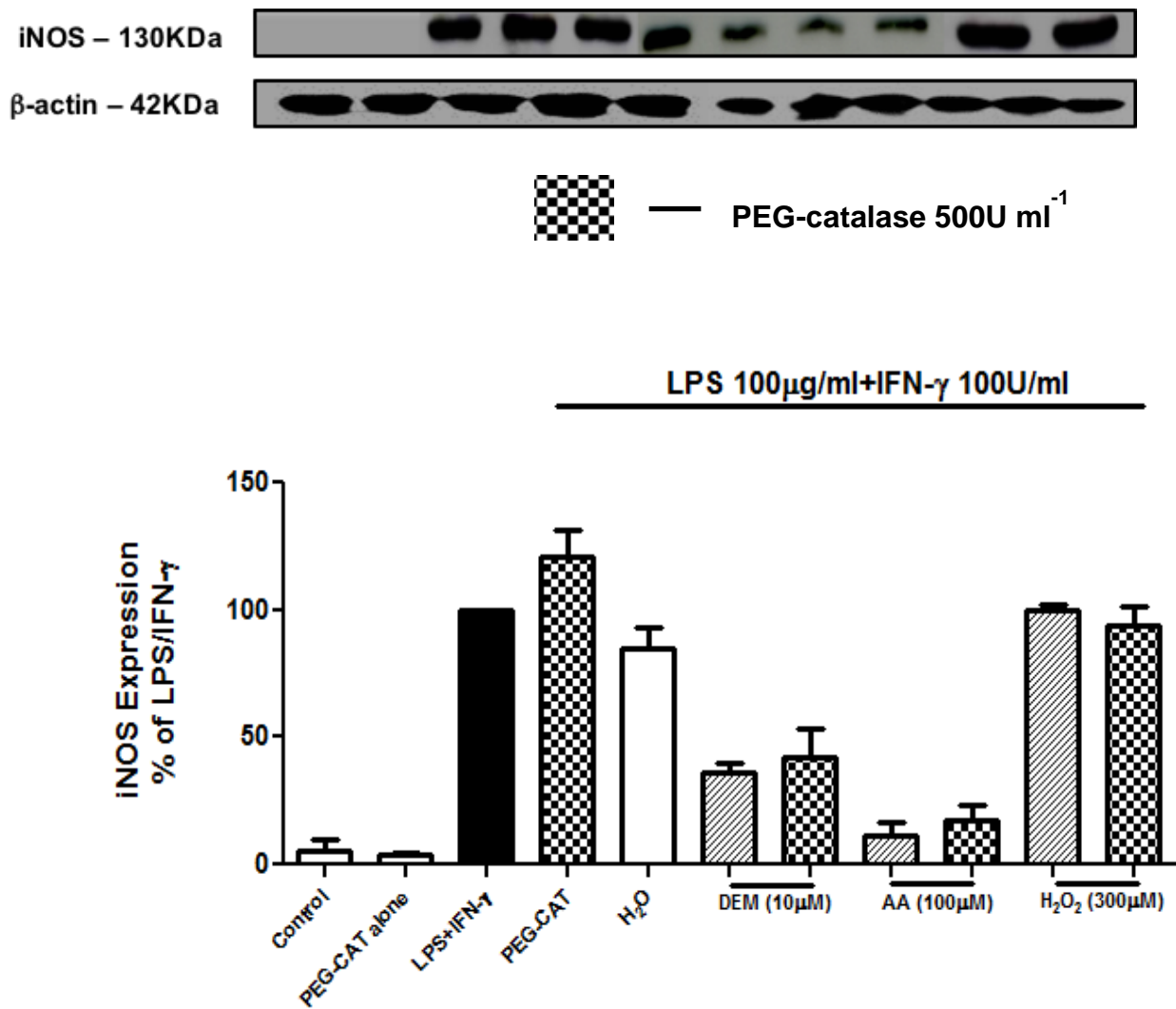


Figure 3.28 Effect of PEG-Catalase on iNOS expression in the presence and absence of DEM and antimycin A in LPS and IFN- γ activated RASMCs

Confluent monolayers of RASMCs in 24-well plate were pre-treated with complete culture medium alone or medium containing PEG-catalase (500U/ml) for 30 minutes prior to incubation with DEM (10 μ M), antimycin A (100 μ M) or H₂O₂(300 μ M) for a further 30 minutes. Cells were then activated with LPS (100 μ g/ml) and IFN- γ (100U/ml) for 24hrs. The expression of iNOS was determined by western blotting as described in the methods (section 2.7). The blot is representative of at least three independent experiments and the bar graph is the densitometric data expressed as % iNOS expression with LPS (100 μ g/ml) + IFN- γ (100U/ml) response taken as 100%. The data represents the means \pm S.E.M of at least three independent experiments.

3.16 Effect of atorvastatin on NO production in the presence and absence of OS inducers

As indicated in the introduction, statins have become one of the critical drugs used in treating patients with coronary heart disease because of their effective lipid lowering effects. However, statins may also have other novel actions, which may be independent of their anti-lipidemic actions. In this regard, and of relevance to this thesis, statins may also have anti-oxidant properties (Davignon *et al.*, 2004). Thus, experiments were carried out to determine whether statins (in particular atorvastatin) regulate NO production. To determine whether Atorvastatin exerted any cytotoxic effects, cells were treated with complete culture medium alone or medium containing various concentrations of Atorvastatin for 24hrs before performing the MTT assay as described in the methods (section 2.6). Control cells showed no decrease in viability and the metabolism of MTT by these cells was considered as 100% and compared to different concentrations of Atorvastatin. Atorvastatin was found to be toxic at 100µM causing a 50-60% decrease in cell viability. Lower concentrations did not show any statistically significant change in cell viability when compared to controls (Figure 3.29). There was no change observed in the above data when Atorvastatin was treated with LPS and IFN- γ . In one series of experiments, cells were pre-treated with different concentrations of atorvastatin for 30minutes before incubating with LPS (100 µg/ml) and IFN- γ (100 U/ml) for 24hrs and nitrite production was determined by the Griess assay as described in the methods (section 2.3). Control cells showed no detectable levels of nitrite while LPS and IFN- γ induced the expected increase in nitrite (Figure 41). Atorvastatin alone did not induce nitrite production but enhanced the effects of LPS and IFN- γ causing a bell-shaped response. Nitrite production was increased with increasing concentration of atorvastatin starting at 1µM, reaching a maximum at 10µM but there was a marginal decrease at 30µM when compared to

LPS (100 µg/ml) and IFN- γ (100 U/ml) alone (Figure 3.30). Further experiments in the presence of OS inducers were conducted using 10µM atorvastatin, which caused the maximum increase in nitrite production when used with LPS and IFN- γ . In these experiments cells were treated with 10µM Atorvastatin for 30minutes before incubating with DEM (1-10µM), antimycin A (25-150µM) or H₂O₂(50-300µM) for a further 30minutes. Cells were then activated with LPS (100 µg/ml) and IFN- γ (100 U/ml) for 24hrs as described in the methods. Once again, control cells showed no nitrite whereas LPS and IFN- γ induced nitrite and this was inhibited in a concentration dependent manner by DEM. Atorvastatin at 10µM was able to completely reverse the inhibition caused by DEM (1-10µM) (Figure 3.31). Antimycin A also significantly inhibited nitrite production in a concentration dependent manner. Treatment with 10µM atorvastatin significantly reversed the inhibitions in nitrite and this effect was more pronounced with the lower (25µM and 50µM) rather than the higher (100 µM and 150 µM) concentrations of antimycin A. In each case however, nitrite levels were higher than those seen with antimycin A alone (Figure 3.32). Hydrogen peroxide did not cause any change in nitrite production with or without 10µM atorvastatin when compared to LPS and IFN- γ alone as seen in figure 3.33.

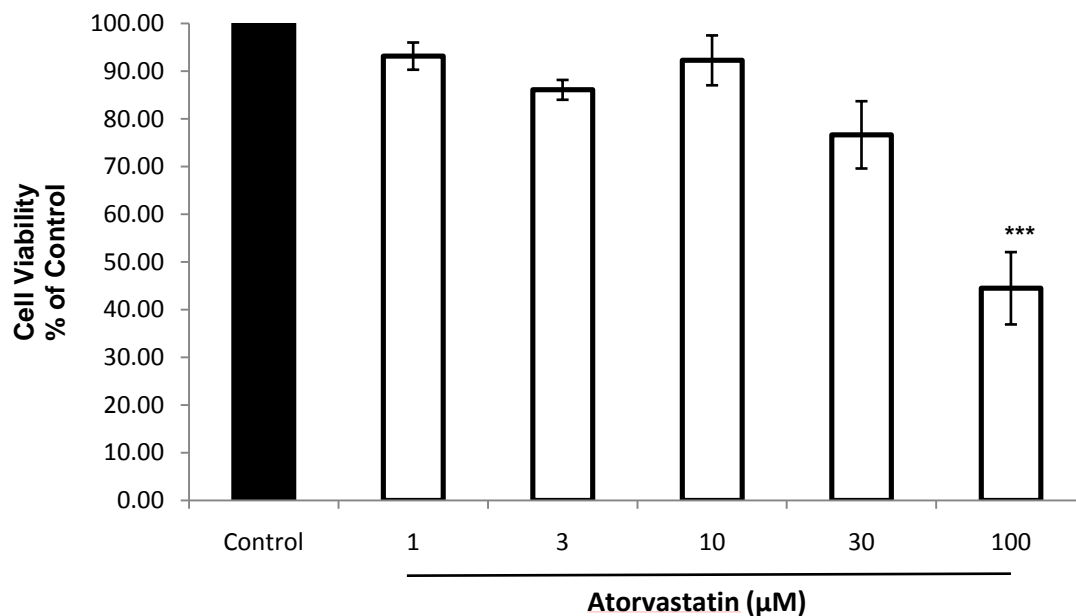


Figure 3.29 Effect of Atorvastatin on viability of RASMCs

Confluent monolayers of cells in 96-well plate were treated with different concentrations of Atorvastatin for 24hrs as described in section 2.6. Following 24hrs incubation, cell viability was determined by performing the MTT assay as described in the methods. The data is presented as % cell viability with control as a 100%. The data represents the means \pm S.E.M. of at least three individual experiments. *** denote $p < 0.001$ when compared to control.

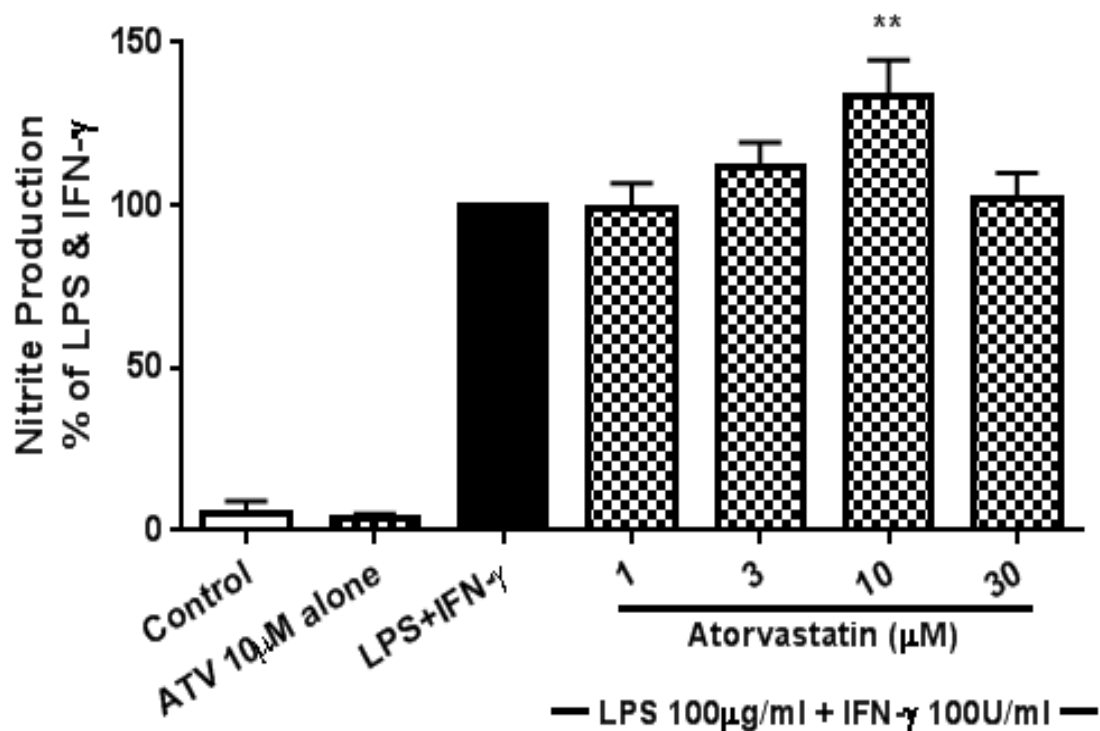


Figure 3.30 Effect of atorvastatin on nitrite production in LPS and IFN- γ activated RASMCs

Confluent monolayers of RASMCs in 24-well plates were pre-treated with complete culture medium alone or medium containing atorvastatin (1 μ M, 3 μ M, 10 μ M, 30 μ M) for 30minutes prior to incubation with LPS (100 μ g/ml) and IFN- γ (100U/ml) for a further 24hrs. Nitrite production was determined as described in the methods (section 2.3). The figure represents % nitrite production with the LPS (100 μ g/ml) + IFN- γ (100U/ml) response taken as 100%. The data represents the means \pm S.E.M of at least three independent experiments. ** denote $p < 0.01$ when compared to LPS (100 μ g/ml) + IFN- γ (100U/ml).

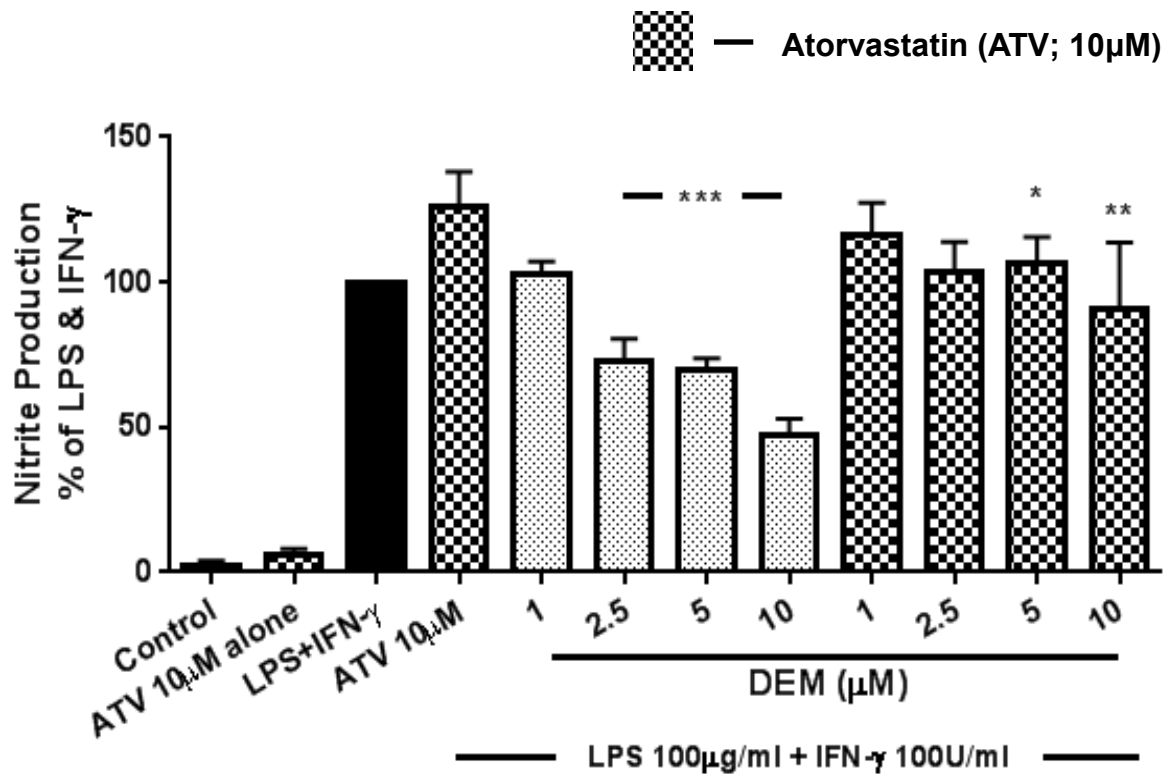


Figure 3.31 Effect of atorvastatin on nitrite production in the presence of DEM in LPS and IFN- γ activated RASMCs

Confluent monolayers of RASMCs in 24-well plates were pre-treated with complete culture medium alone or medium containing atorvastatin (10 μ M) for 30minutes prior to incubation with DEM (1 μ M, 2.5 μ M, 5 μ M and 10 μ M). Cells were then activated with LPS (100 μ g/ml) and IFN- γ (100U/ml) for a further 24hrs. Nitrite production was determined as described in the methods (section 2.3). The figure represents % nitrite production with the LPS (100 μ g/ml) + IFN- γ (100U/ml) response taken as 100%. The data represents the means \pm S.E.M of at least three independent experiments. * denote $p < 0.05$, ** denote $p < 0.01$ and *** denote $p < 0.001$ when compared to LPS (100 μ g/ml) + IFN- γ (100U/ml) and individual concentrations of DEM with or without atorvastatin.

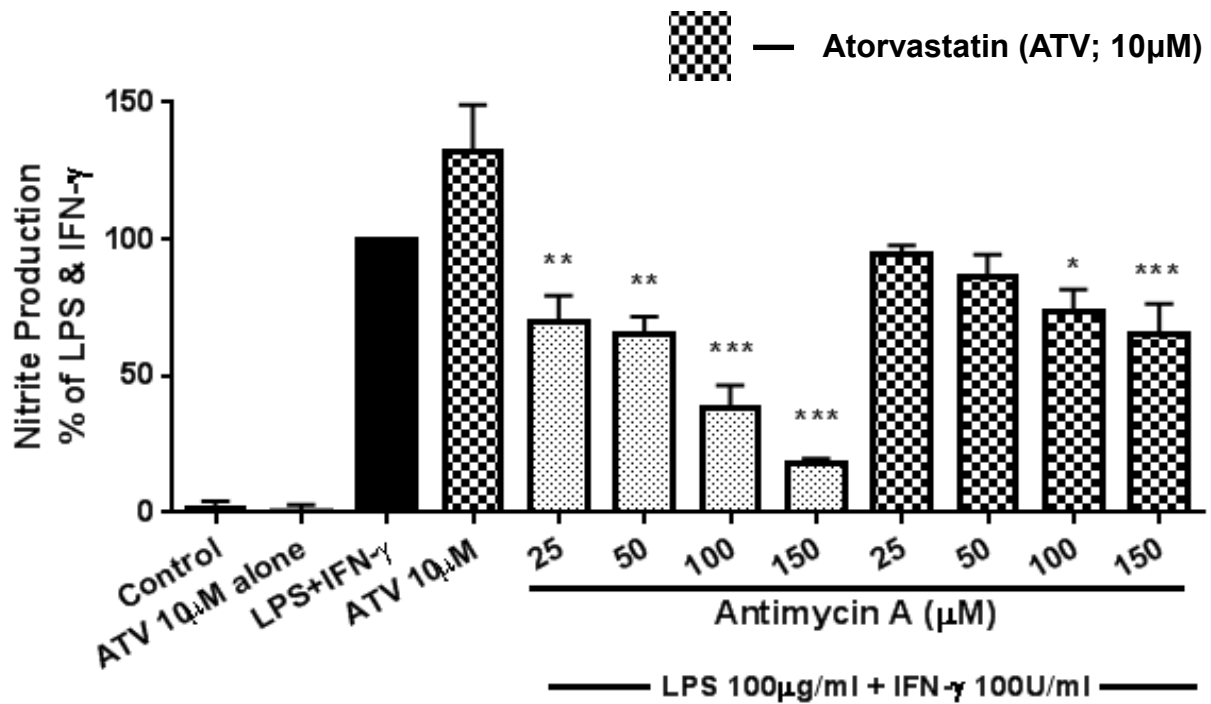


Figure 3.32 Effect of Atorvastatin on nitrite production in the presence of antimycin A in LPS and IFN- γ activated RASMCs

Confluent monolayers of RASMCs in 24-well plates were pre-treated with complete culture medium alone or medium containing atorvastatin (10 μ M) for 30minutes prior to incubation with antimycin A (25 μ M, 50 μ M, 100 μ M and 150 μ M). Cells were then activated with LPS (100 μ g/ml) and IFN- γ (100U/ml) for a further 24hrs. Nitrite production was determined as described in the methods (section 2.3). The figure represents % nitrite production with the LPS (100 μ g/ml) + IFN- γ (100U/ml) response taken as 100%. The data represents the means \pm S.E.M of at least three independent experiments. * denote $p < 0.05$, ** denote $p < 0.01$ and *** denote $p < 0.001$ when compared to LPS (100 μ g/ml) + IFN- γ (100U/ml) and individual concentrations of antimycin A with or without atorvastatin.

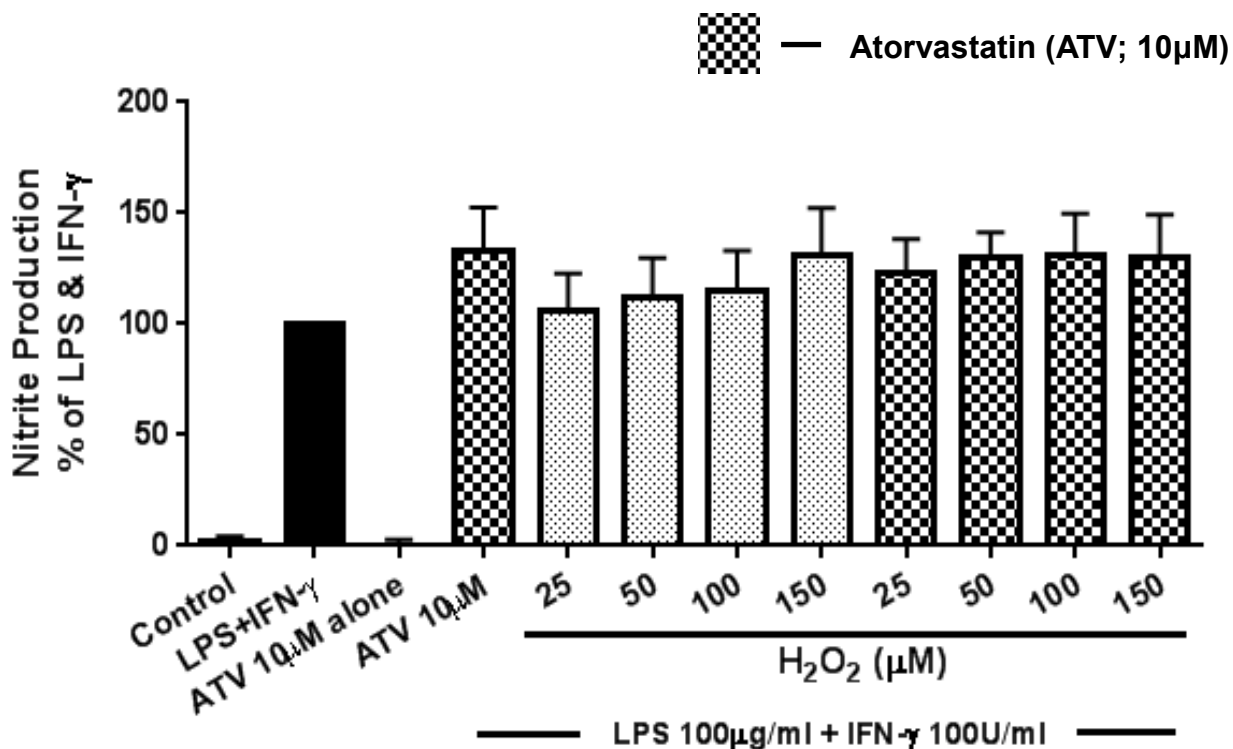


Figure 3.33 Effect of Atorvastatin on nitrite production in the presence of H₂O₂ in LPS and IFN-γ activated RASMCs

Confluent monolayers of RASMCs in 24-well plates were pre-treated with complete culture medium alone or medium containing atorvastatin (10μM) for 30minutes prior to incubation with H₂O₂ (25μM, 50μM, 100μM and 150μM). Cells were then activated with LPS (100μg/ml) and IFN-γ (100U/ml) for a further 24hrs. Nitrite production was determined as described in the methods (section 2.3). The figure represents % nitrite production with the LPS (100μg/ml) + IFN-γ (100U/ml) response taken as 100%. The data represents the means ± S.E.M of at least three independent experiments.

3.17 Effects of atorvastatin on the expression of iNOS in the presence and absence of OS inducers

To determine the effect of atorvastatin on iNOS expression in the presence and absence of OS inducers, cells were pre-treated with different concentrations of atorvastatin for 30 minutes before incubating the cells with LPS (100 µg/ml) and IFN- γ (100 U/ml) for 24 hrs. Lysates were collected and subjected to western blotting as described in the methods. Control cells showed little or no expression of iNOS whereas significant induction was seen with LPS and IFN- γ and this was considered as 100% when compared to OS inducers. Similar to nitrite production, atorvastatin caused an increase in the expression of iNOS with increasing concentrations starting at 1 µM, reaching a maximum at 10 µM and slightly decreasing at 30 µM (Figure 3.34). Further experiments were conducted using 10 µM atorvastatin in the presence and absence of OS inducers as at this concentration there was maximum increase in iNOS expression. In experiments with OS inducers, cells were pre-treated with 10 µM atorvastatin before incubating with DEM (1-10 µM), antimycin A (25-150 µM) or H₂O₂ (50-300 µM) for a further 30 minutes. Cells were then activated with LPS (100 µg/ml) and IFN- γ (100 U/ml) for 24 hrs as described in the methods. Diethyl maleate caused a concentration dependent inhibition on the expression of iNOS. Atorvastatin was able to significantly reduce the inhibition caused by DEM (1-10 µM) (Figure 3.35), completely reversing that seen with 1 µM and causing a 20 to 40% reversal of the inhibitions seen with 2.5 µM, 5 µM and 10 µM DEM. Antimycin A, similar to DEM, significantly inhibited iNOS expression and this was found to be concentration dependent (Figure 3.36). Atorvastatin again reversed the inhibitions caused by antimycin A and this effect was more pronounced at the lower concentrations of antimycin A. Atorvastatin completely restored the inhibition caused by 25 µM whereas it caused a 80-90% reversal of the inhibition caused by 50 µM, 100 µM and 150 µM

antimycin A when compared to antimycin A alone. Consistent with its lack of effect on nitrite production, H₂O₂ did not cause any significant change in iNOS expression with or without 10µM atorvastatin when compared to LPS and IFN-γ alone (Figure 3.37).

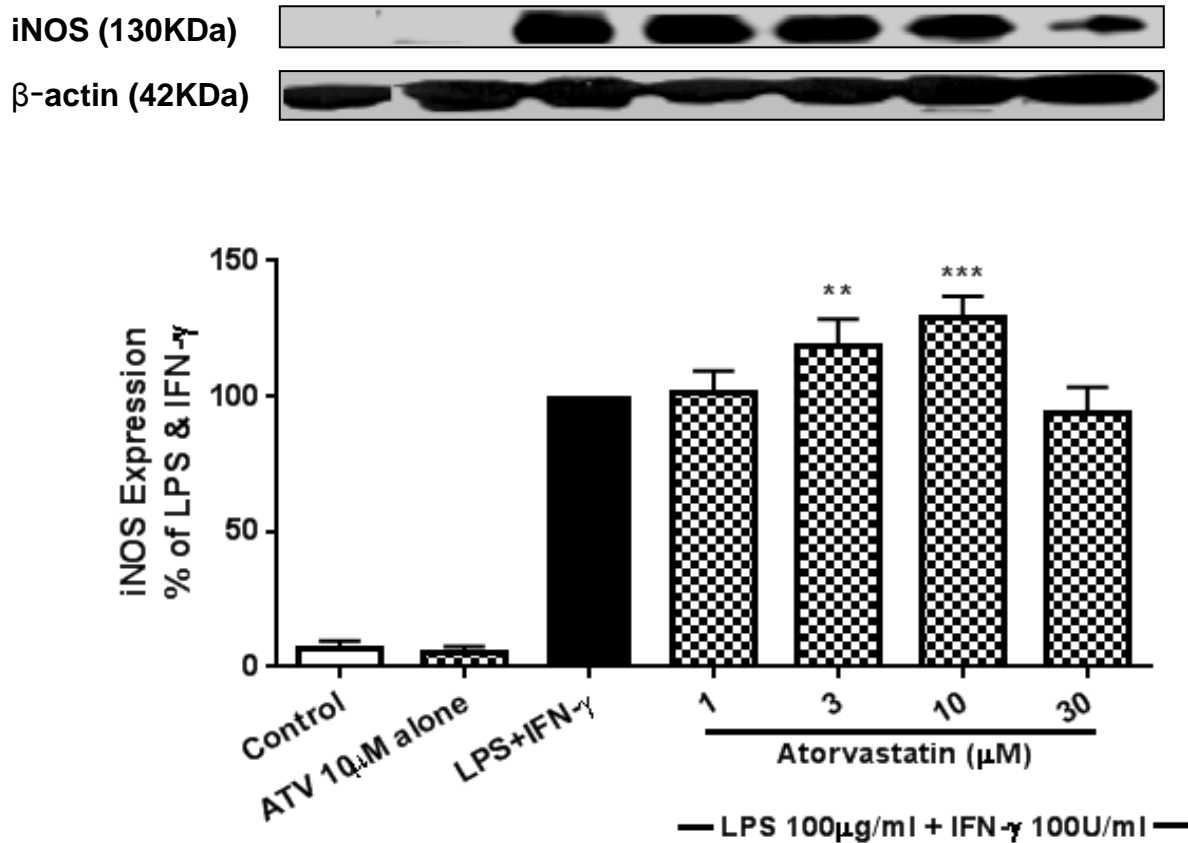


Figure 3.34 Effect of Atorvastatin on iNOS expression in LPS and IFN- γ activated RASMCs

Confluent monolayers of RASMCs in 24-well plates were pre-treated with complete culture medium alone or medium containing atorvastatin (1 μ M, 3 μ M, 10 μ M, 30 μ M) for 30minutes prior to incubation with LPS (100 μ g/ml) and IFN- γ (100U/ml) for a further 24hrs. The expression of iNOS was determined by western blotting as described in the methods (section 2.7). The blot is representative of at least three independent experiments and the bar graph is the densitometric data expressed as % iNOS expression with LPS (100 μ g/ml) + IFN- γ (100U/ml) response taken as 100%. The data represents the means \pm S.E.M of at least three independent experiments.** denote p<0.01 and *** denote p<0.001 when compared to LPS (100 μ g/ml) + IFN- γ (100U/ml).

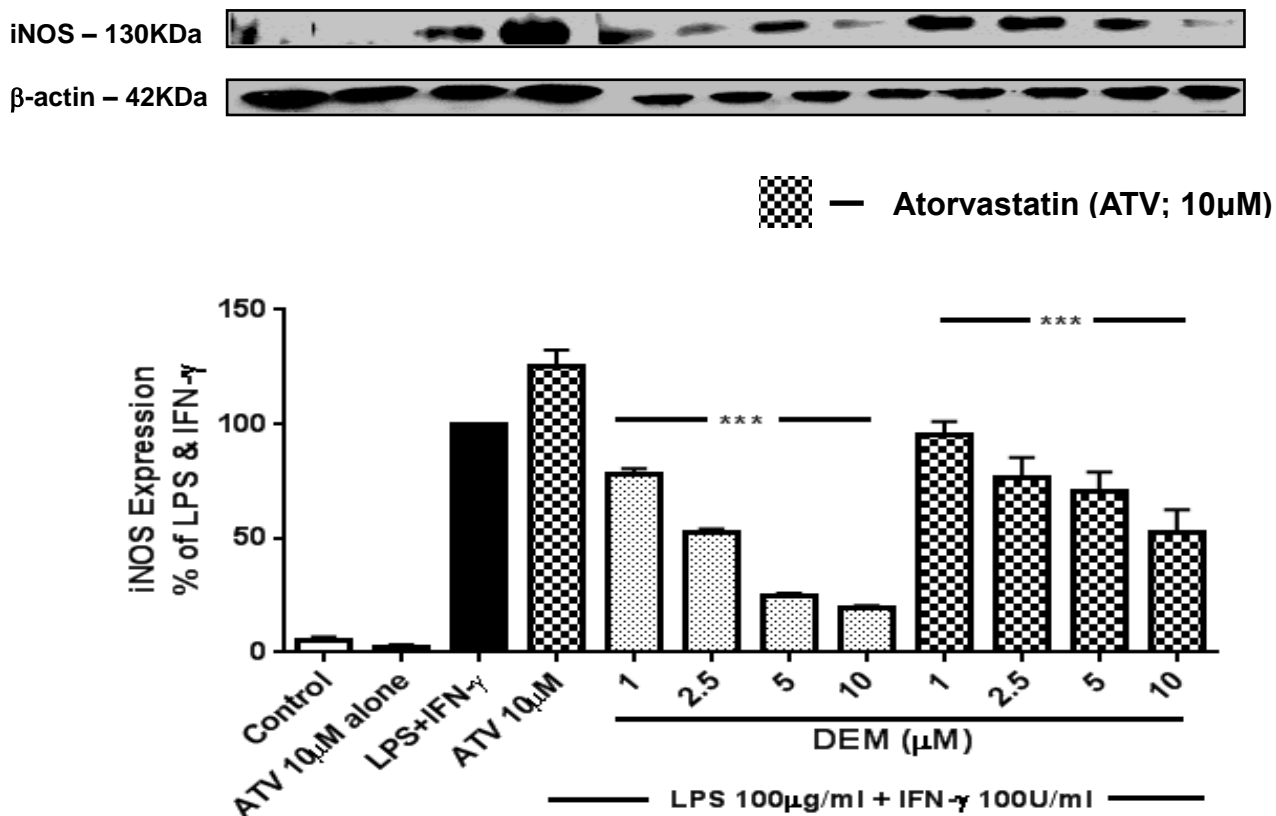


Figure 3.35 Effect of Atorvastatin on iNOS expression in the presence and absence of DEM in LPS and IFN- γ activated RASMCs

Confluent monolayers of RASMCs in 24-well plate were pre-treated with complete culture medium alone or medium containing atorvastatin (10 μ M) for 30minutes prior to incubation with DEM (1 μ M, 2.5 μ M, 5 μ M and 10 μ M) for a further 30minutes. Cells were then activated with LPS (100 μ g/ml) and IFN- γ (100U/ml) for 24hrs. The expression of iNOS was determined by western blotting as described in the methods (section 2.7). The blot is representative of at least three independent experiments and the bar graph is the densitometric data expressed as % iNOS expression with LPS (100 μ g/ml) + IFN- γ (100U/ml) response taken as 100%. The data represents the means \pm S.E.M of at least three independent experiments. ** denote $p < 0.01$ and *** denote $p < 0.001$ when compared to LPS (100 μ g/ml) + IFN- γ (100U/ml) and individual concentrations of DEM with or without atorvastatin.

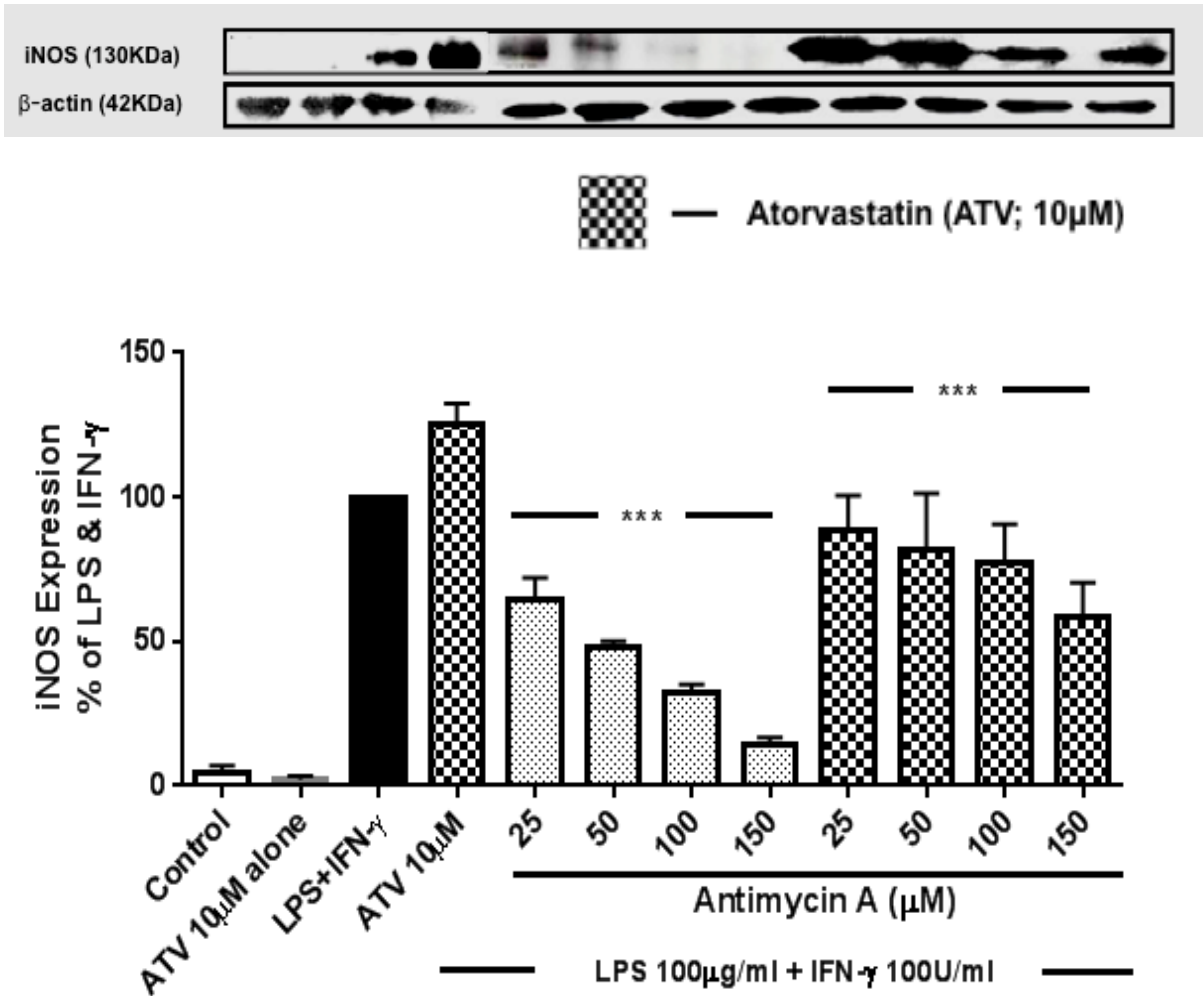


Figure 3.36 Effect of Atorvastatin on iNOS expression in the presence and absence of antimycin A in LPS and $\text{IFN-}\gamma$ activated RASMCs

Confluent monolayers of RASMCs in 24-well plate were pre-treated with complete culture medium alone or medium containing atorvastatin (10 μ M) for 30minutes prior to incubation with antimycin A (25 μ M, 50 μ M, 100 μ M and 150 μ M) for a further 30minutes. Cells were then activated with LPS (100 μ g/ml) and IFN- γ (100U/ml) for 24hrs. The expression of iNOS was determined by western blotting as described in the methods (section 2.7). The blot is representative of at least three independent experiments and the bar graph is the densitometric data expressed as % iNOS expression with LPS (100 μ g/ml) + IFN- γ (100U/ml) response taken as 100%. The data represents the means \pm S.E.M of at least three independent experiments.*** denote $p < 0.001$ when compared to LPS (100 μ g/ml) + IFN- γ (100U/ml) and individual concentrations of antimycin A with or without atorvastatin.



 — Atorvastatin (ATV; 10 μ M)

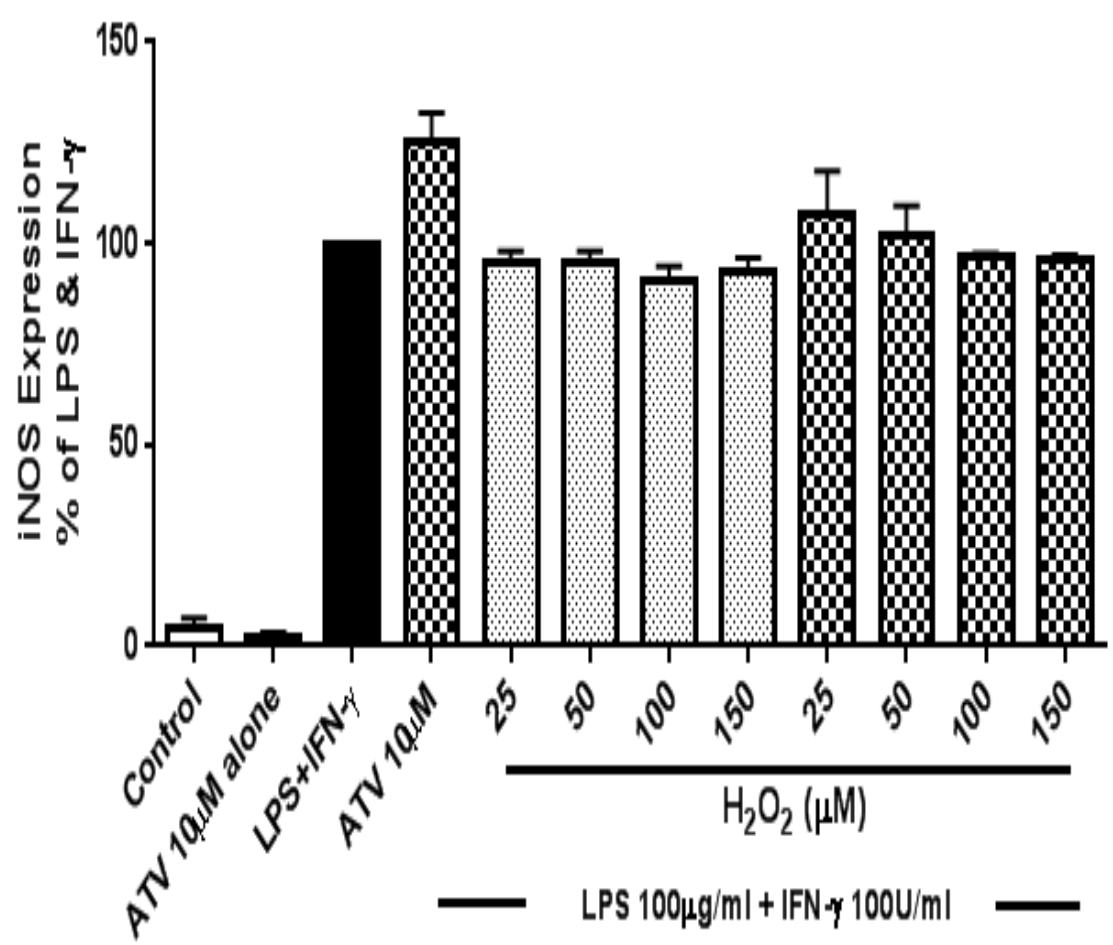


Figure 3.37 Effect of Atorvastatin on iNOS expression in the presence and absence of H₂O₂ in LPS and IFN- γ activated RASMCs

Confluent monolayers of RASMCs in 24-well plate were pre-treated with complete culture medium alone or medium containing atorvastatin (10 μ M) for 30minutes prior to incubation with H₂O₂(25 μ M, 50 μ M, 100 μ M and 150 μ M) for a further 30minutes. Cells were then activated with LPS (100 μ g/ml) and IFN- γ (100U/ml) for 24hrs. The expression of iNOS was determined by western blotting as described in the methods (section 2.7). The blot is representative of at least three independent experiments and the bar graph is the densitometric data expressed as % iNOS expression with LPS (100 μ g/ml) + IFN- γ (100U/ml) response taken as 100%. The data represents the means \pm S.E.M of at least three independent experiments.*** denote p<0.001 when compared to LPS (100 μ g/ml) + IFN- γ (100U/ml).

3.18 Effect of atorvastatin on superoxide radical generation in the presence and absence of OS inducers

To determine whether atorvastatin regulated superoxide radical production by OS inducers, cells were pre-treated with atorvastatin (10 μ M) for 30minutes before incubating the cells with DEM (10 μ M) or antimycin A (100 μ M) for another 30minutes. Cells were then further treated with MitoSOX red (5 μ M) for 10minutes at 37⁰c, washed with HBSS 3 times before viewing under confocal microscope as described in the methods (section 2.8). Control cells and cells treated with atorvastatin (10 μ M) alone did not generate any superoxide radical whereas DEM (10 μ M) and antimycin A (100 μ M) induced significant amount of superoxide radical as previously reported. Antimycin A alone was taken as 100% as it caused maximum generation of superoxide radical. Atorvastatin (10 μ M) caused a 20% reduction in the response to DEM whereas with antimycin A, superoxide radical generation was inhibited down to almost 30-40% of the induced response as shown in figure 3.38.

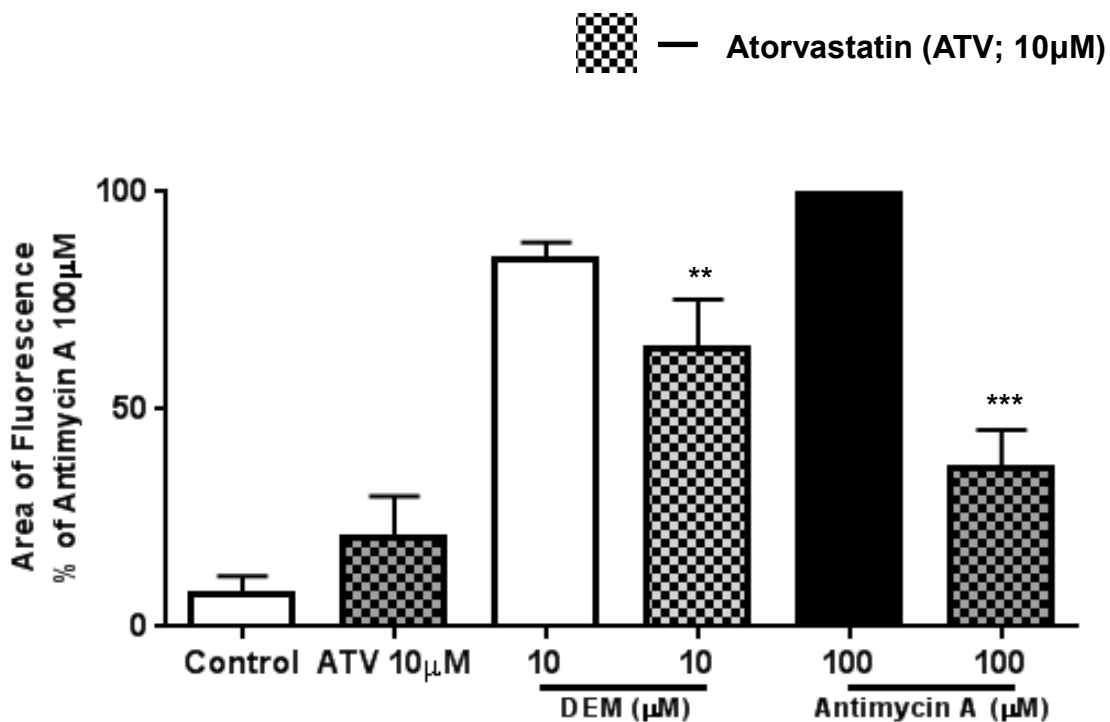


Figure 3.38 Effect of atorvastatin on superoxide radical generation in the presence and absence of OS inducers in RASMCs

RASMCs were seeded into a 12-well plate and was treated with complete culture medium alone or medium containing atorvastatin (10µM) for 30 minutes prior to incubation with DEM (10µM) or antimycin A (100µM) for 24hrs. Cells were then further incubated with MitoSOX for 10 minutes before viewing under a Nikon™ TE-2000 confocal laser scanning microscope as described in the methods (section 2.8). The photographs are representative of at least 3 individual experiments. The bar graph is presented as % area of fluorescence with antimycin A (100µM) as 100%. The data represents the means ± S.E.M of at least 3 independent experiments. ** denote p<0.01 and *** denote p<0.001 when compared to antimycin A or DEM with or without atorvastatin.

3.19 Effect of OS inducers on the phosphorylation of p38 MAPK

To begin to understand whether OS regulated the signalling mechanisms that may be involved in the expression of iNOS, additional studies were carried out investigating the effects of DEM, antimycin A and H₂O₂ on select kinase pathways including the p38 MAPK. The latter was selected as a target because of its critical involvement in iNOS induction by LPS and IFN- γ in RASMCs (Baydoun *et al.*, 1999). To determine the effect of OS inducers on the phosphorylation of p38 MAPK, cells were pre-treated with DEM (2.5-10 μ M), antimycin A (50-150 μ M) or hydrogen peroxide (50-300 μ M) for 30 minutes before activating the cells with LPS (100 μ g/ml) and IFN- γ (100U/ml) for 24hrs. Lysates were collected and western blotting was performed to determine phosphorylation of p38 MAPK expression. Control cells showed no expression of phospho-p38 MAPK whereas maximum phosphorylation was achieved with LPS and IFN- γ . In the presence of LPS and IFN- γ , antimycin A caused an 80-90% reduction in the phosphorylation of p38 MAPK whereas DEM caused a 60-70% reduction and these effects were found to be concentration dependent. On the contrary, H₂O₂ had lesser effect on the phosphorylation of p38 MAPK as only 20-30% reduction was observed with higher concentrations of 100 μ M and 300 μ M as illustrated in figure 3.39.

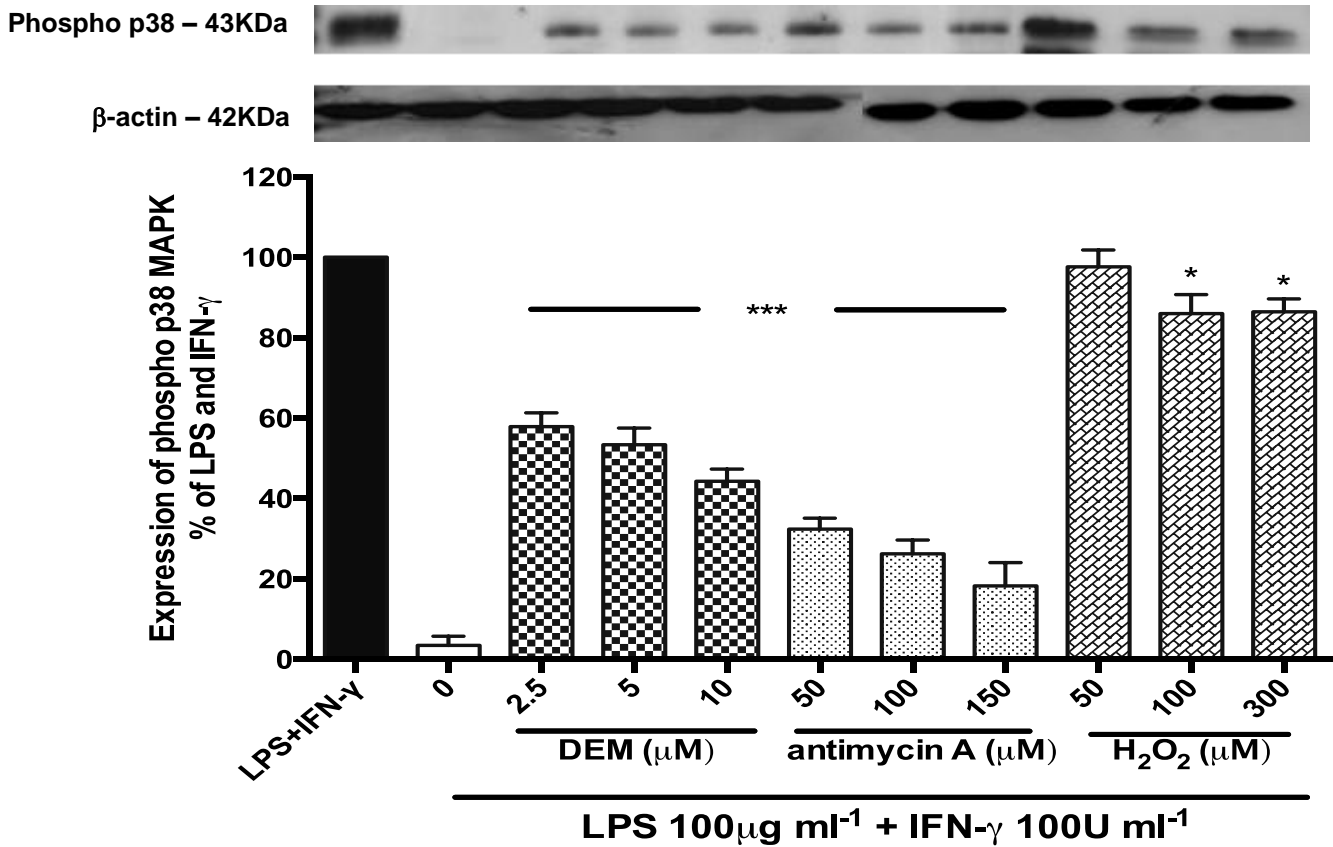


Figure 3.39 Effect of OS inducers on the phosphorylation of p38 MAPK in LPS and IFN- γ activated RASMCs

Confluent monolayers of RASMCs in 24-well plate were pre-treated with complete culture medium alone or medium containing DEM (2.5-10 μ M), antimycin A (50-150 μ M) or hydrogen peroxide (50-300 μ M) for 30minutes. Cells were then activated with LPS (100 μ g/ml) and IFN- γ (100U/ml) for 24hrs. Phosphorylation of p38 MAPK was determined by western blotting as described in the methods (section 2.7). The blot is representative of at least three independent experiments and the bar graph is the densitometric data expressed as % phospho p38 MAPK expression with LPS (100 μ g/ml) + IFN- γ (100U/ml) response taken as 100%. The data represents the means \pm S.E.M of at least three independent experiments. ** denote $p < 0.01$ and *** denote $p < 0.001$ when compared to LPS (100 μ g/ml) + IFN- γ (100U/ml).

3.20 Effect of OS inducers on the phosphorylation of Akt

Another potential key regulator of LPS and IFN- γ induced iNOS expression is the PI3-Akt pathway. Lipopolysaccharides and cytokine stimulates vascular smooth muscle cells leading to the activation of PI3-Akt pathway which activates NF- κ B leading to the induction of iNOS (Hattori *et al.*, 2003). □ To determine the effect of OS inducers on the phosphorylation of Akt, cells were pre-treated with DEM (1-10 μ M), antimycin A (25-100 μ M) or hydrogen peroxide (50-300 μ M) for 30 minutes before activating the cells with LPS (100 μ g/ml) and IFN- γ (100U/ml) for 24hrs. Lysates were collected and western blotting was performed to determine the phosphorylation of Akt expression as described in the methods. Control cells showed no expression of Akt whereas maximum phosphorylation was achieved with LPS and IFN- γ treated cells. Antimycin A caused a 30-60% reduction in the phosphorylation of Akt whereas DEM caused a 50-90% reduction when compared to LPS and IFN- γ response and these effects were found to be concentration dependent. H₂O₂ had lesser effect on the phosphorylation of Akt as only 30% reduction was observed with concentrations of 50-300 μ M as demonstrated in figure 3.40.

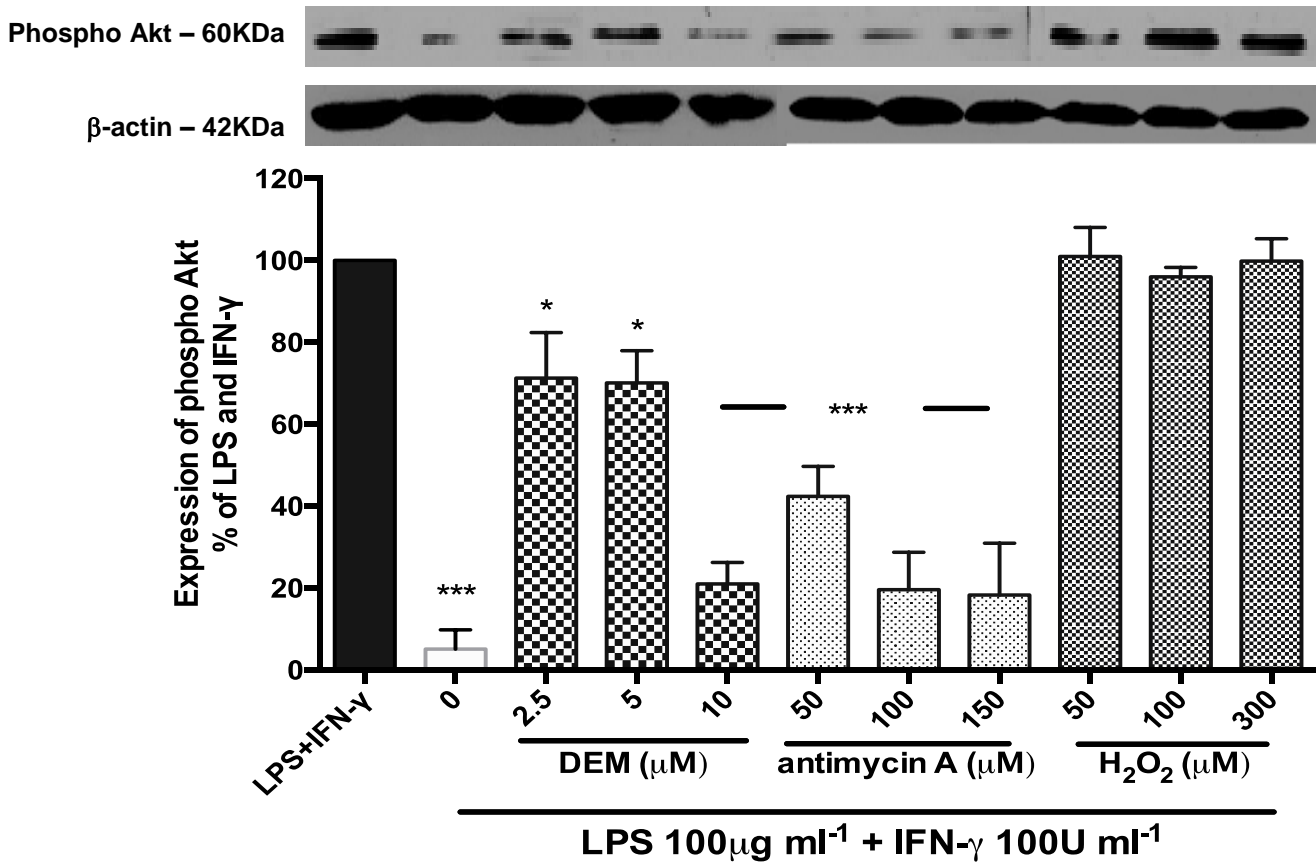


Figure 3.40 Effect of OS inducers on the phosphorylation of Akt in LPS and IFN- γ activated RASMCs

Confluent monolayers of RASMCs in 24-well plate were pre-treated with complete culture medium alone or medium containing DEM (1-10 μ M), antimycin A (25-100 μ M) or hydrogen peroxide (50-300 μ M) for 30minutes. Cells were then activated with LPS (100 μ g/ml) and IFN- γ (100U/ml) for 24hrs. Phosphorylation of Akt was determined by western blotting as described in the methods (section 2.7). The blot is representative of at least three independent experiments and the bar graph is the densitometric data expressed as % phospho Akt expression with LPS (100 μ g/ml) + IFN- γ (100U/ml) response taken as 100%. The data represents the means \pm S.E.M of at least three independent experiments. ** denote $p < 0.01$ and *** denote $p < 0.001$ when compared to LPS (100 μ g/ml) + IFN- γ (100U/ml).

3.21 Effect of Atorvastatin on the phosphorylation of p38 MAPK in the presence and absence of different concentrations of DEM or antimycin A

To determine the effect of atorvastatin on the phosphorylation of p38 MAPK in the presence of DEM or antimycin A, cells were pre-treated with atorvastatin (10 μ M) for 30 minutes before incubating the cells with DEM (1-10 μ M) or antimycin A (25-150 μ M) for a further 30 minutes. Cells were then activated with LPS (100 μ g/ml) and IFN- γ (100U/ml) for 24hrs. Phosphorylation of p38 MAPK was determined using western blotting as described in the methods. Control cells and cells treated with atorvastatin alone did not cause any phosphorylation of p38 MAPK. LPS and IFN- γ alone induced phosphorylation of p38 MAPK and was considered as maximum. Atorvastatin slightly altered LPS and IFN- γ induced phosphorylation of p38 MAPK. In contrast, antimycin A concentration dependently inhibited the phosphorylation of p38 MAPK which was reversed by atorvastatin, but this was only partial at the higher concentrations of 100 μ M and 150 μ M antimycin A (Figure 3.41). As seen with antimycin A, DEM concentration dependently inhibited LPS and IFN- γ induced phosphorylation of p38 MAPK. Atorvastatin at 10 μ M completely reversed the inhibitions caused by 1 μ M and 2.5 μ M of DEM and only partially reversed that seen with 5 μ M but had no effect on the inhibitions caused by 10 μ M DEM (Figure 3.42).

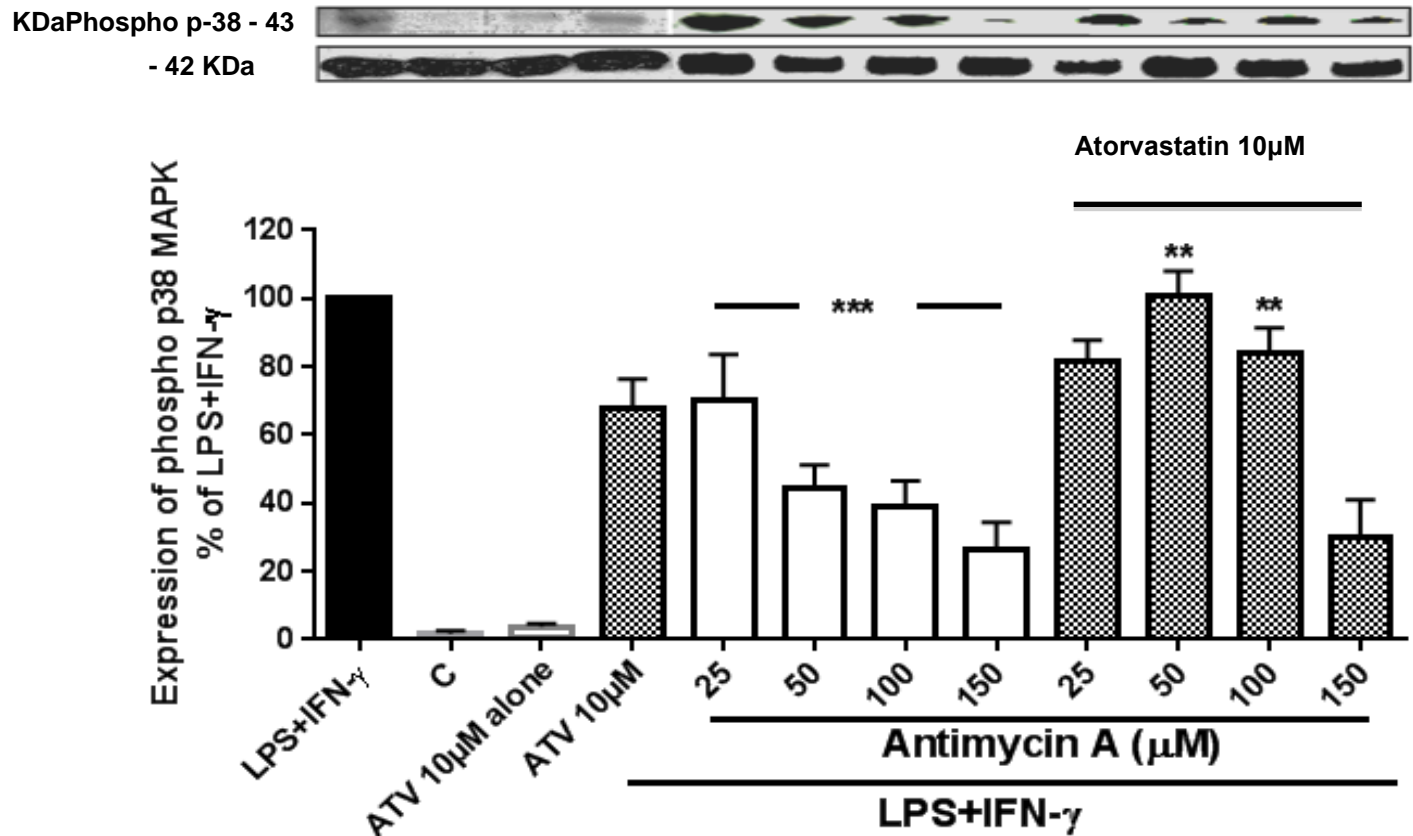


Figure 3.41 Effect of Atorvastatin on the phosphorylation of p38 MAPK in the presence and absence of Antimycin A in LPS and IFN- γ activated RASMCs

Confluent monolayers of RASMCs in 24-well plate were pre-treated with complete culture medium alone or medium containing atorvastatin (10µM) before incubating the cells with antimycin A (25-100µM) for a further 30minutes. Cells were then activated with LPS (100µg/ml) and IFN- γ (100U/ml) for 24hrs. Phosphorylation of p-38 MAPK was determined by western blotting as described in the methods (section 2.7). The blot is representative of at least three independent experiments and the bar graph is the densitometric data expressed as % phospho p38 MAPK expression with LPS (100µg/ml) + IFN- γ (100U/ml) response taken as 100%. The data represents the means \pm S.E.M of at least three independent experiments. ** denote $p < 0.01$ and *** denote $p < 0.001$ when compared to LPS (100µg/ml) + IFN- γ (100U/ml) and individual concentrations of antimycin A with or without atorvastatin

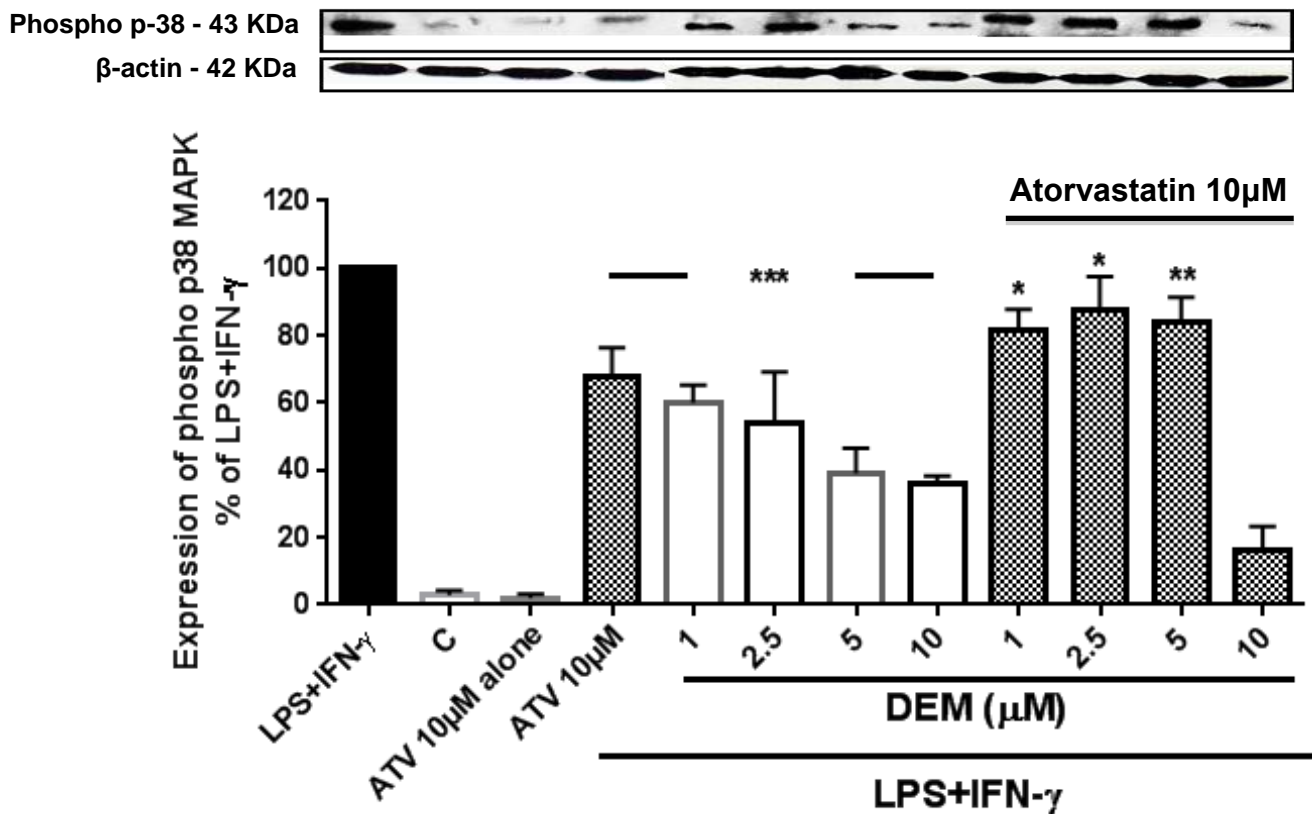


Figure 3.42 Effect of Atorvastatin on the phosphorylation of p38 MAPK in the presence and absence of DEM in LPS and IFN- γ activated RASMCs

Confluent monolayers of RASMCs in 24-well plate were pre-treated with complete culture medium alone or medium containing atorvastatin (10μM) before incubating the cells with DEM (1-10μM) for a further 30minutes. Cells were then activated with LPS (100μg/ml) and IFN- γ (100U/ml) for 24hrs. Phosphorylation of p-38 MAPK was determined by western blotting as described in the methods (section 2.7). The blot is representative of at least three independent experiments and the bar graph is the densitometric data expressed as % phospho p38 MAPK expression with LPS (100μg/ml) + IFN- γ (100U/ml) response taken as 100%. The data represents the means \pm S.E.M of at least three independent experiments. * denote $p < 0.05$, ** denote $p < 0.01$ and *** denote $p < 0.001$ when compared to LPS (100μg/ml) + IFN- γ (100U/ml) and individual concentrations of DEM with or without atorvastatin.

3.22 Effect of Atorvastatin on the phosphorylation of Akt in the presence and absence of different concentrations of DEM or antimycin A

To determine the effect of atorvastatin on the inhibition of Akt phosphorylation caused by DEM or antimycin A, cells were pre-treated with atorvastatin (10 μ M) for 30 minutes before incubating the cells with DEM (1-10 μ M) or antimycin A (25-150 μ M) for a further 30 minutes. Cells were then activated with LPS (100 μ g/ml) and IFN- γ (100U/ml) for 24hrs and lysates subjected to western blotting as described in the methods. Control cells and cells treated with atorvastatin alone did not cause any phosphorylation of Akt. LPS and IFN- γ induced phosphorylation of Akt, which was not significantly altered by atorvastatin, but the latter did reverse the concentration dependent inhibitions of Akt phosphorylation caused by antimycin A. The effects observed were, however, only partial at the higher concentrations of 100 μ M and 150 μ M antimycin A (Figure 3.43). Similarly, the inhibitions caused by DEM were also partially reversed by atorvastatin and the effects were significantly above the responses seen with DEM alone (Figure 3.44).

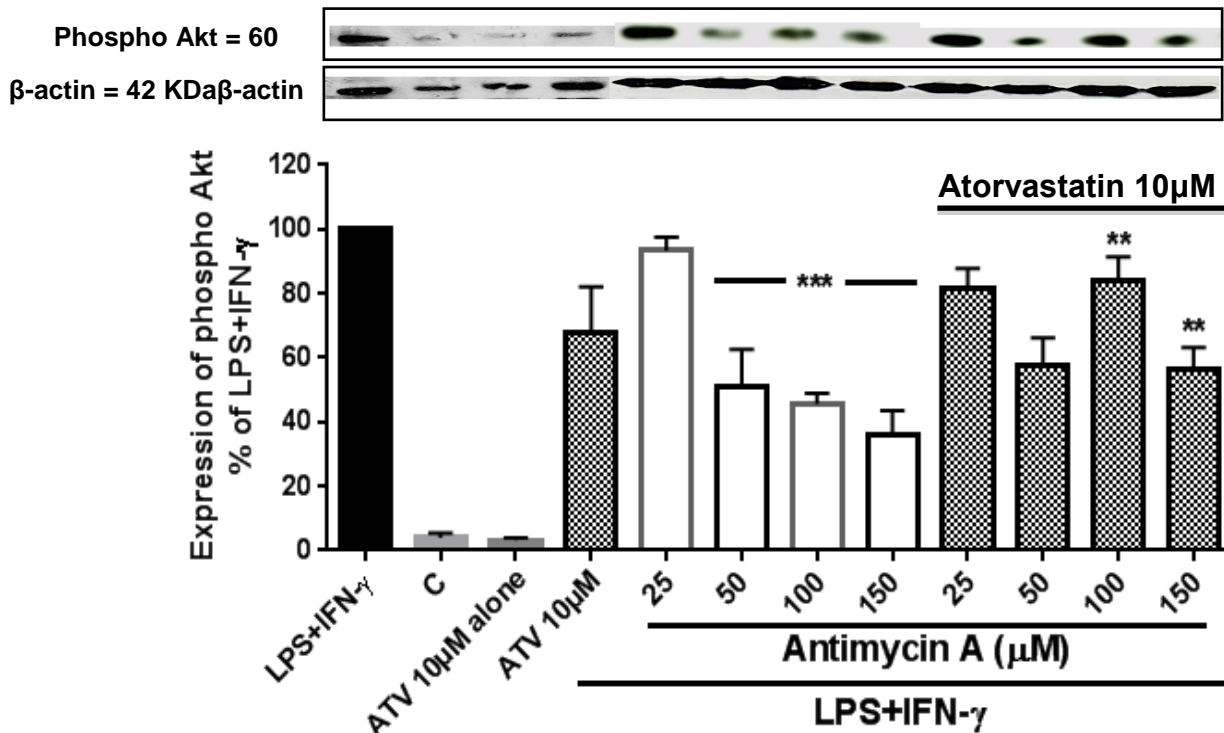


Figure 3.43 Effect of Atorvastatin on the phosphorylation of Akt in the presence and absence of antimycin A in LPS and IFN- γ activated RASMCs

Confluent monolayers of RASMCs in 24-well plate were pre-treated with complete culture medium alone or medium containing atorvastatin (10 μ M) before incubating the cells with antimycin A (25-100 μ M) for a further 30minutes. Cells were then activated with LPS (100 μ g/ml) and IFN- γ (100U/ml) for 24hrs. Phosphorylation of Akt was determined by western blotting as described in the methods (section 2.7). The blot is representative of at least three independent experiments and the bar graph is the densitometric data expressed as % phospho Akt expression with LPS (100 μ g/ml) + IFN- γ (100U/ml) response taken as 100%. The data represents the means \pm S.E.M of at least three independent experiments. ** denote $p < 0.01$ and *** denote $p < 0.001$ when compared to LPS (100 μ g/ml) + IFN- γ (100U/ml) and individual concentrations of antimycin A with or without atorvastatin.

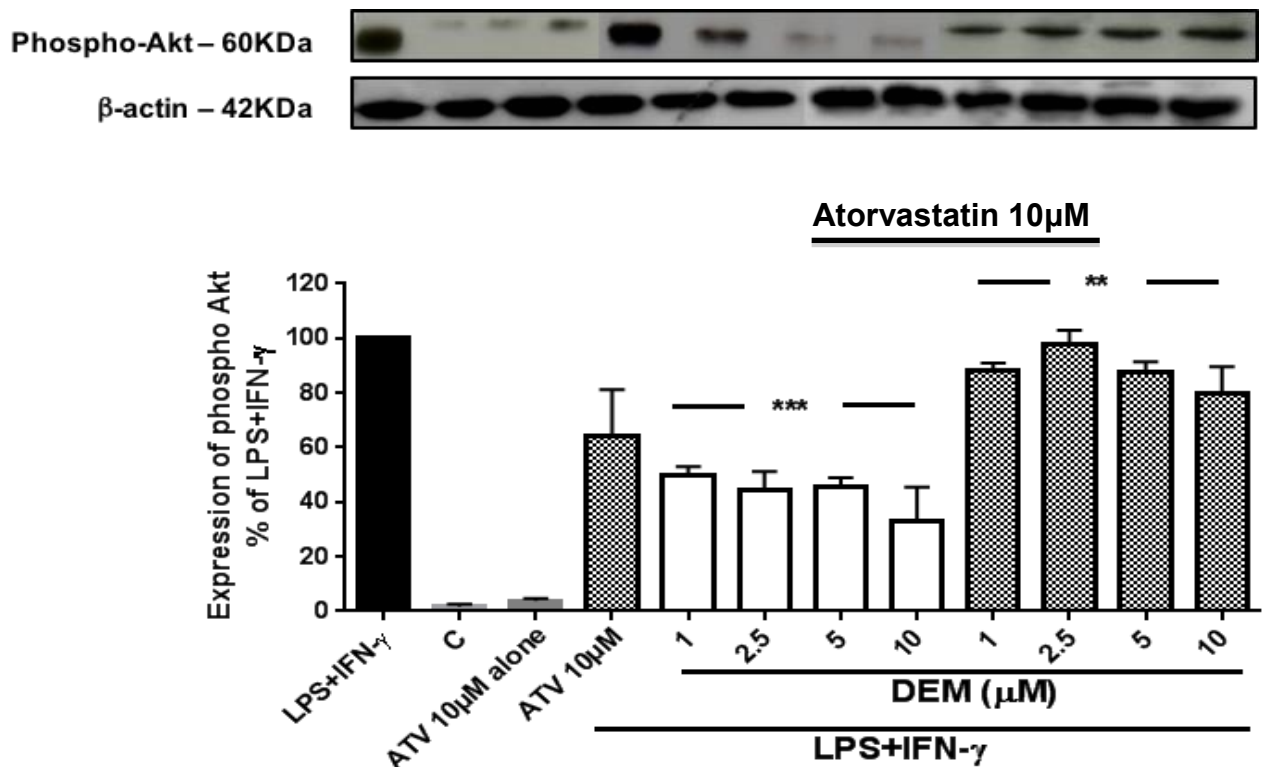


Figure 3.44 Effect of Atorvastatin on the phosphorylation of Akt in the presence and absence of DEM in LPS and IFN- γ activated RASMCs

Confluent monolayers of RASMCs in 24-well plate were pre-treated with complete culture medium alone or medium containing atorvastatin (10 μ M) before incubating the cells with DEM (1-10 μ M) for a further 30minutes. Cells were then activated with LPS (100 μ g/ml) and IFN- γ (100U/ml) for 24hrs. Phosphorylation of Akt was determined by western blotting as described in the methods (section 2.7). The blot is representative of at least three independent experiments and the bar graph is the densitometric data expressed as % phospho Akt expression with LPS (100 μ g/ml) + IFN- γ (100U/ml) response taken as 100%. The data represents the means \pm S.E.M of at least three independent experiments. ** denote $p < 0.01$ and *** denote $p < 0.001$ when compared to LPS (100 μ g/ml) + IFN- γ (100U/ml) and individual concentrations of DEM with or without atorvastatin.

4.0 DISCUSSION

The studies were initiated to examine the regulation of the expression and function of inducible nitric oxide synthase (iNOS) in RASMC's by OS. As already indicated, the role of iNOS in atherosclerosis is controversial. Whilst it is widely believed to have detrimental effects and contribute to the pathogenesis of the disease, recent studies reveal that iNOS induced NO may have cardio-protective functions in the body, which can be helpful in retarding the progression of atherosclerosis (Kanno *et al.*, 2000; Okazaki *et al.*, 2011). Atherosclerotic lesions are found in intimal layer of the artery. These lesions develop due to the endothelial cell injury caused by various stimuli as explained before. The centre of the lesion consists of foam cells and extracellular lipids, which is surrounded by VSMCs. Vascular smooth muscle cells are specialized cells present within the blood vessels and regulates the contraction and relaxation of the vessel (Rensen *et al.*, 2007; Wynne *et al.*, 2009). After the initial injury the endothelial cells, platelets and inflammatory cells release growth mediators and cytokines that causes proliferation and migration of VSMCs leading to plaque formation and extracellular matrix deposition. Smooth muscle cells hence are highly critical in the pathogenesis of atherosclerosis (Gomez and Owens, 2012). The role of iNOS as explained before plays an important role in the pathogenesis of atherosclerosis and although different cell types such as neuronal and endothelial cells generate iNOS it is the expression of iNOS predominantly in smooth muscle cells that may be critical in the pathology. The VSMCs express iNOS to an inflammatory response resulting from an injury or infection. Large amounts of NO are released from iNOS with potential harmful consequences, which can contribute to the pathogenesis of atherosclerosis. Interestingly, emerging evidence now suggest that expression of iNOS may act as a compensatory mechanism to the injury caused to the vascular wall and in turn prevent the progression of the lesions in

atherosclerosis. Hence we studied the activity of iNOS and changes in its expression and function in aortic smooth muscle cells in response to OS. The potential underlying mechanisms associated with any changes observed were also examined, as were the effects of statins, which are rapidly becoming the drugs of choice for patients with atherosclerosis.

Our previous preliminary studies have demonstrated that the expression and function of iNOS may be selectively down regulated by pro-oxidants such as antimycin A and DEM. Inducible nitric oxide synthase induced NO reduces oxidation of LDL (Rikitake *et al.*, 1998) and it is possible that the beneficial effects of iNOS-induced NO may be abolished under conditions of OS. Hence we hypothesized that the deleterious effects of OS may involve suppression of iNOS induced NO thereby preventing its protective actions. This may occur through ROS generated during OS reacting with NO, thereby decreasing the bioavailability of the latter or, alternatively, elements of OS may suppress iNOS expression through regulating the induction of this enzyme. Antimycins represent a group of secondary metabolites resulted from *Streptomyces* bacteria. Antimycin A with an empirical formula $C_{28}H_{40}O_9N_2$ (Figure 4.1) prevents the oxidation of ubiquinol by binding to the Qi site of cytochrome c reductase during the electron transport chain of oxidative phosphorylation in the mitochondria. This leads to the disruption of formation of proton gradient through the inner membrane. As a result protons become incapable to stream through the ATP synthase complex resulting in inhibition of ATP synthesis. Instead, a large quantity of toxic free radical superoxide is formed which causes OS. Antimycin A has been extensively used to detect the specific sites of reactive radical species produced in mitochondria isolated from skeletal muscle (Huang *et al.*, 2005).

Diethyl maleate (DEM) is a maleate ester produced as a result of formal condensation of both carboxy groups of maleic acid with ethanol (as shown in figure 4.2). In organic synthesis, it is generally used as a dienophile for diels-alder type cycloaddition reaction. It prevents formation of anti-oxidant glutathione by inhibiting glutathione synthase enzyme(Kaur *et al.*, 2006). As a result there is an increase in the pro-oxidant levels causing deleterious effects. Hydrogen peroxide by comparison is a compound with an oxygen-oxygen single bond (as shown in figure 4.3) and is a colourless liquid having viscosity slightly higher than water. It acts as a major factor in free radical associated aging and has an important role as a signalling molecule in the regulation of numerous biological processes (Romero and Lamas, 2014). Hydrogen peroxide is thermodynamically unstable and readily gets converted to water and oxygen thus leading to the formation of OH^\cdot radical. These OH^\cdot radicals further damage vital cellular components, especially those of the mitochondria causing oxidative DNA impairment (Halliwell *et al.*, 2000).

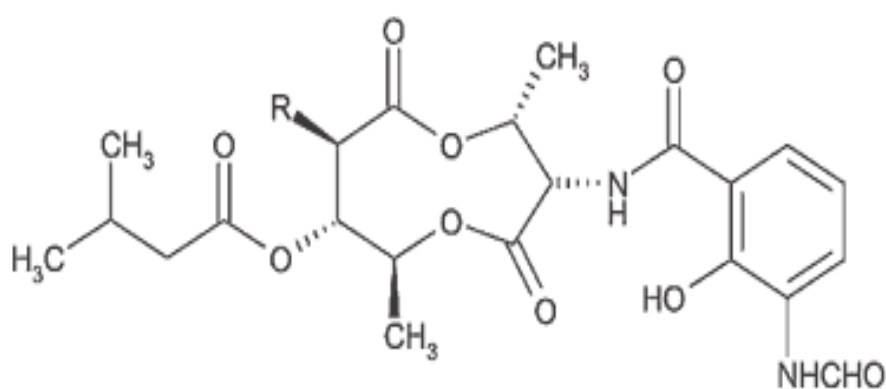


Figure 4.1 Structural Representation of antimycin A

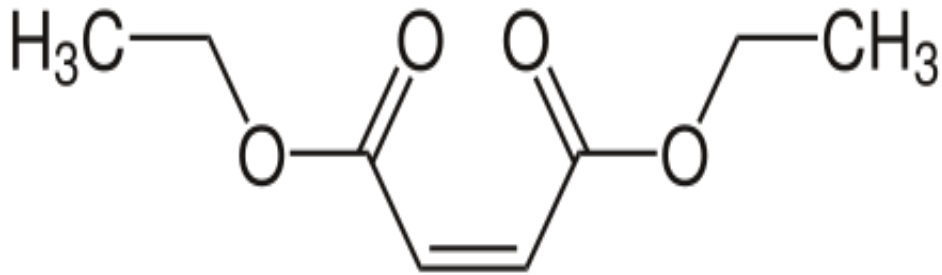


Figure 4.2 Structural Representation of diethyl maleate

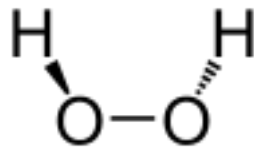


Figure 4.3 Structural Representation of Hydrogen Peroxide

Experiments were carried out using each of these agents for comparison. In each case cells were pre-incubated with the pro-oxidants: antimycin A, DEM or H₂O₂. Further incubating with LPS and IFN- γ then subsequently activated the cells and the expression of iNOS and NO production were investigated (Wileman *et al.*, 2003). These studies revealed antimycin A and DEM showed concentration dependent decrease of NO production induced by LPS and IFN- γ . Intriguingly H₂O₂ was without any effect. Antimycin A and DEM but not H₂O₂ also caused a concentration dependent decrease in detectable iNOS protein, suggesting that the suppression of NO production was caused by inhibition of iNOS expression. The results with DEM are consistent with the observations made by Kang *et al.* (1999) showing that DEM

inhibits the expression and function of iNOS but in macrophages and hepatocytes. Moreover, these findings suggest a relationship between glutathione and the induction of iNOS, which may be under critical regulation by cellular glutathione levels. With regards to the effects of antimycin A, it is likely that these may be linked to ATP depletion in cells. Indeed, ATP production is essential in regulating the expression of iNOS during inflammation (Chan *et al.*, 2001). Thus, decreases in the levels of iNOS and nitrite could be attributed to the effects of antimycin A in inhibiting ATP production. However unlike DEM and antimycin A, H₂O₂ did not regulate either iNOS or nitrite. Our findings with H₂O₂ further strengthened the available literature that supports no change in the expression of iNOS and subsequently nitrite production when incubated with H₂O₂ due to its inability to activate the key signalling molecules that leads to the induction of iNOS gene (Thirunavukkarasu *et al.*, 2006; Mendes *et al.*, 2003).

In addition to examining the effects of pro-oxidants on iNOS protein expression and function, further experiments were also initiated at the transcriptional level by looking at the effects of OS inducers on the iNOS mRNA. The results obtained showed a similar trend with that seen on iNOS protein expression/function. Antimycin A and DEM concentration dependently inhibited the mRNA of iNOS whereas H₂O₂ was without any effect when compared to the LPS and IFN- γ response. This results further explains our observations made earlier about the differences in the regulation of iNOS by DEM, antimycin A and H₂O₂. This confirms, at least in our model, that H₂O₂ was not able to effect the iNOS expression and function, as it did not regulate the transcription of iNOS gene. This further suggests that the effect may be independent of OS or may be specific free radicals generated by OS regulate the

signalling cascade that govern the induction of iNOS gene. Also as all three pro-oxidants generate free radicals, differences can also be attributed to the type of free radical species generated. These results strongly indicate that pro-oxidants, or at least antimycin A and DEM, regulate the expression of iNOS at the nuclear level, potentially regulating gene transcription. This would be consistent with other literature reporting that both DEM and antimycin A markedly inhibited LPS induced mRNA synthesis for iNOS in hepatocytes and macrophages (Kang *et al.*, 1999) which is similar to effects seen in this project on iNOS protein expression and function. Interestingly, H₂O₂ has been reported to up-regulate the expression of iNOS through the induction of NF- κ B and p38 MAPK in macrophages (Aktan, 2004). However, as already discussed, H₂O₂ was without effects in our studies. At present these discrepancies cannot be unequivocally explained but it is likely that the effects of H₂O₂ depends on the cell type. As discussed above the H₂O₂ activates iNOS in macrophages and up-regulates iNOS, however it did not affect the NF- κ B and further iNOS in bovine articular chondrocytes and rat islets (Mendes *et al.*, 2003; Cnop *et al.*, 2005). This clearly indicates the differential actions of H₂O₂ in different cell types and the effects we have seen in our cell culture model might reflect the same. Also H₂O₂ pre-dominantly generates OH⁻ radicals compared to DEM and antimycin A, which produces high amounts of both O₂⁻ and OH⁻ radicals. Therefore it is likely that the pro-oxidants generating O₂⁻ might regulate the expression and function of iNOS or the effects might be independent of OS...

Experiments were also conducted to investigate the cytotoxic effects of the selected compounds to see whether the above effects observed were specific or a consequence of any non-selective cytotoxic action of any of the pro-oxidants. The

Results showed no cytotoxic effects with the concentrations used suggesting the effects observed were not related to any cytotoxic effects of antimycin A, DEM or H_2O_2 . To additionally rule out any possible direct solvent effects on nitrite production and iNOS expression, experiments were also carried out by incubating the cells with various concentrations of ethanol. These studies revealed no solvent effects at the concentration ranges used, as ethanol alone did not alter nitrite synthesis or iNOS expression. Hence the effects reported were due to the treatment conditions.

As suggested above the effects seen with the pro-oxidants may or may not be independent of OS. Thus, it was essential to establish whether under treatment conditions, cells generated free radicals, which may be indicative of OS and may contribute to the consequences of OS in the studies. This is particularly important to establish especially as H_2O_2 did not cause any detectable changes in any of the parameters determined, making it difficult to establish what role OS actually plays in suppressing iNOS expression in our cell system or whether the inhibitions observed with AA and DEM are a consequence of ROS generation or due to other events which can directly or indirectly suppress the NOS gene and thus iNOS expression. Generation of ROS was therefore detected by fluorescence when cells were exposed to the three pro-oxidants and levels of ROS detected were correlated with the degree of inhibition of iNOS expression and NO production. These studies enabled us to explore the differences in the actions of H_2O_2 , antimycin A and DEM that we have observed previously and establish whether the suppression of iNOS is indeed mediated through ROS generation.

The species and/or site of ROS generation may also be of importance and as a result studies were carried out using confocal imaging where cells were loaded with an appropriate ROS probes and the reaction of ROS with the selected dye imaged. Fluorogenic, chemiluminescent or chromogenic probes such as 2', 7' – dichlorofluorescein (DCFH) and dihydroethidium (DHE) have been extensively used in tissue culture experiments to evaluate the production of ROS. The diacetate of DCFH (DCFH-DA) is added to cells and is hydrolysed by various intracellular esterases to DCFH. Upon oxidation the DCFH is converted to highly fluorescent DCF as elucidated in figure 59. Oxidation occurs in the presence of various OS molecules present within the cells. Peroxynitrite, the product formed between the reaction of NO and superoxide, can also oxidize DCFH (Kooy *et al.*, 1997; Royall and Ischiropoulos, 1993).

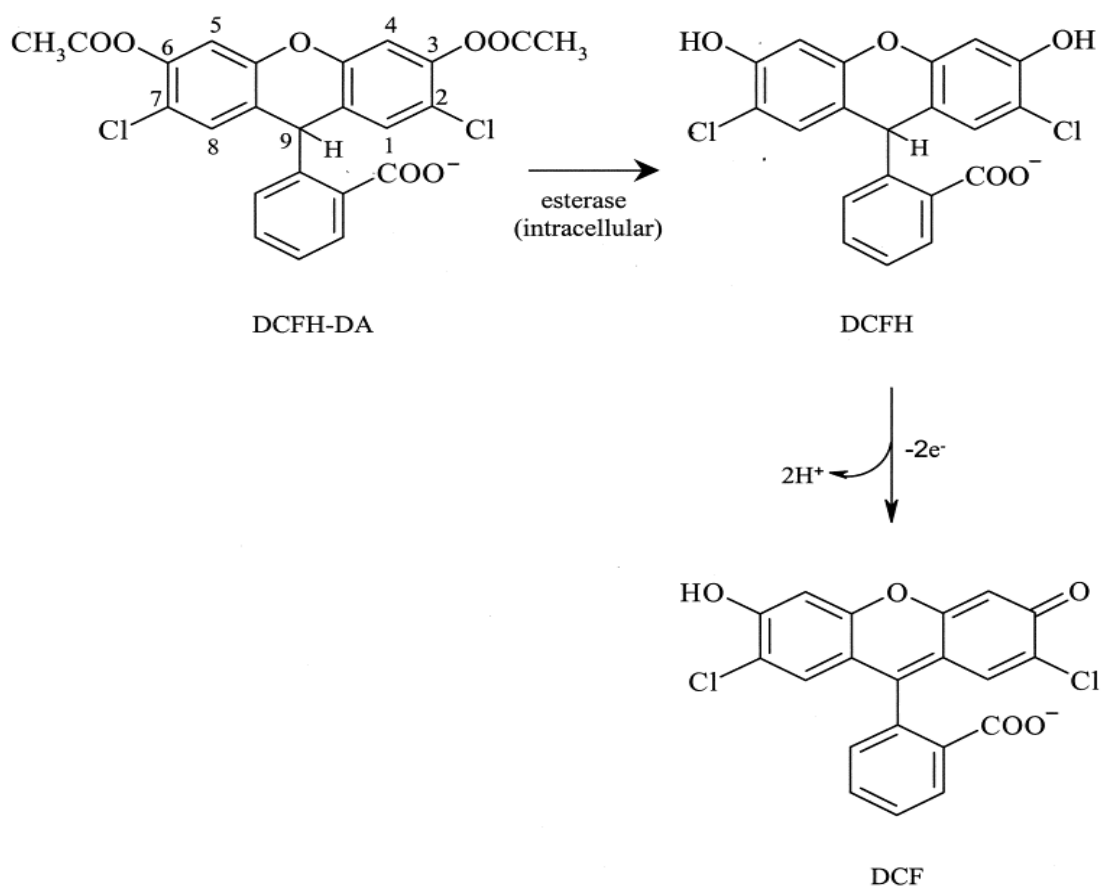


Figure 4.4 Structural representation of hydrolysis and oxidation of DCFH

Antimycin A, DEM and H_2O_2 caused significant generation of free radicals when incubated with the cells for 24hrs and subsequently probing with the DCF dye. Free radical production was found to be concentration dependent. The effects were more pronounced with higher concentrations such as $100\mu\text{M}$ and $150\mu\text{M}$ for antimycin A; $5\mu\text{M}$ and $10\mu\text{M}$ for DEM and $100\mu\text{M}$ and $300\mu\text{M}$ for H_2O_2 . The generation of ROS production was time dependent, with all three pro-oxidants inducing free radicals as early as 5min and reaching a peak at 6hr. However the effects were more pronounced with DEM and antimycin A when compared to H_2O_2 . At early time points more amounts of free radicals were generated with DEM and antimycin A compared to H_2O_2 . This indicates that DEM and antimycin A were quick to produce good amount of free radicals as early as 5min. However all three pro-oxidants generated

significant amounts of free radicals at 6hr. These results clearly demonstrate that all three pro-oxidants could induce significant levels of free radicals and strongly suggest that they may induce OS in our cell system. This however raises the question why H₂O₂ was without any noticeable effects on either iNOS expression or on NO production and suggest, to a certain degree, that OS may not regulate iNOS or NO production. There is however the alternative hypothesis that the outcome of OS may be dependent on the free radical species generated and that O₂⁻ generation may impact differently on iNOS and NO when compared to OH⁻ radicals. Thus, to further address the differences between these pro-oxidants, studies were extended to examine the specific free radicals generated by these agents. As O₂⁻ is the major free radical produced during the oxidative burst, experiments were conducted to establish the ability of antimycin A, DEM and H₂O₂ to produce superoxide radical. MitoSOX Red, a mitochondrial superoxide indicator and a cationic derivative of dihydroethidium, was used as a probe. MitoSOX Red is designed for highly specific detection of superoxide in the mitochondria of live cells. Mitochondrial superoxide is generated as a by-product of oxidative phosphorylation or by uncoupling of NOS. In an otherwise tightly coupled electron transport chain, a few proportion of mitochondrial oxygen is partly reduced and these electrons readily react with superoxide anion, the predominant reactive oxygen species in mitochondria. As explained earlier, uncoupling of NOS due to the deficiency in co-factors such as BH₄ also leads to the generation of O₂⁻ instead of NO thus contributing to the free radical accumulation (Kudin *et al.*, 2004; Batandier *et al.*, 2002; Luo *et al.*, 2014).

The triphenyl phosphonium constituent of MitoSOX red is responsible for the uptake of the dye into the actively respiring mitochondria. Oxidation of the dye by superoxide radicals results in the hydroxylation leading to the formation of 2-hydroxyethidium (as shown in Figure 61), which exhibits fluorescence at a wavelength of 400nm that falls in the spectrum of superoxide anion but not of the other ROS. Thus this dye enables selective detection of superoxide radical (Robinson *et al.*, 2008; Zielonka *et al.*, 2008).

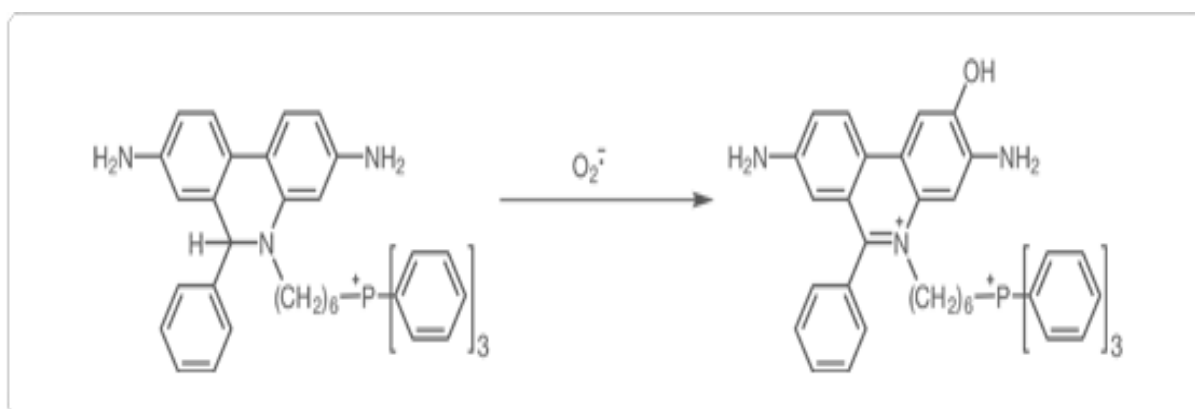


Figure 4.5 Oxidation of MitoSOX to 2-hydroxy-5-(triphenylphosphonium) hexylethidium by superoxide ($\bullet\text{O}_2^-$).

Cells were incubated with antimycin A, H_2O_2 and DEM for 24hrs and subsequent detection of superoxide radical with MitoSOX red. As described in the results, antimycin A and DEM produced significant amount of superoxide radical whereas hydrogen peroxide did not induce any superoxide radical generation. This data suggests the dissimilarities between these pro-oxidants and explains to an extent their difference in actions on the expression and function of iNOS. Moreover, these findings would suggest that the reduction in the expression of iNOS and consequent

inhibition of nitrite production might be achieved by the pro-oxidants that have the ability to generate superoxide anion rather than hydroxyl radicals.

To confirm the above proposal, further studies were conducted using specific free radical scavengers following treatment of cells with pro-oxidants. Polyethylene glycol superoxide dismutase (PEG-SOD) and polyethylene glycol catalase (PEG-catalase) were employed as inhibitors, which reduce the levels of superoxide and hydroxyl radicals respectively. Polyethylene glycol is covalently linked to superoxide dismutase and to catalase to increase the plasma half-life and allow cellular penetration thus making these scavengers more effective and long acting. Polyethylene glycol superoxide dismutase has been proposed as an effective agent for reducing free radical mediated ischemia-reperfusion injury (Galinares *et al.*, 1992). It provides protection against O_2^- anion by catalysing its oxidation and reduction into oxygen and hydrogen peroxide. Polyethylene glycol catalase acts by inhibiting OH^- radical and reducing H_2O_2 to water (Parastatidis *et al.*, 2014).

Cells treated with PEG-SOD or with PEG-catalase before incubation with DEM or antimycin A revealed that PEG-SOD at 500 U/ml was able to significantly inhibit the levels of superoxide generated whereas PEG-catalase only marginally altered the levels of superoxide generated by DEM and antimycin A. The marginal effect of PEG-catalase is not unexpected as it shows selectivity for hydroxyl radicals. The inhibition of superoxide anion by PEG-catalase may however be attributed to its effect, albeit small, on the mechanisms by which superoxide anion is produced. In this regard, PEG-catalase has been reported to inhibit the angiotensin II system that activates the NADPH enzyme, a major source of superoxide anion (Nagata *et al.*,

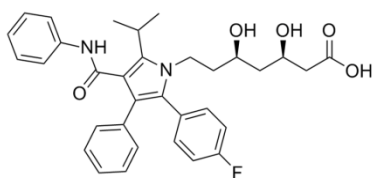
2004). Although there was no angiotensin II used in our studies, PEG-catalase may possibly regulate the activation of pathways that lead to the generation of superoxide radicals and this, although marginal, could explain to an extent the inhibition of superoxide seen in this project.

To confirm the importance of the specific free radical species in inhibiting iNOS expression and function, experiments were conducted using PEG-SOD and PEG-catalase to see if the inhibitions caused by DEM and antimycin A on nitrite production and iNOS expression could be restored. PEG-SOD at 500 U/ml was able to partially yet considerably reverse the inhibitions caused by these pro-oxidants, thus significantly restoring the expression of iNOS and thus nitrite production. However, as the expression of iNOS was already diminished resulting in low protein levels, the PEG-SOD could only partially restore the levels of nitrite. PEG-catalase did not have any effect on the inhibitions caused by AA and DEM suggesting the importance of superoxide anion in regulating the expression and function of iNOS. These results confirm the previous effects we have seen with the pro-oxidants in differentially regulating superoxide anion production and is consistent with their effects on the expression of iNOS and thus nitrite production.

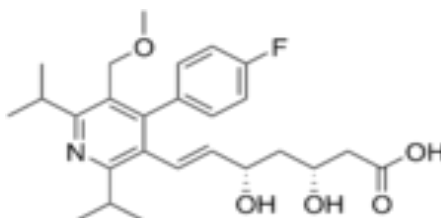
Statins are known to inhibit cholesterol synthesis in the body. These drugs however have other beneficial effects apart from their lipid lowering activity. Statins inhibit the effects of OS inducers and preserve the protective functions of NO and expression of iNOS (Mazzeiet *al.*, 2010). Similarly, in previous studies from our group, atorvastatin was shown to reverse the suppression of iNOS by antimycin A and by DEM but another statin, pravastatin, was without effect. Thus it is possible that this action of

atorvastatin is not common to all statins but perhaps specific to this particular drug or other members belonging to the same family of molecules.

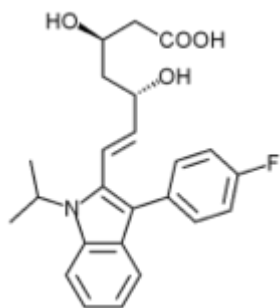
Statins are classified into two categories. Natural statins include lovastatin and synthetic derivatives include atorvastatin, simvastatin, pravastatin, fluvastatin and rosuvastatin. The different types of statins along with their molecular structure are shown below:



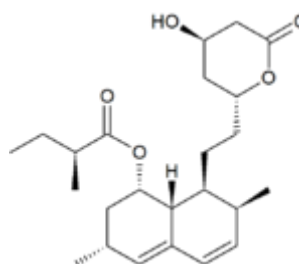
Atorvastatin



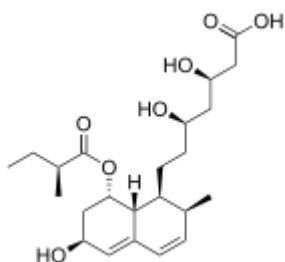
cerivastatin



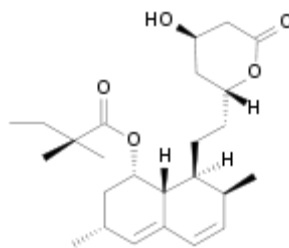
Fluvastatin



Lovastatin



Pravastatin



simvastatin

Statins prevent the occurrence of cardiovascular diseases by maintaining plaque stability, reducing endothelial dysfunction, modulating inflammatory response and preventing thrombus formation. Statins are known to raise the quantity of NO through the surge in the levels of catalase and tetrahydrobiopterin (BH₄) and inhibition of LDL oxidation while at the same time restores vitamins C and E levels and endogenous antioxidants such as ubiquinone and glutathione. The antioxidant vitamins C and E inhibit the oxidative process and may lead to the prevention of atherosclerotic lesions. Vitamin C activates NO synthase, stimulates BH₄ and reduces endothelial dysfunction (Munzelet *et al.*, 2005).

Fluvastatin decreases the generation of superoxide and also reduces the susceptibility of LDL to oxidation (Kugi *et al.*, 2002). Simvastatin inhibited the elevation of thiobarbituric acid and plasma F2-isoprostanes that are the markers of OS (Mohamadin *et al.*, 2011). Hence reduction in oxidative molecules can increase the bioavailability of NO enhancing its protective actions. Atorvastatin inhibits angiotensin-II induced superoxide formation by NADPH oxidase in vascular smooth muscle cells (Hong *et al.*, 2006; Pignatelli *et al.*, 2010; Violi *et al.*, 2014). Also, atorvastatin has been shown to increase paraoxanase activity and reduce cellular

uptake of oxLDL. Paraoxanase is an anti-oxidant enzyme present in HDL. It protects plasma lipoproteins from oxidative modification by ROS (Harangi *et al.*, 2004).

Studies were therefore initiated to examine the effects of atorvastatin on the expression and function of iNOS. Atorvastatin caused an increase in the expression of iNOS and nitrite production in a concentration dependent manner reaching a peak at 10 μ M and then decreasing with further concentrations causing a bell-shaped response. Atorvastatin at 10 μ M appeared to cause a maximum increase in the expression and function of iNOS and this concentration was used for further experiments. The increase in the expression of iNOS and subsequent nitrite production by atorvastatin suggests a possible action at the molecular level. Atorvastatin regulate the pathways associated with iNOS expression as evidenced by the literature that it activates PI3/Akt kinase and NF-kB, which are essential in inducing iNOS expression (Ye *et al.*, 2008; Nakata *et al.*, 2007). Thus, further studies were conducted to investigate whether atorvastatin could reverse the inhibitions caused by DEM and antimycin A on nitrite production and iNOS expression. Atorvastatin significantly restored both nitrite production and iNOS expression inhibited by DEM and antimycin A. These results confirm the novel role of atorvastatin in restoring the expression and function of iNOS and thus providing a protective mechanism against atherosclerosis.

Additional studies examined the effect of atorvastatin on superoxide radical generation in the presence and absence of DEM or antimycin A. Atorvastatin at 10 μ M significantly inhibited the generation of superoxide radical induced by antimycin A and DEM and on its own did not induce any superoxide radical

generation above that seen in controls. These results support the potential cellular anti-oxidant effects of atorvastatin (Wassmann *et al.*, 2002).

Studies were aimed at understanding the underlying cellular mechanism that mediates the suppression of iNOS following treatment of cells with pro-oxidants. In this regard, it has been reported that OS regulates various signalling pathways including those, which are involved in the transcription of iNOS (Park *et al.*, 2005; Schieber and Chandel, 2014). Thus experiments were carried out where changes in select kinase signalling were examined under our experimental conditions to determine whether pro-oxidants exert effects through suppression of these critical pathways. The transcriptional regulation of iNOS has been extensively characterised. Many regulatory elements have been identified to be important in LPS and IFN- γ induction of iNOS including the mitogen activated protein kinases (MAPKs). These are serine-threonine kinases, which are responsible for activation of transcription factors such as activator protein-1 (AP-1) and NF- κ B (Khalaf *et al.*, 2010) as shown in figure 4.6. Mitogen activated protein kinases are composed of three family members, which are diverse with each other: p38 MAPKs, extracellular signal-regulated kinases (ERKs) and c-jun terminal kinases (JNKs) or stress activated protein kinases (SAPKs) (Cargnello and Roux, 2011). Mitogen activated protein kinases are activated by MAPK kinases (MKKs), that phosphorylate MAPKs on specific threonine and tyrosine residues: MKK4 and MKK7 (also known as JNKK1 and JNKK2 or SAPK/ERK kinase (SEK)-1 and -2) activate the JNK/SAPKs, MKK3 and MKK6 activate the p38MAPKs, and MAPK/ERK kinase (MEK)-1 and -2 activate the ERKs (Stalheim and Johnson, 2008). Further upstream, JNK and ERK pathways were stimulated by the MEK kinases (MEKKs) and other kinases such as germinal

center kinase, mixed-lineage kinase, p21-activated kinase, and tyrosine phenol-lyase. Apart from MAPKs the other pathway involved is Janus kinase/signal transducers and activators of transcription (JAK/STAT). It is the principal signaling mechanism through which the cytokines and growth factors exert their effects. They are involved in cell proliferation, migration, differentiation and apoptosis. The IFN- γ used in our studies activates the JAK/STAT pathway through the receptor interferon-gamma receptor (IFN- γ R). The receptor activates the JAK's which are comprised of JAK1, JAK2 and JAK3. The activation of JAKs leads to the phosphorylation of downstream targets and its major substrates STAT's. STAT's are present in the cytoplasm in an inactivated form. Activation by JAK's phosphorylates STAT's into the nucleus where it further activates the target genes (Rawlings *et al.*, 2004). STAT's then activate the interferon regulatory factor 1 (IRF-1) which functions as a transcription activator for a variety of target genes. Interferon regulatory factor 1 then stabilizes the iNOS mRNA in the nucleus leading to the expression of iNOS and subsequent NO production (figure 4.6). Some of these kinase pathways were investigated in this study but limited to p38 MAPK and Akt because of the restricted time available and also because these have been identified as the critical and most widely reported signaling pathway for the induction of iNOS.

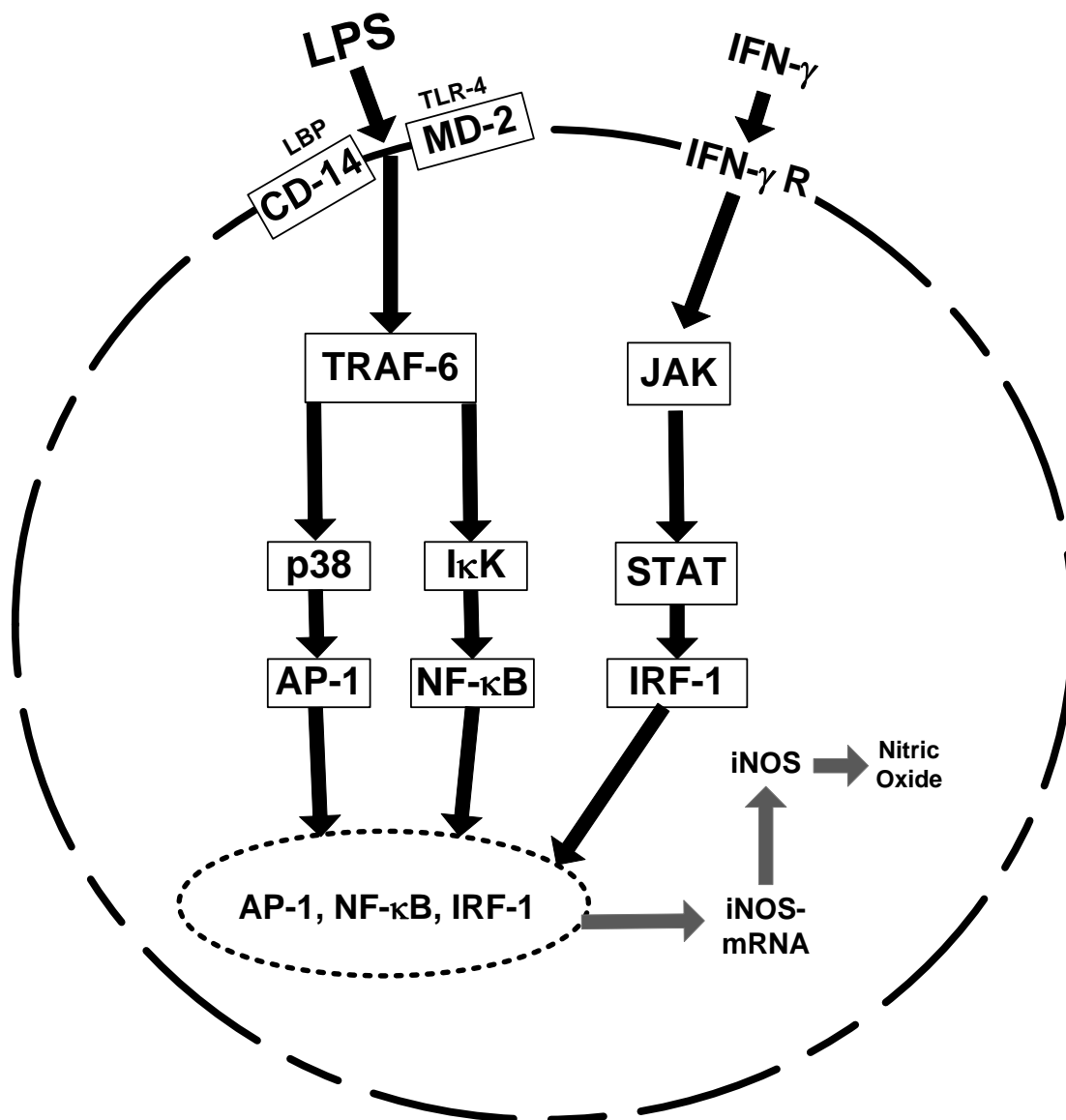


Figure 4.6 Schematic Representation of LPS and IFN- γ Signalling

Cells were treated with DEM, antimycin A or H₂O₂ before activating with LPS and IFN- γ . Antimycin A and DEM but not H₂O₂ down-regulated the phosphorylation of p38 MAPK and this was found to be concentration dependent. These effects were similar to the observations we have seen with the OS inducers on the expression of iNOS and nitrite production. This confirms the importance of p38 MAPK in regulating iNOS expression and, more importantly, tells us that OS regulates the expression

and function of iNOS by inhibiting this important signalling molecule. Similar studies were also conducted on the phosphorylation of Akt. This signalling molecule was found to be upstream to various MAP kinases and its shown to activate downstream targets such as NF- κ B, AP-1 etc (Kane *et al.*, 2002). Additionally, the literature suggests that Akt is predominantly involved in regulating the expression of iNOS by activating various signalling molecules that lead to the expression of iNOS (Isenovic *et al.*, 2002). Similar to the effects with p38, antimycin A and DEM concentration dependently inhibited the phosphorylation of Akt. These studies suggest that DEM and antimycin A down-regulate the expression and function of iNOS by inhibiting the phosphorylation of both Akt and p38 MAPK, which are the important signalling molecules that regulate iNOS. Also H₂O₂ was without any effect because of its inability in regulating these signalling molecules. These novel findings confirm the difference in OS inducers in regulating iNOS expression. Antimycin A and DEM inhibited the iNOS expression/function but not H₂O₂ because of their difference on the activity of the key signalling molecules that induce iNOS gene transcription.

Recent studies reveal that there is a link between statins and the protein kinase Akt. Low concentrations of Statins enhanced angiogenesis by activating Akt kinase and subsequent increase in NO production (Wong *et al.*, 2006). Literature suggests that atorvastatin exerted cardio protection through increase in the expression of iNOS and subsequently NO production (Zhou *et al.*, 2007). In case of ischaemic preconditioning, atorvastatin activated the transcription of protein kinase C, NF- κ B and JAK-STAT signalling leading to the expression of iNOS. When the activation of iNOS is blocked the myocardial infarct size limiting capacity of Atorvastatin was abrogated suggesting the need of up-regulation of iNOS in reducing the infarct size (Ye *et al.*,

2008; subramani *et al.*, 2009). Atorvastatin improved the endothelial dysfunction and vascular tone by scavenging the free radicals and thus reducing the oxidative stress (Li *et al.*, 2015; Crespo and Quidgley, 2015). There are various pathways that have been suggested through which the Atorvastatin activates iNOS. Of all the pathways, MAPKs were considered to be the important pathway through which it regulates the expression of iNOS. Atorvastatin phosphorylates Akt leading to the expression of downstream targets such as p38 MAPK, NF- κ B. some studies suggests that Atorvastatin at 34-68micromol/L raised the nitrite levels and iNOS activity by 9-fold and also increased the mRNA of iNOS (Kolyada *et al.*, 2001; Kesavan *et al.*, 2014). These reports gives a strong indication that atorvastatin may be exerting its observed effects in our studies by acting, at least in part, on some of the signalling identified above. Since we have already identified a role for phospho-p38 and phospho-Akt, the next series of experiments examined whether these kinases may be regulated by atorvastatin.

Indeed atorvastatin was able to significantly restore the phosphorylation of both p38 MAPK and Akt inhibited by antimycin A and DEM in a concentration dependent manner. These results confirm that atorvastatin suppresses the inhibition caused by DEM and antimycin A on nitrite production and iNOS expression by restoring the phosphorylation of both p38 MAPK and Akt. Hence these novel and exciting studies confirm the importance of Akt and p38 MAPK as the key signalling molecules targeted in OS in regulating the expression of iNOS. Thus by suppressing OS and restoring the mechanisms of the iNOS gene transcription we can achieve the desired iNOS and nitrite levels and hence help in retarding the progression of atherosclerotic lesions.

4.1 Summary and Conclusions

The data generated in this thesis showed the difference in the regulation by OS inducers on the expression and function of iNOS. The key finding is both DEM and antimycin A inhibited iNOS expression and function whereas intriguingly H₂O₂ was without any effect. However all three OS inducers generated significant amount of ROS but only DEM and antimycin A produced superoxide anion. The results confirms the difference between the three OS inducers and demonstrate clearly that effect on iNOS expression/function depends on the ability of the OS inducers to generate superoxide anion which may then act at targeted signalling molecules to suppress iNOS mRNA and subsequent protein expression. Indeed this was confirmed in the second part of the studies which focused on the molecular mechanisms through which OS inducers inhibited iNOS expression and function. The important findings are the effects of OS inducers on the key signalling molecules, p38 MAPK and Akt that regulate the iNOS gene transcription. Both antimycin A and DEM inhibited iNOS expression by down-regulating the activation of both the p38 MAPK and Akt. These findings further strengthened the importance of these signalling molecules in regulating iNOS expression and also revealed a novel mechanism by which antimycin A and DEM inhibit the iNOS expression and subsequent nitrite production. Also studies conducted using atorvastatin showed an increase in the expression of iNOS suggesting an effect at the molecular level. Atorvastatin restored the inhibitions caused by OS inducers on the expression of iNOS and nitrite production by reversing their effects on key signalling molecules, p38 MAPK and Akt.

Taken together, the data suggest novel actions for both pro-oxidants and atorvastatin, which may have important implications in coronary artery disease where suppression of iNOS may be deleterious and maintaining its expression may be cardio-protective.

5.0 FUTURE WORK

Further experiments can be carried out by looking at the effects of OS inducers on the anti-oxidant signalling molecules and its comparison with the levels of iNOS expression and nitrite production. Some of the anti-oxidant signalling molecules and transcription factors that can be verified include HO-1, Nrf-2, Klotho etc.

We have looked at the effects of anti-oxidants, PEG-SOD and PEG-catalase, on the expression and function of iNOS in the presence and absence of OS inducers. Studies can be extended to the signalling mechanisms that regulate the expression of iNOS in the presence of OS inducers. These studies can establish whether the free radicals such as O_2^- and OH^\cdot have an effect on key signalling molecules.

Different statins have distinct lipid lowering effects. Hence it would be interesting to evaluate the effects of other statins such as simvastatin, cerivastatin, rosuvastatin etc. on the iNOS expression/function and also on the signalling pathways following treatment of cells with OS inducers.

6.0 REFERENCES

- Abd El-Aleem, S., Ragab, S., & Ahmed, R. (2008). Upregulation of the Inducible Nitric Oxide Synthase in Rat Hippocampus in A Model of Alzheimer's Disease: A possible Mechanism of Aluminium Induced Alzheimer's, *32*(1), 173–180.
- Abraham, N. G., & Kappas, A. (2008). Pharmacological and clinical aspects of heme oxygenase. *Pharmacological Reviews*, *60*, 79–127.
- Aktan, F. (2004). iNOS-mediated nitric oxide production and its regulation. *Life Sciences*, *75*(2004), 639–653.
- Alderton, W. K., Cooper, C. E., & Knowles, R. G. (2001). Nitric oxide synthases: structure, function and inhibition. *The Biochemical Journal*, *357*(Pt 3), 593–615.
- Alfieri, A., Srivastava, S., Siow, R. C. M., Mudo, M., Fraser, P. a, & Mann, G. E. (2011). Targeting the Nrf2-Keap1 antioxidant defence pathway for neurovascular protection in stroke. *The Journal of Physiology*, *589*(April), 4125–4136.
- Annuk, M., Zilmer, M., & Fellström, B. (2003). Endothelium-dependent vasodilation and oxidative stress in chronic renal failure: impact on cardiovascular disease. *Kidney International. Supplement*, *63*(84), S50–3.
- Arnaud, C., Laubriet, a, Joyeux, M., Godin-Ribuot, D., Rochette, L., Demenge, P., & Ribuot, C. (2001). Role of nitric oxide synthases in the infarct size-reducing effect conferred by heat stress in isolated rat hearts. *British Journal of Pharmacology*, *132*(8), 1845–51.

- Atar, S., Ye, Y., Lin, Y., Freeberg, S. Y., Nishi, S. P., Rosanio, S., ... Birnbaum, Y. (2006). Atorvastatin-induced cardioprotection is mediated by increasing inducible nitric oxide synthase and consequent S-nitrosylation of cyclooxygenase-2. *American Journal of Physiology. Heart and Circulatory Physiology*, 290, H1960–H1968.
- Athyros, V. G., Kakafika, A., Karagiannis, A., & Mikhailidis, D. P. (2007). Statins and regression of coronary atherosclerosis. *JAMA: The Journal of the American Medical Association*.
- Aviram, M., Rosenblat, M., Bisgaier, C. L., & Newton, R. S. (1998). Atorvastatin and gemfibrozil metabolites, but not the parent drugs, are potent antioxidants against lipoprotein oxidation. *Atherosclerosis*, 138(2), 271–80.
- Bae, Y. S., Lee, J. H., Choi, S. H., Kim, S., Almazan, F., Witztum, J. L., & Miller, Y. I. (2009). Macrophages generate reactive oxygen species in response to minimally oxidized low-density lipoprotein: Toll-like receptor 4- and spleen tyrosine kinase-dependent activation of NADPH oxidase 2. *Circulation Research*, 104, 210–218.
- Baker, C. S. R., Hall, R. J. C., Evans, T. J., Pomerance, a., Maclouf, J., Creminon, C., ... Polak, J. M. (1999). Cyclooxygenase-2 Is Widely Expressed in Atherosclerotic Lesions Affecting Native and Transplanted Human Coronary Arteries and Colocalizes With Inducible Nitric Oxide Synthase and Nitrotyrosine Particularly in Macrophages. *Arteriosclerosis, Thrombosis, and Vascular Biology*, 19(3), 646–655.

- Balogun, E., Hoque, M., Gong, P., Killeen, E., Green, C. J., Foresti, R., ... Motterlini, R. (2003). Curcumin activates the haem oxygenase-1 gene via regulation of Nrf2 and the antioxidant-responsive element. *The Biochemical Journal*, 371(Pt 3), 887–95.
- Bao, X.-M., Wu, C.-F., & Lu, G.-P. (2010). Atorvastatin inhibits homocysteine-induced oxidative stress and apoptosis in endothelial progenitor cells involving Nox4 and p38MAPK. *Atherosclerosis*, 210(1), 114–21.
- Batandier, C., Fontaine, E., Kériel, C., & Lerverve, X. M. (2002). Determination of mitochondrial reactive oxygen species: methodological aspects. *Journal of Cellular and Molecular Medicine*, 6, 175–87.
- Bedard, K., & Krause, K.-H. (2007). The NOX family of ROS-generating NADPH oxidases: physiology and pathophysiology. *Physiological Reviews*, 87, 245–313.
- Bell, R. M., & Yellon, D. M. (2003). Atorvastatin, administered at the onset of reperfusion, and independent of lipid lowering, protects the myocardium by up-regulating a pro-survival pathway. *Journal of the American College of Cardiology*, 41(3), 508–515.
- Bianchi, A. L., Denavit-Saubié, M., & Champagnat, J. (1995). Central control of breathing in mammals: neuronal circuitry, membrane properties, and neurotransmitters. *Physiological Reviews*, 75, 1–45.
- Blancher, C., & Jones, A. (2001). SDS -PAGE and Western Blotting Techniques. *Methods in Molecular Medicine*, 57, 145–162.

- Bureau, J. F., Bihl, F., Brahic, M., & Le Paslier, D. (1995). The gene coding for interferon-gamma is linked to the D12S335 and D12S313 microsatellites and to the MDM2 gene. *Genomics*, *28*(1), 109–12.
- Buttery, L. D., Springall, D. R., Chester, a H., Evans, T. J., Standfield, E. N., Parums, D. V, ... Polak, J. M. (1996). Inducible nitric oxide synthase is present within human atherosclerotic lesions and promotes the formation and activity of peroxynitrite. *Laboratory Investigation; a Journal of Technical Methods and Pathology*, *75*, 77–85.
- Cai, H., & Harrison, D. G. (2000). Endothelial Dysfunction in Cardiovascular Diseases: The Role of Oxidant Stress. *Circulation Research*, *87*(10), 840–844
- Cargnello, M., & Roux, P. P. (2011). Activation and function of the MAPKs and their substrates, the MAPK-activated protein kinases. *Microbiology and Molecular Biology Reviews : MMBR*, *75*(1), 50–83.
- Carr, a. C., Zhu, B.-Z., & Frei, B. (2000). Potential Antiatherogenic Mechanisms of Ascorbate (Vitamin C) and -Tocopherol (Vitamin E). *Circulation Research*, *87*(5), 349–354.
- Cassina, P. (2002). Peroxynitrite triggers a phenotypic transformation in spinal cord astrocytes that induces motor neuron apoptosis. *J. Neurosci. Res.*, *67*, 21–29.

Chan, E. D., Morris, K. R., Belisle, J. T., Remigio, L. K., Brennan, P. J., David, W. H., ... Riches, D. W. H. (2001). Induction of Inducible Nitric Oxide Synthase-NO[·] by Lipoarabinomannan of *Mycobacterium tuberculosis* Is Mediated by Signaling Pathways Induction of Inducible Nitric Oxide Synthase-NO[·] by Lipoarabinomannan of *Mycobacterium tuberculosis* Is Mediated by MEK1. *Infection and Immunity*, 69(4), 2001–2010.

Chan, E. D., & Riches, D. W. (2001). IFN-gamma + LPS induction of iNOS is modulated by ERK, JNK/SAPK, and p38(mapk) in a mouse macrophage cell line. *American Journal of Physiology. Cell Physiology*, 280, C441–C450.

Channon, K. M., Qian, H., & George, S. E. (2000). Nitric oxide synthase in atherosclerosis and vascular injury: insights from experimental gene therapy. *Arteriosclerosis, Thrombosis, and Vascular Biology*, 20, 1873–1881.

Chen, H., Ikeda, U., Shimpo, M., Ikeda, M., Minota, S., & Shimada, K. (2000). Fluvastatin Upregulates Inducible Nitric Oxide Synthase Expression in Cytokine-Stimulated Vascular Smooth Muscle Cells. *Hypertension*, 36(6), 923–928.

Chen, K., & Popel, A. S. (2009). Nitric oxide production pathways in erythrocytes and plasma. *Biorheology*.

Chu, L. W., Chen, J. Y., Yu, K. L., Cheng, K. I., Chen, I. J., Wu, P. C., & Wu, B. N. (2012). Neuroprotective and anti-inflammatory activities of atorvastatin in a rat chronic constriction injury model. *International Journal of Immunopathology and Pharmacology*.

- Cnop, M., Welsh, N., Jonas, J., Jo, A., & Lenzen, S. (2014). Many Differences, Few Similarities, *54*(6), 97–107.
- Coller, B. S. (2005). Leukocytosis and ischemic vascular disease morbidity and mortality: Is it time to intervene? *Arteriosclerosis, Thrombosis, and Vascular Biology*, *25*, 658–670.
- Cruse, I., & Maines, M. D. (1988). Evidence suggesting that the two forms of heme oxygenase are products of different genes. *Journal of Biological Chemistry*, *263*(7), 3348–3353.
- Cui, W., Matsuno, K., Iwata, K., Ibi, M., Katsuyama, M., Kakehi, T., ... Yabe-Nishimura, C. (2009). NADPH oxidase isoforms and anti-hypertensive effects of atorvastatin demonstrated in two animal models. *Journal of Pharmacological Sciences*, *111*, 260–268.
- Da Silva, J. L., Morishita, T., Escalante, B., Staudinger, R., Drummond, G., Goligorsky, M. S., ... Abraham, N. G. (1996). Dual role of heme oxygenase in epithelial cell injury: contrasting effects of short-term and long-term exposure to oxidant stress. *The Journal of Laboratory and Clinical Medicine*, *128*(3), 290–6.
- Da Silva, J. L., Zand, B. a, Yang, L. M., Sabaawy, H. E., Lianos, E., & Abraham, N. G. (2001). Heme oxygenase isoform-specific expression and distribution in the rat kidney. *Kidney International*, *59*, 1448–1457.

- Dae, S. J., Min, H. Y., Jeong, Y. H., Sang, K. L., & Seo, E. K. (2004). Di- and sesquiterpenoids isolated from the pods of *Sindora sumatrana* and their potential to inhibit lipopolysaccharide-induced nitric oxide production. *Archives of Pharmacal Research*, 27, 291–294.
- Davey, G. P., Tipton, K. F., & Murphy, M. P. (1992). Uptake and accumulation of 1-methyl-4-phenylpyridinium by rat liver mitochondria measured using an ion-selective electrode. *Biochem. J.*, 288, 439–443.
- Davis, N. E. (2005). Atherosclerosis--an inflammatory process. *Journal of Insurance Medicine*, 37: 72–75.
- Davis, R. L., Sanchez, A. C., Lindley, D. J., Williams, S. C., & Syapin, P. J. (2005). Effects of mechanistically distinct NF-kappaB inhibitors on glial inducible nitric oxide synthase expression. *Nitric Oxide : Biology and Chemistry / Official Journal of the Nitric Oxide Society*, 12(4), 200–9.
- De Frutos, T., de Miguel, L. S., García-Durán, M., González-Fernández, F., Rodríguez-Feo, J. a, Montón, M., ... López-Farré, a. (1999). NO from smooth muscle cells decreases NOS expression in endothelial cells: role of TNF-alpha. *The American Journal of Physiology*, 277, H1317–H1325.
- Demir, B. Ç., Uyar, Y., Ozbilgin, K., & Köse, C. (2013). Effect of raloxifene and atorvastatin in atherosclerotic process in ovariectomized rats. *Journal of Obstetrics and Gynaecology Research*, 39, 229–236.

- Dichtl, W. (2002). HMG-CoA Reductase Inhibitors Regulate Inflammatory Transcription Factors in Human Endothelial and Vascular Smooth Muscle Cells. *Arteriosclerosis, Thrombosis, and Vascular Biology*, 23(1), 58–63.
- Ding, Y., & Vaziri, N. D. (1998). Calcium channel blockade enhances nitric oxide synthase expression by cultured endothelial cells. *Hypertension*, 32, 718–723.
- Doronzo, G., Viretto, M., Russo, I., Mattiello, L., Di Martino, L., Cavalot, F., ... Trovati, M. (2011). Nitric oxide activates PI3-K and MAPK signalling pathways in human and rat vascular smooth muscle cells: influence of insulin resistance and oxidative stress. *Atherosclerosis*, 216(1), 44–53.
- Drummond, G. R., Selemidis, S., Griendling, K. K., & Sobey, C. G. (2011). Combating oxidative stress in vascular disease: NADPH oxidases as therapeutic targets. *Nature Reviews. Drug Discovery*, 10, 453–471.
- Dupont, G. P., Huecksteadt, T. P., Marshall, B. C., Ryan, U. S., Michael, J. R., & Hoidal, J. R. (1992). Regulation of xanthine dehydrogenase and xanthine oxidase activity and gene expression in cultured rat pulmonary endothelial cells. *The Journal of Clinical Investigation*, 89, 197–202.
- Ebrahimi, M., & Sadeghizadeh, M. (2002). EXPRESSION OF INDUCIBLE NITRIC OXIDE SYNTHASE GENE (iNOS) STIMULATED BY HYDROGEN PEROXIDE IN HUMAN, 13(1), 15–18.
- Finkel, T., & Holbrook, N. J. (2000). Oxidants, oxidative stress and the biology of ageing. *Nature*, 408(November), 239–247.

- Förstermann, U. (2010). Nitric oxide and oxidative stress in vascular disease. *Pflügers Archiv: European Journal of Physiology*, 459(6), 923–39.
- Förstermann, U., & Sessa, W. C. (2012). Nitric oxide synthases: Regulation and function. *European Heart Journal*, 33, 829–837.
- Furchgott, R. F., & Zawadzki, J. V. (1980). The obligatory role of endothelial cells in the relaxation of arterial smooth muscle by acetylcholine. *Nature*, 288, 373–376.
- Galinanes, M., Ferrari, R., Qiu, Y., Cargnoni, A., Ezrin, A., & Hearse, D. J. (1992). PEG-SOD and myocardial antioxidant status during ischaemia and reperfusion: Dose-response studies in the isolated blood perfused rabbit heart. *Journal of Molecular and Cellular Cardiology*, 24, 1021–1030.
- Garcia, X., & Stein, F. (2006). Nitric oxide. *Seminars in Pediatric Infectious Diseases*, 17(2), 55–7.
- Ginnan, R., Guikema, B. J., Halligan, K. E., Singer, H. a, & Jourd'heuil, D. (2008). Regulation of smooth muscle by inducible nitric oxide synthase and NADPH oxidase in vascular proliferative diseases. *Free Radical Biology & Medicine*, 44(7), 1232–45.
- Gobe, G., & Crane, D. (2010). Mitochondria, reactive oxygen species and cadmium toxicity in the kidney. *Toxicology Letters*, 198(1), 49–55.
- Gomez, D., & Owens, G. K. (2012). Smooth muscle cell phenotypic switching in atherosclerosis. *Cardiovascular Research*, 95, 156–164.

- Gorren, a C., & Mayer, B. (1998). The versatile and complex enzymology of nitric oxide synthase. *Biochemistry. Biokhimiia*, 63, 734–743.
- Green, K., Brand, M. D., & Murphy, M. P. (2004). Prevention of mitochondrial oxidative damage as a therapeutic strategy in diabetes. *Diabetes*, 53(suppl 1), S110–118.
- Gregory, E. M., Goscin, S. a, & Fridovic.I. (1974). Superoxide-Dismutase and Oxygen Toxicity in a Eukaryote. *Journal of Bacteriology*, 117(2), 456–460.
- Griendling, K. K., Sorescu, D., & Ushio-Fukai, M. (2000). NAD(P)H Oxidase : Role in Cardiovascular Biology and Disease. *Circulation Research*, 86(5), 494–501.
- Guzik, T. J., West, N. E. J., Black, E., Mcdonald, D., Pillai, R., Channon, K. M., & Ratnatunga, C. (2006). UltraRapid Communication Association With Endothelial Dysfunction and Clinical Risk Factors. *Clinical Risk*.
- Hadi, H. a R., Carr, C. S., & Al Suwaidi, J. (2005). Endothelial dysfunction: cardiovascular risk factors, therapy, and outcome. *Vascular Health and Risk Management*, 1(3), 183–198.
- Hajjar, R. J., & Leopold, J. a. (2006). Xanthine oxidase inhibition and heart failure: Novel therapeutic strategy for ventricular dysfunction? *Circulation Research*, 98(1), 169–171.
- Halliwell, B., Clement, M. V, & Long, L. H. (2000). Hydrogen peroxide in the human body. *FEBS Letters*, 486(1), 10–3.

- Hamilton, C. a, Miller, W. H., Al-Benna, S., Brosnan, M. J., Drummond, R. D., McBride, M. W., & Dominiczak, A. F. (2004). Strategies to reduce oxidative stress in cardiovascular disease. *Clinical Science (London, England: 1979)*, 106(3), 219–34.
- Hansson, G. K., Robertson, A.-K. L., & Söderberg-Nauclér, C. (2006). Inflammation and atherosclerosis. *Annual Review of Pathology*, 1, 297–329.
- Harangi, M., Seres, I., Varga, Z., Emri, G., Szilvássy, Z., Paragh, G., & Remenyik, É. (2004). Atorvastatin effect on high-density lipoprotein-associated paraoxonase activity and oxidative DNA damage. *European Journal of Clinical Pharmacology*, 60, 685–691.
- Hattori, Y., Hattori, S., & Kasai, K. (2003). Lipopolysaccharide activates Akt in vascular smooth muscle cells resulting in induction of inducible nitric oxide synthase through nuclear factor-kappa B activation. *European Journal of Pharmacology*, 481(2-3), 153–158.
- Hecker, M., Cattaruzza, M., & Wagner, a H. (1999). Regulation of inducible nitric oxide synthase gene expression in vascular smooth muscle cells. *General Pharmacology*, 32(1), 9–16.
- Hill, K. E., Zollinger, L. V., Watt, H. E., Carlson, N. G., & Rose, J. W. (2004). Inducible nitric oxide synthase in chronic active multiple sclerosis plaques: Distribution, cellular expression and association with myelin damage. *Journal of Neuroimmunology*, 151, 171–179.

- Hong, H., Zeng, J.-S., Kreulen, D. L., Kaufman, D. I., & Chen, A. F. (2006). Atorvastatin protects against cerebral infarction via inhibition of NADPH oxidase-derived superoxide in ischemic stroke. *American Journal of Physiology. Heart and Circulatory Physiology*, 291, H2210–H2215.
- Howden, R. (2013). Nrf2 and cardiovascular defense. *Oxidative Medicine and Cellular Longevity*, 2013.
- Huang LS, Cobessi D, T. E. (2005). Binding of the Respiratory Chain Inhibitor Antimycin to the Mitochondrial bc1 Complex@2011-10-25T23:51:12.pdf. *J Mol Biol*.
- Hughes, J. P., Staton, P. C., Wilkinson, M. G., Strijbos, P. J. L. M., Skaper, S. D., Arthur, J. S. C., & Reith, A. D. (2003). Mitogen and stress response kinase-1 (MSK1) mediates excitotoxic induced death of hippocampal neurones. *Journal of Neurochemistry*, 86, 25–32.
- Irani, K. (2000). Oxidant Signaling in Vascular Cell Growth, Death, and Survival: A Review of the Roles of Reactive Oxygen Species in Smooth Muscle and Endothelial Cell Mitogenic and Apoptotic Signaling. *Circulation Research*, 87(3), 179–183.
- Isenovic, E. R., Meng, Y., Divald, A., Milivojevic, N., & Sowers, J. R. (2002). Role of phosphatidylinositol 3-kinase/Akt pathway in angiotensin II and insulin-like growth factor-1 modulation of nitric oxide synthase in vascular smooth muscle cells. *Endocrine*, 19, 287–292.

- Ito, D., Ito, O., Mori, N., Muroya, Y., Cao, P.-Y., Takashima, K., ... Kohzuki, M. (2010). Atorvastatin upregulates nitric oxide synthases with Rho-kinase inhibition and Akt activation in the kidney of spontaneously hypertensive rats. *Journal of Hypertension*, *28*, 2278–2288.
- Jorens, P. G., Matthys, K. E., & Bult, H. (1995). Modulation of nitric oxide synthase activity in macrophages. *Mediators of Inflammation*, *4*, 75–89.
- Kandasamy, K., Prawez, S., Choudhury, S., More, A. S., Ahanger, A. A., Singh, T. U., ... Mishra, S. K. (2011). Atorvastatin prevents vascular hyporeactivity to norepinephrine in sepsis: role of nitric oxide and α_1 -adrenoceptor mRNA expression. *Shock (Augusta, Ga.)*.
- Kane, L. P., Mollenauer, M. N., Xu, Z., Turck, C. W., & Weiss, A. (2002). Akt-dependent phosphorylation specifically regulates Cot induction of NF-kappa B-dependent transcription. *Molecular and Cellular Biology*, *22*, 5962–5974.
- Kang, K. W., Pak, Y. M., & Kim, N. D. (1999). Diethylmaleate and buthionine sulfoximine, glutathione-depleting agents, differentially inhibit expression of inducible nitric oxide synthase in endotoxemic mice. *Nitric Oxide: Biology and Chemistry / Official Journal of the Nitric Oxide Society*, *3*(3), 265–271.
- Kanno, S., Lee, P. C., Zhang, Y., Ho, C., Griffith, B. P., Shears, L. L., & Billiar, T. R. (2000). Attenuation of myocardial ischemia/reperfusion injury by superinduction of inducible nitric oxide synthase. *Circulation*, *101*, 2742–2748.

- Kaur, P., Kalia, S., & Bansal, M. P. (2006). Effect of diethyl maleate induced oxidative stress on male reproductive activity in mice: Redox active enzymes and transcription factors expression. *Molecular and Cellular Biochemistry*, 291, 55–61.
- Kavya, R., Saluja, R., Singh, S., & Dikshit, M. (2006). Nitric oxide synthase regulation and diversity: Implications in Parkinson's disease. *Nitric Oxide - Biology and Chemistry*, 15, 280–294.
- Khalaf, H., Jass, J., & Olsson, P.-E.(2010). Differential cytokine regulation by NF-kappaB and AP-1 in Jurkat T-cells.*BMC Immunology*, 11, 26.
- Kiang, J. G. (2004). Inducible heat shock protein 70 kD and inducible nitric oxide synthase in hemorrhage/resuscitation-induced injury. *Cell Research*, 14(6), 450–459.
- Kishore, R., McMullen, M. R., Cocuzzi, E., & Nagy, L. E. (2004). Lipopolysaccharide-mediated signal transduction: Stabilization of TNF-alpha mRNA contributes to increased lipopolysaccharide-stimulated TNF-alpha production by Kupffer cells after chronic ethanol feeding. *Comparative Hepatology*, 3 Suppl 1, S31.
- Kissner, R., & Koppenol, W. H. (2002). Product distribution of peroxynitrite decay as a function of pH, temperature, and concentration.*Journal of the American Chemical Society*, 124(2), 234–9.

- Kiyoshima, T., Enoki, N., Kobayashi, I., Sakai, T., Nagata, K., Wada, H., ... Sakai, H. (2012). Oxidative stress caused by a low concentration of hydrogen peroxide induces senescence-like changes in mouse gingival fibroblasts. *International Journal of Molecular Medicine*, 30, 1007–1012.
- Kleinert, H., Pautz, A., Linker, K., & Schwarz, P. M. (2004). Regulation of the expression of inducible nitric oxide synthase. *European Journal of Pharmacology*, 500(1-3), 255–66.
- Kojda, G., & Harrison, D. (1999). Interactions between NO and reactive oxygen species: Pathophysiological importance in atherosclerosis, hypertension, diabetes and heart failure. *Cardiovascular Research*, 43, 562–571.
- Kolyada, a. Y., Fedtsov, a., & Madias, N. E. (2001). 3-Hydroxy-3-Methylglutaryl Coenzyme A Reductase Inhibitors Upregulate Inducible NO Synthase Expression and Activity in Vascular Smooth Muscle Cells. *Hypertension*, 38(5), 1024–1029.
- Kooy, N. W., Lewis, S. J., Royall, J. a, Ye, Y. Z., Kelly, D. R., & Beckman, J. S. (1997). Extensive tyrosine nitration in human myocardial inflammation: evidence for the presence of peroxynitrite. *Critical Care Medicine*.
- Kröncke, K. D., Fehsel, K., & Kolb-Bachofen, V. (1998). Inducible nitric oxide synthase in human diseases. *Clinical and Experimental Immunology*.
- Kudin, A. P., Bimpong-Buta, N. Y. B., Vielhaber, S., Elger, C. E., & Kunz, W. S. (2004). Characterization of Superoxide-producing Sites in Isolated Brain Mitochondria. *Journal of Biological Chemistry*, 279, 4127–4135.

- Kugi, M., Matsunaga, A., Ono, J., Arakawa, K., & Sasaki, J. (2002). Antioxidative effects of fluvastatin on superoxide anion activated by angiotensin II in human aortic smooth muscle cells. *Cardiovascular Drugs and Therapy / Sponsored by the International Society of Cardiovascular Pharmacotherapy*, 16, 203–207.
- Kuivenhoven, J. A., Jukema, J. W., Zwinderman, A. H., de Knijff, P., McPherson, R., Brusckhe, A. V. G., ... Kastelein, J. J. P. (1998). The Role of a Common Variant of the Cholesteryl Ester Transfer Protein Gene in the Progression of Coronary Atherosclerosis. *New England Journal of Medicine*, 338, 86–93.
- Kyaw, M., Yoshizumi, M., Tsuchiya, K., Izawa, Y., Kanematsu, Y., & Tamaki, T. (2004). Atheroprotective effects of antioxidants through inhibition of mitogen-activated protein kinases. *Acta Pharmacologica Sinica*, 25(8), 977–85.
- Lahera, V., Goicoechea, M., de Vinuesa, S. G., Miana, M., de las Heras, N., Cachofeiro, V., & Luño, J. (2007). Endothelial dysfunction, oxidative stress and inflammation in atherosclerosis: beneficial effects of statins. *Current Medicinal Chemistry*, 14, 243–248.
- Lee, S., Bai, S., & Lee, K. (2003). Astaxanthin Inhibits Nitric Oxide Production and Inflammatory Gene Expression by Suppressing I... B Kinase-dependent NF-... B Activation. *Molecules*:16(1), 97–105
- Lee, S. S., Gao, W., Mazzola, S., Thomas, M. N., Csizmadia, E., Otterbein, L. E., ... Wang, H. (2007). Heme oxygenase-1, carbon monoxide, and bilirubin induce tolerance in recipients toward islet allografts by modulating T regulatory cells. *FASEB Journal : Official Publication of the Federation of American Societies for Experimental Biology*, 21(13), 3450–7

- Leifeld, L., Fielenbach, M., Dumoulin, F.-L., Speidel, N., Sauerbruch, T., & Spengler, U. (2002). Inducible nitric oxide synthase (iNOS) and endothelial nitric oxide synthase (eNOS) expression in fulminant hepatic failure. *Journal of Hepatology*, 37(5), 613–9.
- Li, Y., Zhu, H., & Trush, M. a. (1999). Detection of mitochondria-derived reactive oxygen species production by the chemilumigenic probes lucigenin and luminol. *Biochimica et Biophysica Acta*, 1428(1), 1–12.
- Lirk, P., Hoffmann, G., & Rieder, J. (2002). Inducible nitric oxide synthase--time for reappraisal. *Current Drug Targets. Inflammation and Allergy*, 1(1), 89–108
- Liu, W., Kato, M., Itoigawa, M., Murakami, H., Yajima, M., Wu, J., ... Nakashima, I. (2001). Distinct Involvement of NF- κ B and p38 Mitogen- Activated Protein Kinase Pathways in Serum Deprivation- Mediated Stimulation of Inducible Nitric Oxide Synthase and Its Inhibition by 4-Hydroxynonenal, 280.
- Liu, Y., & Schubert, D. R. (2009). The specificity of neuroprotection by antioxidants. *Journal of Biomedical Science*.98.
- Lowenstein, C. J., & Padalko, E. (2004). iNOS (NOS2) at a glance. *Journal of Cell Science*, 117, 2865–2867.
- Lu, Y.-H., Su, M.-Y., Huang, H.-Y., Lin-Li, & Yuan, C.-G. (2010). Protective effects of the citrus flavanones to PC12 cells against cytotoxicity induced by hydrogen peroxide. *Neuroscience Letters*, 484(1), 6–11.

- Madamanchi, N. R., Vendrov, A., & Runge, M. S. (2005). Oxidative stress and vascular disease. *Arteriosclerosis, Thrombosis, and Vascular Biology*, 25(Cvd), 29–38.
- Magenta, A., Greco, S., Capogrossi, M. C., Gaetano, C., & Martelli, F. (2014). Nitric oxide, oxidative stress, and p66Shc interplay in diabetic endothelial dysfunction. *BioMed Research International*, 2014.
- Mann, G. E., Bonacasa, B., Ishii, T., & Siow, R. C. (2009). Targeting the redox sensitive Nrf2-Keap1 defense pathway in cardiovascular disease: protection afforded by dietary isoflavones. *Current Opinion in Pharmacology*, 9(2), 139–45.
- Mason, J. C. (2003). Statins and their role in vascular protection. *Clinical Science (London, England : 1979)*, 105(3), 251–66.
- Mazzei, L., García, I. M., Cacciamani, V., Benardón, M. E., & Manucha, W. (2010). WT-1 mRNA expression is modulated by nitric oxide availability and Hsp70 interaction after neonatal unilateral ureteral obstruction. *Biocell*, 34(3), 121–132.
- Mendes, A. F., Caramona, M. M., Carvalho, a P., & Lopes, M. C. (2003). Differential roles of hydrogen peroxide and superoxide in mediating IL-1-induced NF-kappa B activation and iNOS expression in bovine articular chondrocytes. *Journal of Cellular Biochemistry*, 88, 783–793.
- Menshikova, E. B., Tkachev, V. O., & Zenkov, N. K. (2010). Redox-dependent signaling system Nrf2/ARE in inflammation. *Molecular Biology*, 44(3), 343–357.

- Meraz, M. a, White, J. M., Sheehan, K. C., Bach, E. a, Rodig, S. J., Dighe, a S., ... Schreiber, R. D. (1996). Targeted disruption of the Stat1 gene in mice reveals unexpected physiologic specificity in the JAK-STAT signaling pathway. *Cell*, 84(3), 431–42.
- Merényi, G., Lind, J., Czapski, G., & Goldstein, S. (2000). The decomposition of peroxyxynitrite does not yield nitroxyl anion and singlet oxygen. *Proceedings of the National Academy of Sciences of the United States of America*, 97(15), 8216–8.
- Mezzetti, a, Di Ilio, C., Calafiore, a M., Aceto, A., Marzio, L., Frederici, G., & Cuccurullo, F. (1990). Glutathione peroxidase, glutathione reductase and glutathione transferase activities in the human artery, vein and heart. *Journal of Molecular and Cellular Cardiology*, 22, 935–938.
- Milstien, S., & Katusic, Z. (1999). Oxidation of tetrahydrobiopterin by peroxyxynitrite: implications for vascular endothelial function. *Biochemical and Biophysical Research Communications*, 263(3), 681–4.
- Miyamoto, S., Ronsein, G. E., Corrêa, T. C., Martinez, G. R., Medeiros, M. H. G., & Di Mascio, P. (2009). Direct evidence of singlet molecular oxygen generation from peroxyxynitrate, a decomposition product of peroxyxynitrite. *Dalton Transactions (Cambridge, England : 2003)*, (29), 5720–9.
- Modlinger, P. S., Wilcox, C. S., & Aslam, S. (2004). Nitric oxide, oxidative stress, and progression of chronic renal failure. *Seminars in Nephrology*, 24(4), 354–365.

- Moens, A. L., Takimoto, E., Tocchetti, C. G., Chakir, K., Bedja, D., Cormaci, G., ... Kass, D. a. (2008). Reversal of cardiac hypertrophy and fibrosis from pressure overload by tetrahydrobiopterin efficacy of recoupling nitric oxide synthase as a therapeutic strategy. *Circulation*, *117*, 2626–2636.
- Mohamadin, A. M., Elberry, A. A., Gawad, H. S. A., Morsy, G. M., & Al-abbasi, F. A. (2011). Protective Effects of Simvastatin , an HMG- CoA Reductase Inhibitor , Against Oxidative Damage in Experimental Diabetic Rats, *3*, 1780–1795.
- Moore, K. J., & Tabas, I. (2011). Macrophages in the pathogenesis of atherosclerosis. *Cell*, *145*(3), 341–355.
- Morrison, D. K. (2012). MAP kinase pathways. *Cold Spring Harbor Perspectives in Biology*, *4*.
- Morse, D., & Choi, A. M. K. (2005). Heme oxygenase-1: from bench to bedside. *American Journal of Respiratory and Critical Care Medicine*, *172*(6), 660–70.
- Mukhopadhyay, P., Rajesh, M., Hasko, G., Hawkins, B. J., Madesh, M., & Pacher, P. (2007). Simultaneous detection of apoptosis and mitochondrial superoxide production in live cells by flow cytometry and confocal microscopy. *Nat. Protoc.*, *2*, 2295–2301.
- Münzel, T., Daiber, A., Ullrich, V., & Mülsch, A. (2005). Vascular consequences of endothelial nitric oxide synthase uncoupling for the activity and expression of the soluble guanylyl cyclase and the CGMP-dependent protein kinase. *Arteriosclerosis, Thrombosis, and Vascular Biology*, *25*, 1551–1557.

- Murphy, M. P. (2009). How mitochondria produce reactive oxygen species. *The Biochemical Journal*, 417, 1–13.
- Nagata, D., Takeda, R., Sata, M., Satonaka, H., Suzuki, E., Nagano, T., & Hirata, Y. (2004). AMP-activated protein kinase inhibits angiotensin II-stimulated vascular smooth muscle cell proliferation. *Circulation*, 110, 444–451.
- Nakata, S., Tsutsui, M., Shimokawa, H., Yamashita, T., Tanimoto, A., Tasaki, H., ... Yanagihara, N. (2007). Statin treatment upregulates vascular neuronal nitric oxide synthase through Akt/NF-kappaB pathway. *Arteriosclerosis, Thrombosis, and Vascular Biology*, 27(1), 92–8.
- Nedeljkovic, Z. S., Gokce, N., & Loscalzo, J. (2003). Mechanisms of oxidative stress and vascular dysfunction. *Postgraduate Medical Journal*, 79, 195–199; quiz 198–200.
- O'Donnell, V. B., & Freeman, B. a. (2001). Interactions Between Nitric Oxide and Lipid Oxidation Pathways: Implications for Vascular Disease. *Circulation Research*, 88(1), 12–21.
- Okazaki, T., Otani, H., Shimazu, T., Yoshioka, K., Fujita, M., Katano, T., ... Iwasaka, T. (2011). Reversal of inducible nitric oxide synthase uncoupling unmasks tolerance to ischemia/reperfusion injury in the diabetic rat heart. *Journal of Molecular and Cellular Cardiology*, 50, 534–544.
- Öllinger, R., Bilban, M., Erat, A., Froio, A., McDaid, J., Tyagi, S., ... Bach, F. H. (2005). A natural inhibitor of vascular smooth muscle cell proliferation. *Circulation*, 112, 1030–1039.

- Ollinger, R., Wang, H., Yamashita, K., Wegiel, B., Thomas, M., Margreiter, R., & Bach, F. H. (2007). Therapeutic applications of bilirubin and biliverdin in transplantation. *Antioxidants & Redox Signaling*, 9, 2175–2185.
- Ozbek, E., Cekmen, M., Ilbey, Y. O., Simsek, A., Polat, E. C., & Somay, A. (2009). Atorvastatin prevents gentamicin-induced renal damage in rats through the inhibition of p38-MAPK and NF-kappaB pathways. *Renal Failure*, 31(May 2008), 382–392.
- Parastatidis, I., Weiss, D., Joseph, G., & Taylor, W. R. (2013). Overexpression of catalase in vascular smooth muscle cells prevents the formation of abdominal aortic aneurysms. *Arteriosclerosis, Thrombosis, and Vascular Biology*, 33, 2389–2396.
- Park, J. Y., Cho, H. Y., Kim, J. K., Noh, K. H., Yang, J. R., Ahn, J. M., ... Song, Y. S. (2005). Chlorella dichloromethane extract ameliorates NO production and iNOS expression through the down-regulation of NF- κ B activity mediated by suppressed oxidative stress in RAW 264.7 macrophages. *Clinica Chimica Acta*, 351, 185–196.
- Pehar, M. (2007). Mitochondrial superoxide production and nuclear factor erythroid 2-related factor 2 activation in p75 neurotrophin receptor-induced motor neuron apoptosis. *J. Neurosci.*, 27, 7777–7785.

- Perrotta, I., Brunelli, E., Sciangula, A., Conforti, F., Perrotta, E., Tripepi, S., ... Cassese, M. (2011). iNOS induction and PARP-1 activation in human atherosclerotic lesions: an immunohistochemical and ultrastructural approach. *Cardiovascular Pathology: The Official Journal of the Society for Cardiovascular Pathology*, 20(4), 195–203.
- Qiao, W., Chaoshu, T., Hongfang, J., & Junbao, D. (2010). Endogenous hydrogen sulfide is involved in the pathogenesis of atherosclerosis. *Biochemical and Biophysical Research Communications*, 396(2), 182–6.
- Ramana, C. V, Gil, M. P., Schreiber, R. D., & Stark, G. R. (2002). Stat1-dependent and -independent pathways in IFN-gamma-dependent signaling. *Trends in Immunology*, 23(2), 96–101.
- Rasmussen, S. E., Frederiksen, H., Struntze Krogholm, K., & Poulsen, L. (2005). Dietary proanthocyanidins: occurrence, dietary intake, bioavailability, and protection against cardiovascular disease. *Molecular Nutrition & Food Research*, 49(2), 159–74.
- Rensen, S. S. M., Doevendans, P. a F. M., & van Eys, G. J. J. M. (2007). Regulation and characteristics of vascular smooth muscle cell phenotypic diversity. *Netherlands Heart Journal: Monthly Journal of the Netherlands Society of Cardiology and the Netherlands Heart Foundation*, 15(3), 100–108.
- Rikitake, Y., Hirata, K., Kawashima, S., Akita, H., & Yokoyama, M. (1998). Inhibitory effect of inducible type nitric oxide synthase on oxidative modification of low density lipoprotein by vascular smooth muscle cells. *Atherosclerosis*, 136(1), 51–7.

- Rikitake, Y., & Liao, J. K. (2005). Rho GTPases, statins, and nitric oxide. *Circulation Research*, 97(12), 1232–1235.
- Robinson, K. M. (2006). Selective fluorescent imaging of superoxide in vivo using ethidium-based probes. *Proc. Natl. Acad. Sci. USA*, 103, 15038–15043.
- Robinson, K. M., Janes, M. S., & Beckman, J. S. (2008). The selective detection of mitochondrial superoxide by live cell imaging. *Nat. Protocols*, 3(6), 941–947.
- Roe, N. D., & Ren, J. (2012). Nitric oxide synthase uncoupling: a therapeutic target in cardiovascular diseases. *Vascular Pharmacology*, 57(5-6), 168–72.
- Ross, M. F. (2005). Lipophilic triphenylphosphonium cations as tools in mitochondrial bioenergetics and free radical biology. *Biochemistry Mosc.*, 70, 222–230.
- Ross, R. (1995). Cell biology of atherosclerosis. *Annual Review of Physiology*, 57, 791–804.
- Rothe, G., & Valet, G. (1990). Flow cytometric analysis of respiratory burst activity in phagocytes with hydroethidine and 2[prime],7[prime]-dichlorofluorescin. *J. Leukoc. Biol.*, 47, 440–448.
- Royall, J. A., & Ischiropoulos, H. (1993). Evaluation of 2',7'-dichlorofluorescin and dihydrorhodamine 123 as fluorescent probes for intracellular H₂O₂ in cultured endothelial cells. *Archives of Biochemistry and Biophysics*, 302(2), 348–55.

- Salvemini, D., Wang, Z. Q., Stern, M. K., Currie, M. G., & Misko, T. P. (1998). Peroxynitrite decomposition catalysts: therapeutics for peroxynitrite-mediated pathology. *Proceedings of the National Academy of Sciences of the United States of America*, *95*(5), 2659–63.
- Sena, C. M., Matafome, P., Crisóstomo, J., Rodrigues, L., Fernandes, R., Pereira, P., & Seica, R. M. (2012). Methylglyoxal promotes oxidative stress and endothelial dysfunction. *Pharmacological Research*, *65*, 497–506.
- Shigenaga, M. K., Hagen, T. M., & Ames, B. N. (1994). Oxidative damage and mitochondrial decay in aging. *Proc. Natl. Acad. Sci. USA*, *91*, 10771–10778.
- Shih, A. Y., Erb, H., & Murphy, T. H. (2007). Dopamine activates Nrf2-regulated neuroprotective pathways in astrocytes and meningeal cells. *Journal of Neurochemistry*, *101*, 109–119.
- Shishehbor, M. H., Brennan, M. L., Aviles, R. J., Fu, X., Penn, M. S., Sprecher, D. L., & Hazen, S. L. (2003). Statins promote potent systemic antioxidant effects through specific inflammatory pathways. *Circulation*, *108*, 426–431.
- Sirker, A., Zhang, M., & Shah, A. M. (2011). NADPH oxidases in cardiovascular disease: insights from in vivo models and clinical studies. *Basic Research in Cardiology*, *106*(5), 735–47.
- Spitaler, M. M., & Graier, W. F. (2002). Vascular targets of redox signalling in diabetes mellitus. *Diabetologia*.
- Stalheim, L., & Johnson, G. L. (2008). MAPK kinase kinase regulation of SAPK/JNK pathways. *Topics in Current Genetics*, *20*, 1–15.

- Stancu, C., & Sima, a. (2001). Statins: mechanism of action and effects. *Journal of Cellular and Molecular Medicine*, 5(4), 378–387.
- Subramani J, K. K. (2009). Atorvastatin restores the impaired vascular endothelium-dependent relaxations mediated by nitric oxi. *J Cardiovasc Pharmacol.*, 54(6):526-.
- Sugiyama, M., Ohashi, M., Takase, H., Sato, K., Ueda, R., & Dohi, Y. (2005). Effects of atorvastatin on inflammation and oxidative stress. *Heart and Vessels*, 20(4), 133–6.
- Tarpey, M. M., & Fridovich, I. (2001). Methods of Detection of Vascular Reactive Species: Nitric Oxide, Superoxide, Hydrogen Peroxide, and Peroxynitrite. *Circulation Research*, 89(3), 224–236.
- Teng, X., Zhang, H., Snead, C., & Catravas, J. D. (2002). Molecular mechanisms of iNOS induction by IL-1 beta and IFN-gamma in rat aortic smooth muscle cells. *American Journal of Physiology. Cell Physiology*, 282, C144–C152.
- Thirunavukkarasu, C., Watkins, S. C., & Gandhi, C. R. (2006). Mechanisms of endotoxin-induced NO, IL-6, and TNF-alpha production in activated rat hepatic stellate cells: role of p38 MAPK. *Hepatology (Baltimore, Md.)*, 44(II), 389–398.
- Tong, K. I., Padmanabhan, B., Kobayashi, A., Shang, C., Hirotsu, Y., Yokoyama, S., & Yamamoto, M. (2007). Different electrostatic potentials define ETGE and DLG motifs as hinge and latch in oxidative stress response. *Molecular and Cellular Biology*, 27(21), 7511–21.

- Troiano, L. (2007). Multiparametric analysis of cells with different mitochondrial membrane potential during apoptosis by polychromatic flow cytometry. *Nat. Protoc.*, 2, 2719–2727.
- Tsikakos, D. (2007). Analysis of nitrite and nitrate in biological fluids by assays based on the Griess reaction: appraisal of the Griess reaction in the L-arginine/nitric oxide area of research. *Journal of Chromatography. B, Analytical Technologies in the Biomedical and Life Sciences*, 851(1-2), 51–70.
- Tufekci, K. U., Civi Bayin, E., Genc, S., & Genc, K. (2011). The Nrf2/ARE Pathway: A Promising Target to Counteract Mitochondrial Dysfunction in Parkinson's Disease. *Parkinson's Disease*, 2011, 314082. <http://doi.org/10.4061/2011/314082>
- Valko, M., Morris, H., & Cronin, M. T. D. (2005). Metals, toxicity and oxidative stress. *Current Medicinal Chemistry*, 12, 1161–1208.
- Vanhoutte, P. M. (1992). Inducible nitric oxide synthase and vascular smooth muscle. *Japanese Journal of Pharmacology*, 58 Suppl 2, 192P–199P.
- Víteček, J., Lojek, A., Valacchi, G., & Kubala, L. (2012). Arginine-based inhibitors of nitric oxide synthase: Therapeutic potential and challenges. *Mediators of Inflammation*, 2012.
- Vogiatzi, G., Tousoulis, D., & Stefanadis, C. (2009). The role of oxidative stress in atherosclerosis. *Hellenic Journal of Cardiology: HJC = Hellēnikē Kardiologikē Epitheōrēsē*, 50(5), 402–9.

- Walker, J. M. (1994). The bicinchoninic acid (BCA) assay for protein quantitation. *Methods in Molecular Biology (Clifton, N.J.)*, 32, 5–8.
- Wang, Y., Zuo, Z., Lee, K. K. H., & Chow, M. S. S. (2007). Evaluation of HO-1-u-1 cell line as an in vitro model for sublingual drug delivery involving passive diffusion--Initial validation studies. *International Journal of Pharmaceutics*, 334(1-2), 27–34.
- Wassmann, S. (2002). Cellular Antioxidant Effects of Atorvastatin In Vitro and In Vivo. *Arteriosclerosis, Thrombosis, and Vascular Biology*, 22, 300–305.
- Wei, C., Huang, K., Chou, Y., Hsieh, P., Lin, K., & Lin, W. (2006). The Role of Rho-Associated Kinase in Differential Regulation by Statins of Interleukin-1 α - and Lipopolysaccharide-Mediated Nuclear Factor κ B Activation and Inducible Nitric Oxide Synthase Gene Expression in Vascular Smooth Muscle Cells, 69(3), 960–967.
- Weitz-Schmidt, G., Welzenbach, K., Brinkmann, V., Kamata, T., Kallen, J., Bruns, C., ... Hommel, U. (2001). Statins selectively inhibit leukocyte function antigen-1 by binding to a novel regulatory integrin site. *Nat Med*, 7(6), 687–692.
- Wen, J., Ribeiro, R., & Zhang, Y. (2011). Specific PKC isoforms regulate LPS-stimulated iNOS induction in murine microglial cells. *Journal of Neuroinflammation*, 8(1), 38.
- Wierzbicki, A. S., Poston, R., & Ferro, A. (2003). The lipid and non-lipid effects of statins. *Pharmacology & Therapeutics*, 99(1), 95–112.

- Wileman, S. M., Mann, G. E., & Baydoun, A. R. (1995). Induction of L-arginine transport and nitric oxide synthase in vascular smooth muscle cells: synergistic actions of pro-inflammatory cytokines and bacterial lipopolysaccharide. *British Journal of Pharmacology*, *116*, 3243–3250.
- Wileman, S. M., Mann, G. E., Pearson, J. D., & Baydoun, A. R. (2003). Role of L-citrulline transport in nitric oxide synthesis in rat aortic smooth muscle cells activated with LPS and interferon-gamma. *British Journal of Pharmacology*, *140*(1), 179–85.
- Wong, C. H., Liu, T.-Z., Chye, S.-M., Lu, F.-J., Liu, Y.-C., Lin, Z.-C., & Chen, C.-H. (2006). Sevoflurane-induced oxidative stress and cellular injury in human peripheral polymorphonuclear neutrophils. *Food and Chemical Toxicology: An International Journal Published for the British Industrial Biological Research Association*, *44*(8), 1399–407.
- Yamada, T. (2009). [Regulation of the expression of inducible nitric oxide synthase by prostanoids]. *Yakugaku Zasshi: Journal of the Pharmaceutical Society of Japan*, *129*(10), 1211–4.
- Ye, Y., Martinez, J. D., Perez-Polo, R. J., Lin, Y., Uretsky, B. F., & Birnbaum, Y. (2008). The role of eNOS, iNOS, and NF-kappaB in upregulation and activation of cyclooxygenase-2 and infarct size reduction by atorvastatin. *American Journal of Physiology. Heart and Circulatory Physiology*, *295*, H343–H351.

- Zhang, Y., Guo, W., Wen, Y., Xiong, Q., Liu, H., Wu, J., ... Zhu, Y. (2012). SCM-198 attenuates early atherosclerotic lesions in hypercholesterolemic rabbits via modulation of the inflammatory and oxidative stress pathways. *Atherosclerosis*, 224(1), 43–50.
- Zhou, L., & Zhu, D.-Y. (2009). Neuronal nitric oxide synthase: structure, subcellular localization, regulation, and clinical implications. *Nitric Oxide: Biology and Chemistry / Official Journal of the Nitric Oxide Society*, 20(4), 223–230.
- Zhou, Q., & Liao, J. K. (2009). Rho kinase: an important mediator of atherosclerosis and vascular disease. *Current Pharmaceutical Design*, 15(27), 3108–3115.
- Zhou, Y., Chen, M.-H., & Liu, J.-H.(2007). Cardioprotective effects of atorvastatin preconditioning via iNOS upregulation in a rabbit ischemia/reperfusion model. *Zhonghua Xin Xue Guan Bing Za Zhi [Chinese Journal of Cardiovascular Diseases]*.
- Zielonka, J., Vasquez-Vivar, J., & Kalyanaraman, B. (2008). Detection of 2-hydroxyethidium in cellular systems: a unique marker product of superoxide and hydroethidine. *Nat. Protocols*, 3(1), 8–21.